Iowa State University
Digital Repository

1973

Tungsten bronzes as indicating potentiometric electrodes

Paul Balser Hahn
Iowa State University

INFORMATION TO USERS

This material was produced from a microfilm copy of the original document. While the most advanced technological means to photograph and reproduce this document have been used, the quality is heavily dependent upon the quality of the original submitted.

The following explanation of techniques is provided to help you understand markings or patterns which may appear on this reproduction.

1. The sign or "target" for pages apparently lacking from the document photographed is "Missing Page(s)". if it was possible to obtain the missing page(s) or section, they are spliced into the film along with adjacent pages. This may have necessitated cutting thru an image and duplicating adjacent pages to insure you complete continuity.

2. When an image on the film is obliterated with a large round black mark, it is an indication that the photographer suspected that the copy may have moved during exposure and thus cause a blurred image. You will find a good image of the page in the adjacent frame.

3. When a map, drawing or chart, etc., was part of the material being photographed the photographer followed a definite method in "sectioning" the material. It is customary to begin photoing at the upper left hand corner of a large sheet and to continue photoing from left to right in equal sections with a small overlap. If necessary, sectioning is continued again — beginning below the first row and continuing on until complete.

4. The majority of users indicate that the textual content is of greatest value, however, a somewhat higher quality reproduction could be made from "photographs" if essential to the understanding of the dissertation. Silver prints of "photographs" may be ordered at additional charge by writing the Order Department, giving the catalog number, title, author and specific pages you wish reproduced.

5. PLEASE NOTE: Some pages may have indistinct print. Filmed as received.

74-542

HAHN, Paul Balser, 1940-
   TUNGSTEN BRONZES AS INDICATING POTENTIOMETRIC
   ELECTRODES.

   Iowa State University, Ph.D., 1973
   Chemistry, analytical

University Microfilms, A XEROX Company, Ann Arbor, Michigan

Tungsten bronzes as indicating potentiometric electrodes

by

Paul Balser Hahn

A Dissertation Submitted to the

Graduate Faculty in Partial Fulfillment of

The Requirements for the Degree of

DOCTOR OF PHILOSOPHY

Department: Chemistry
Major: Analytical Chemistry

Approved:

In Charge of Major Work

For the Major Department

For the Graduate College

Iowa State University
Ames, Iowa

1973

TABLE OF CONTENTS

INTRODUCTION

The recent discovery that the metal tungsten bronzes are extremely versatile potentiometric-indicating electrodes for following acid-base and redox titrations and for determining the concentration of certain reducible metals initiated this study into the possible further uses of tungsten bronze electrodes in analytical chemistry.

These investigations led to two significant discoveries: the ability of sodium tungsten bronze to act as a potentiometric-selective electrode for dissolved oxygen in basic solution and as a potentiometric-indicating electrode for following chelometric titrations of a large number of metals with EDTA in basic solution. These characteristics were found to be unique to the cubic sodium tungsten bronzes among the highly conducting alkali metal tungsten bronzes. Significant effort was directed toward demonstrating the analytical applicability of these discoveries.

The mechanism for the response of the sodium tungsten bronze to dissolved oxygen and in the chelometric titrations was not at all obvious. The extremely large response to oxygen (120 mV/decade instead of the expected 15 or 30 mV/decade) and the ability to perform chelometric titrations of nonreducible metals such as calcium made it impossible to explain the response on the basis of simple redox reactions. An adsorption mechanism involving the adsorption and displacement of hydroxide ions at the electrode surface was first proposed on the basis of a number of early observations. Subsequent observations however, which included voltammetric studies of several tungsten bronze electrodes, provided extremely strong evidence of a mixed-potential mechanism for the response of the sodium

tungsten bronze electrode in basic solution. The mixed potential established at the sodium tungsten bronze electrode was found to be the result of the spontaneous oxidation of the electrode surface to tungstate by oxygen or other oxidizing agents. The oxygen response, the response in chelometric titrations and a number of other intriguing observations are explained by the mixed-potential mechanism.

THE TUNGSTEN BRONZES

The tungsten bronzes, due to their many unique and interesting properties, have been the object of considerable physical and chemical studies in the past four decades. They are nonstoichiometric metal-like oxides containing tungsten and at least one other metallic element located at a different site in the crystal lattice than the tungsten atom. The tungsten bronzes are not considered to be mixed oxides with the second metal replacing a portion of the tungsten atoms but rather a solid solution of tungstic oxide and the second metal which occupies vacant interstices between interlocking WO_3 octahedra. When only one other metal is present the general formula is represented by M_xWO_3 in which $0 < x < 1$. Tungsten bronzes containing the alkali and alkaline earth metals, lanthanum and other rare earths, aluminum, cobalt, nickel, copper, zinc, gallium, silver, cadmium, indium, thallium, tin, lead, thorium, and uranium have been reported (1-3). The concentration of the second metal is continuously variable within definite ranges depending on its ionic radius, its location in the crystal lattice and the overall structure of the bronze. In addition to the metal tungsten bronzes, hydrogen and ammonium tungsten bronzes have also been reported (4,5).

The first tungsten bronze reported was that of sodium, prepared by Wöhler (6) in 1823 by passing dry hydrogen over a molten mixture of Na_2WO_4 and WO_3 producing golden yellow crystals with a metallic appearance. Potassium tungsten bronze was first prepared by Laurent (7) in 1838 by the reduction of a K_2WO_4-WO_3 melt with hydrogen. First mention of the synthesis of similar compounds containing lithium and rubidium was made in the

early 1900's. Hallopeau (8) and Brunner (9) obtained dark blue crystals of Li_xWO_3 by reducing paratungstate melts (Li_2WO_4-WO_3) by electrolysis or with tin metal, and Schaefer (10) prepared Rb_xWO_3 by reducing a Rb_2CO_3-H_2WO_4 melt with a hydrogen-methane gas mixture. Tungsten bronzes containing metals other than the alkali metals and more than one other metal have only recently been prepared and characterized.

For many years it was thought that these oxide bronzes were unique to tungsten. However, investigations since the late 1940's have shown it possible to prepare analogous bronzes of molybdenum, vanadium, niobium, tantalum, titanium and rhenium having properties similar to those of the tungsten bronzes. Several excellent review articles on the oxide bronzes may be found in the recent literature (1-3).

Tungsten bronzes have been prepared by three methods; vapor phase reaction of a metal vapor and WO_3 vapor, chemical reduction in a molten mixture containing a salt of the secondary metal and tungstic oxide or electrolytic reduction at a platinum, tungsten or other electrode in a similar melt.

The vapor phase reaction is limited to metals appreciably volatile at high temperatures. Excellent single crystals of Tl_xWO_3 were prepared by Sienko (11), and Straumanis and Hsu (12) reported the production of Li_xWO_3 using this technique.

A number of investigators have prepared bronzes in the form of a powder or small single crystals using a variety of chemical reductants. Tungsten metal has been widely used in a molten mixture of WO_3 and the metal tungstate or oxide to produce Na_xWO_3 (13-16) and a number of rare earth tungsten bronzes (17,18). A typical reaction may be represented by

equation 1.

$$3xNa_2WO_4 + (6-4x)WO_3 + xW \longrightarrow 6Na_xWO_3 \tag{1}$$

Tungsten dioxide has also been widely used as the reducing agent for the production of alkali metal bronzes from M_2O-WO_3 melts (19), for the production of Pb_xWO_3 from $PbCO_3-WO_3$ and $PbWO_4-WO_3$ melts (20), and for the production of a number of alkali and alkaline earth and other tungsten bronzes from a metal halide-WO_3 melt (21).

$$xMCl_2 + xWO_2 + WO_3 \longrightarrow M_xWO_3 + xWO_2Cl_2 \tag{2}$$
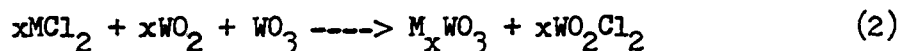
Other reducing agents have included hydrogen for the production of tetragonal K_xWO_3 from K_2O-WO_3 melts and hexagonal Rb_xWO_3 from Rb_2O-WO_3 melts (19,22) and cubic sodium bronzes from $Na_2WO_4-WO_3$ melts (23), Sn and Zn metals for the production of alkali metal bronzes from similar melts (19) and alkali azides for the production of alkali metal bronzes from WO_3 melts at pressures of 100-3000 atm (24).
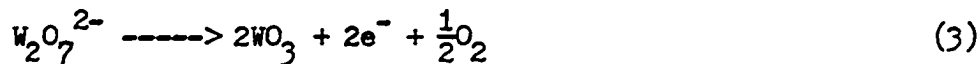
In the production of the tungsten bronzes by chemical reduction the reaction generally proceeds at temperatures of 500-1000°C for periods of time ranging from a few minutes to several days. Oxygen must be excluded to avoid competing reactions and the reduction is performed either in a vacuum or under an inert atmosphere (argon). The final composition of the bronze (x value) can be adjusted by varying the molar ratios of WO_3 and the secondary metal oxide or tungstate. Such reactions are generally far from complete and the relationship between melt composition and final bronze composition is at best very empirical.

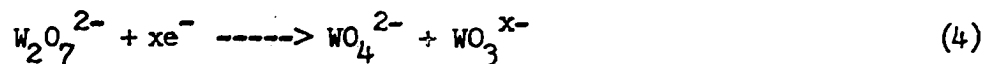The third and perhaps the most useful method of tungsten bronze

production is by electrolytic reduction in melts similar to those described above. The primary advantage of the electrolytic method is that large single crystals may be grown. Currents in the range of a few tenths of a milliampere to several amperes with voltages up to 6 volts have been employed to form and deposit the bronze at metal cathodes with the evolution of oxygen at the anode (11,19,25-30). As in the case of preparation by chemical reduction, melts are maintained at temperatures of $500-1000^{\circ}C$ and the final bronze composition is a function of the melt composition. Electrolyses have been carried out for periods of time ranging from a few hours to several days.

Only recently has the electrochemistry of this bronze preparative technique been investigated. Fredlein and Damjanovic (31) studied the deposition and dissolution of $Na_2WO_4-WO_3$ melts and established from voltammetric curves that dissolution was not the simple reverse of deposition. They further established that the composition of the bronze was constant if deposited at a constant potential but that during dissolution, the ratio of Na and W dissolution rates changed. Meites et al. (32) studied the voltammetric behavior of Na, Li and K tungstate and polytungstate melts at Pt electrodes. From similar studies, Whittingham and Huggins (33) proposed the following electrochemical reactions for the production of M_xWO_3 from tungstate-tungstic oxide melts:
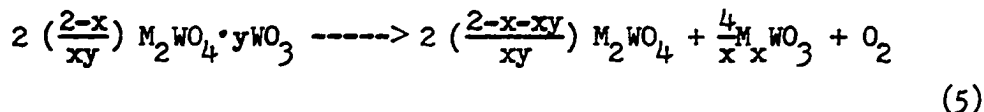
Anode reaction:

$$W_2O_7^{2-} \longrightarrow 2WO_3 + 2e^- + \tfrac{1}{2}O_2 \tag{3}$$

Cathode reaction:

$$W_2O_7{}^{2-} + xe^- \longrightarrow WO_4{}^{2-} + WO_3{}^{x-} \tag{4}$$

Overall reaction (alkali metal):

$$2 \left(\frac{2-x}{xy}\right) M_2WO_4 \cdot yWO_3 \longrightarrow 2 \left(\frac{2-x-xy}{xy}\right) M_2WO_4 + \frac{4}{x}M_xWO_3 + O_2 \tag{5}$$

After preparation the bronzes are generally washed with boiling water or alkali hydroxide solutions to remove tungstates and tungstic oxide. It is also possible to alter the secondary metal content (x value) of such bronzes after they have been prepared. This was demonstrated by de Jong (34) as early as 1932 when he prepared tetragonal "blue Na-W bronze" by reducing cubic Na_xWO_3 with H_2 or Zn. Straumanis (13) also found it possible to remove sodium from Na_xWO_3 with I_2 vapor at 800°C. More recently, McNeill (15) and McNeill and Conroy (16) prepared cubic Na_xWO_3 (x = 0.363, 0.291, 0.234) by mixing finely divided stoichiometric amounts of $Na_{0.693}WO_3$ and WO_3 for the desired final sodium concentration and heating in a vacuum at 920°C for 9 days.

The characterization of the tungsten bronzes in terms of stoichiometry and crystal structure, chemical properties, and electrical and magnetic properties has been directed primarily toward the alkali metal bronzes with the major emphasis on the sodium compounds. In the early 1930's de Jong (34,35) and Hagg (36,37) established on the basis of X-ray measurements that the sodium tungsten bronzes could exist in the cubic perovskite structure with W at the center of the cube, the oxygen atoms arranged octahedrally at the face centers and the sodium atoms occupying a fraction of the interstitial sites at the cube corners. They also noted the characteristic color change of the sodium tungsten bronzes from gold

through orange red and violet to blue as the sodium content decreased. Hägg was the first to demonstrate that the various cubic sodium bronzes were not separate compounds but a continuous series of solid solutions of variable composition with an extended homogeneity range. He determined the lattice constants of these compounds and was the first to observe the contraction of the lattice with decreasing sodium content. De Jong also demonstrated a tetragonal structure for a low concentration sodium tungsten bronze.

The sodium tungsten bronzes are now known to exist in the cubic structure for x values from approximately 0.3 to nearly 1.0 (16,19). Brown and Banks (38) determined the relationship between the sodium concentration and the cubic lattice constant to be $a(\text{Å}) = 0.0819x + 3.7846$ by X-ray measurements coupled with chemical analysis. This linear relationship was later confirmed by Reuland and Voigt (39) using neutron activation analysis. The crystal structure of Na_xWO_3 decreases in symmetry as the sodium content decreases passing through two tetragonal phases ($0.05 < x < 0.4$) to the monoclinic structure of WO_3 itself (1,19,40,41).

The other alkali metal tungsten bronzes follow similar phase transitions as the x value varies. Li_xWO_3 is observed to have similar structures as its sodium analog, existing in the cubic form for $0.1 < x < 0.4$ and a tetragonal form for $0.05 < x < 0.3$ (19,29). Potassium bronzes may exist in the cubic form for $x \approx 0.9$ (24), the tetragonal form for $0.40 < x < 0.57$ (1,19) and in a hexagonal form for x, approximately 0.3 (19, 42,43). Rubidium and cesium tungsten bronzes have only been observed in the hexagonal form with x approximately 0.3 (19,42,43).

Considerable interest in the bronzes has resulted from their

unusually low electrical resistivities typical of metals rather than metal oxides. Resistivities of various tungsten bronzes have been determined by a number of investigators and are summarized by Dickens and Whittingham (1), Sienko (44) and Shanks et al. (45). Resistivities for a number of alkali tungsten bronzes (cubic sodium and lithium, tetragonal potassium and sodium) were found to range from about 20μ ohm cm for x values of 0.9 to approximately 400μ ohm cm for x values approaching 0.3 (45). The resistivities of the bronzes rise linearly with temperature indicating metal-like conduction and appear to be more a function of x value rather than the alkali metal or the crystal structure. At lower alkali metal concentration (x<0.25) the resistivity of the tungsten bronzes is very much larger and they are semiconductors.

Measurements of the Hall and Seebeck effects in the highly conducting bronzes has confirmed that one free electron exists per alkali metal atom (two for alkaline earth, three for rare earth) in the bronze lattice and that the carrier mobility is comparable to that of free electrons in the conduction band of typical metals (1,44-47). Magnetic measurements on the cubic alkali metal tungsten bronzes has shown only a small temperature-independent paramagnetism showing the absence of two isolated spin states for tungsten (48). The old theory of the tungsten bronzes being solid solutions containing tungsten in two oxidation states $W^{VI}O_3$ and $MW^{V}O_3$) has thus given way to the theory that they are solutions of M in a WO_3 matrix with the ionized secondary metal providing the free electrons which are located in a delocalized conduction band (1).

Three models have been proposed concerning the origin of the conduction band. Mackintosh (49) and Fuchs (50) considered that the conduction

band results from direct overlap of the alkali metal 3p orbitals while

Sienko (44) proposed that the band results only from W-W bonding via

direct overlap of the W $5d(t_{2g})$ orbitals. Two observations placed serious

doubt on the Mackintosh-Fuchs model (1). Nuclear magnetic resonance mea-

surements showed no significant 3p character of the conduction band, and

ReO_3 which is isoelectric with $Na_{1.0}WO_3$ exhibits metallic conductivity

without any alkali metal present. The third model, proposed by Goodenough

and coworkers (51-53), refines that of Sienko by mixing oxygen $p\pi$ orbitals

with tungsten t_{2g} orbitals. This model was based on the observation that

Sr_2MgReO_6, a compound with the necessary symmetry for $Re(t_{2g})$ overlap but

not for $Re(t_{2g})-O(p\pi)$ overlap, showed only semiconducting properties.

The tungsten bronzes are insoluble in water and are extremely resistant

toward acids developing an insoluble surface film of tungstic acid.

Na_xWO_3 is insoluble in basic solution in the absence of oxidizing agents

but dissolves slowly with the formation of tungstate in the presence of

oxygen and rapidly in the presence of sodium peroxide (12,13). Ammoniacal

silver nitrate also oxidizes Na_xWO_3 with the spontaneous plating of metallic

silver and the formation of WO_4^{2-}. Other tungsten bronzes including Li_xWO_3

and mixed $Li_xNa_yWO_3$ appear much more resistant toward oxidation. They are

not attacked by hot, concentrated base in the presence of oxygen (54).

Much of the practical interest in the tungsten bronzes has been

concerned with their catalytic activity in gas phase reactions and their

electrocatalytic activity as electrodes in aqueous solution. The sodium

tungsten bronzes have been demonstrated to catalyze the decomposition of

formic acid at high temperature (14), the ortho-para hydrogen conversion

and hydrogen-deuterium exchange in the gas phase (55). Their catalytic

activity for the dehydration of certain alcohols however, was shown to
be very small (56). As electrodes in electrolytic cells the sodium
tungsten bronzes were found to catalyze the evolution of hydrogen in acid
solution (57), the oxidation of carbon monoxide and reformer gas (78% H_2,
2% CO, 20% CO_2) in acid electrolyte fuel cells (58), and the reduction of
oxygen in acid solution (59-70).

In the past decade there has been considerable interest in the
ability of the bronzes to catalyze the reduction of oxygen, perhaps to
serve as an economically feasible oxygen electrode in fuel cells. Their
high conductivity, resistance to attack, and low cost compared to the
noble metal catalysts were certainly in their favor. Early studies by
Damjanovic, Sepa and Bockris (59,60) showed Na_xWO_3 to be almost as good
as platinum (the best catalyst known) for catalyzing the reduction of O_2
in acid solution. More recent investigations however, have demonstrated
this catalytic activity to be due to trace platinum impurities incorpora-
ted in the bronzes during their preparation by electrolysis on Pt cathodes
(62,64-66,68,70). Bockris and McHardy (70) have quantitatively evaluated
the influence of Pt and other dopants on the catalytic effect of the
sodium tungsten bronzes and proposed models for the increased activity.

The tungsten and other transition metal bronzes have been found to
act as potentiometric-indicating electrodes for a number of electroactive
species. Koksharov and Ust-Kachkinsev found the cubic sodium tungsten
bronzes (71) and the strontium niobium bronzes (72) to have linear
potentiometric response to pH over a wide interval (pH 0-14) with slopes
of response $(\Delta E/\Delta pH)$ of 58 mV for Na_xWO_3 and 40-50 mV for the strontium
niobium bronze. They demonstrated the utility of these electrodes for

acid-base titrations in both aqueous and alcoholic solution and in the
presence of oxidizing (MnO_4^{2-}) and reducing ($Fe(II)$) agents which
appeared to have little effect on the potential developed at the bronze
electrode. The same authors found only minimal pH response for tetra-
gonal Na_xWO_3 (71) and for copper and silver vanadium bronzes (73).
Wechter et al. (74) recently demonstrated the pH response of the cubic
Na_xWO_3 electrode and the ability to perform acid-base titrations in
aqueous and non aqueous systems.

The inability of the bronzes to respond to oxidizing and reducing
agents has, however, been discredited by two groups of investigators.
Weser and Pungor (75) demonstrated that cubic Na_xWO_3 and ReO_3 electrodes
exhibited a potentiometric response similar to that of platinum for the
$Fe(II)-Fe(III)$ and the ferro-ferricyanide redox couples in acid solution.
Wechter et al. (74) showed the Na_xWO_3 electrode to respond to both the
$Fe(II)-Fe(III)$ and the $Ce(IV)-Ce(III)$ redox couples by titrating $Fe(II)$
with $Ce(IV)$ in acid solution. In this titration the bronze electrode
response was found to lag slightly behind that of a platinum electrode
affording the opportunity to directly obtain an excellent first derivative
titration curve if the potential between a bronze and Pt electrode is
monitored.

Wechter et al. also demonstrated the ability of the Na_xWO_3 electrode
to function as a potentiometric-indicating electrode for a number of
easily reducible metals in acid solution. Nernstian response was found for
$Ag(I)$ (60 mV/decade), $Hg(II)$ and $Cu(II)$ (30 mV/decade) for concentrations
ranging from 10^{-1} to nearly $10^{-7}M$.

EXPERIMENTAL

Materials and Apparatus

Crystals of the alkali metal tungsten bronzes, M_xWO_3, used for electrodes were grown by the electrolysis of a melt of the metal tungstate (M_2WO_4) and tungstic oxide (WO_3) (26,27). After preparation they were washed with dilute NaOH and deionized water to remove any tungstate or tungstic oxide adhering to the surface. The metal content or the x value of the bronzes had been previously determined by activation analysis, the measurement of lattice parameters (39,76,77), or by estimation on the basis of the electrolytic melt composition during preparation.

Individual electrodes were prepared from pieces either cut with a diamond saw or chipped from larger single crystals of bronze. The crystals which were cut had smooth flat surfaces, while those chipped from the parent crystal had jagged uneven surfaces. One series of sodium tungsten bronzes was annealed at $650°C$ in an argon atmosphere for several days and cooled at a rate of $50°C/hr$ to achieve a greater degree of homogeneity.

The electrodes themselves were prepared by cementing the crystals to glass tubing with epoxy compound and making electrical contact through a mercury pool to a copper wire (Figure 1). The electrical resistance of each electrode was checked with an ohmmeter; those exhibiting a resistance greater than 1-2 ohms were not used. The exposed surface areas of the bronze electrodes were estimated to vary between 0.05 and 0.2 cm^2. Table 1 lists the characteristics of the tungsten bronze electrodes used in this investigation.

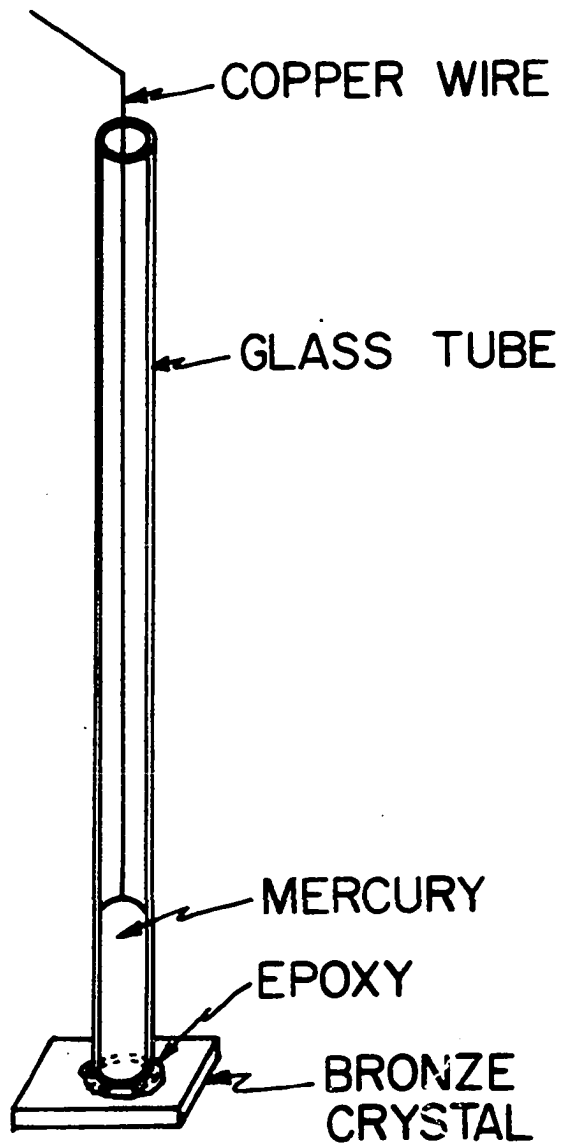All solutions used in this study were prepared from reagent grade

Figure 1. The tungsten bronze electrode

Table 1. Characteristics of the tungsten bronze electrodes

Electrode	x value	Crystal structure	Remarks
Na_xWO_3	0.507	cubic	chipped
Na_xWO_3	0.626	cubic	chipped
Na_xWO_3	0.65	cubic	cut (4x4x2mm), annealed
Na_xWO_3	0.718	cubic	chipped
Na_xWO_3	0.81	cubic	chipped
Na_xWO_3	0.907	cubic	chipped
Li_xWO_3	0.35	cubic	chipped
K_xWO_3	0.3	hexagonal	chipped
K_xWO_3	0.5	tetragonal	chipped
Rb_xWO_3	0.3	hexagonal	chipped
Cs_xWO_3	0.3	hexagonal	chipped

chemicals and deionized water; no attempt was made to prepare carbonate-free basic solutions. Gases used for oxygen equilibration were dry 99.995% nitrogen and 99.6% oxygen, Matheson "Zero" grade air, and specific oxygen-nitrogen gas mixtures (10.12, 3.27, 0.99, 0.35 and 0.10% O_2 by volume) prepared and analyzed ($\pm$ 2 relative percent) by Matheson Gas Products.

Potentiometric measurements were made with Beckman Zeromatic SS-3 or H-5 pH meters or a Keithley Model 640 vibrating capacitor electrometer. The output from these was fed into a Sargent Model MR recorder to monitor electrode response as a function of time. All potential measurements

were made vs. a Beckman saturated calomel reference electrode.

Voltammetric studies of the tungsten bronze electrodes were performed

with a Leeds and Northrup Electro-Chemograph Model E polaragraph. A

large surface area saturated calomel electrode (78) was used as the

reference electrode in these studies.

Procedures

Dissolved oxygen measurement

The potentiometric response to dissolved oxygen was determined in

pH 9.2 (0.0246M $Na_2B_4O_7$, 0.0018M NaOH), pH 10.5 (0.0172M $Na_2B_4O_7$,

0.031M NaOH), and pH 12.0 (0.161M KCl, 0.0387M NaOH, 0.5mM EDTA) buffer

solutions (79) and in 0.1M KOH-1.0mM EDTA.

Three separate techniques were employed to establish or indepen-

dently measure the concentration of dissolved oxygen in these solutions.

The first was by mixing varying volumes of nitrogen-saturated and oxygen-

saturated solutions and calculating the relative oxygen concentration on

the basis of the volumes, assuming no loss of dissolved gases upon mixing.

In the second, air and nitrogen were purged into solution at varying

rates and the dissolved oxygen was determined voltammetrically with a

rotating platinum disc electrode (80). In this method the dissolved

oxygen concentration was calculated from the observed diffusion limited

current for the $2H_2O + O_2 + 4e^- \longrightarrow 4OH^-$ reaction (Equation 6).

$$C = \frac{i_1}{0.62 \, n \, F(\pi r^2) \, D^{2/3} \omega^{1/2} \nu^{-1/6}} \tag{6}$$

In this equation C is the concentration in moles/liter, i_1 the limiting

current in mA, n the number of electrons involved in the redox reaction, πr^2 the area of the electrode (0.470 cm^2), D the diffusion coefficient for O_2 in aqueous solution (2.6 X 10^{-5} cm^2/sec) (81), ω the angular velocity of the rotating electrode (168 radians/sec), and ν the kinematic viscosity of the solution (0.01002 poise) (79).

The third technique made use of the pre-mixed N_2-O_2 gases described above to establish the oxygen concentration. This technique was used in most of the experiments because it was much easier than the other two and provided much better stability in oxygen concentration over long periods of time.

The oxygen concentrations in the solutions may be calculated assuming Henry's Law. The effect of KOH on the solubility of oxygen has been determined by Davis et al. (82) who found the relation

$$\log s = \log 1.26 \text{ X } 10^{-3} - 0.1746 \text{ M} \tag{7}$$

between the solubility of oxygen, s, in moles per liter and the KOH concentration, M, also in moles per liter at 25°C. Calculated values of the oxygen concentrations in the solution used in most of the measurements, 0.1M KOH - 1mM EDTA, are given in Table 2. The effect of 0.1M KOH is to reduce the solubility from that in pure water by about 4%. Except for the oxygen and air there is an uncertainty of $\pm 2\%$ in these values based on the analyses provided with the gas mixtures.

All potentiometric measurements were performed in a rapidly stirred solution after the electrode was allowed to equilibrate for 2-10 minutes. When the equilibrating gases were used the temperature of the solution was controlled within a few tenths of a degree with a constant temperature bath.

Table 2. Calculated oxygen concentrations in 0.1M KOH-1mM EDTA at 25°C as a function of equilibrating gas

Equilibrating gas volume % O_2		O_2 Concentration	
		M	ppm
100	(O_2)	1.21×10^{-3}	38.7
20.9	(air)	2.53×10^{-4}	8.10
10.12		1.23×10^{-4}	3.94
3.27		3.96×10^{-5}	1.27
. 0.99		1.20×10^{-5}	0.384
0.35		4.24×10^{-6}	0.136
0.10		1.21×10^{-6}	0.039

The potentiometric response to dissolved oxygen was also determined in several flow-through systems having the basic design illustrated in Figure 2. The sample solution equilibrated with one of the gas mixtures, and the deoxygenated KOH-EDTA reagent solution were simultaneously introduced into a mixing chamber and allowed to flow sequentially past the bronze and saturated calomel reference electrodes. The sample solution was introduced by gravity at a rate of 2-5 times that of the reagent solution which was introduced either by gravity or under 1-2 lb/in^2 nitrogen pressure.

Chelometric titrations

Chelometric titrations were performed with 10^{-1}, 10^{-2}, or 10^{-3}M disodium EDTA solutions in either 1M NH_4OH or a pH 10 buffer solution
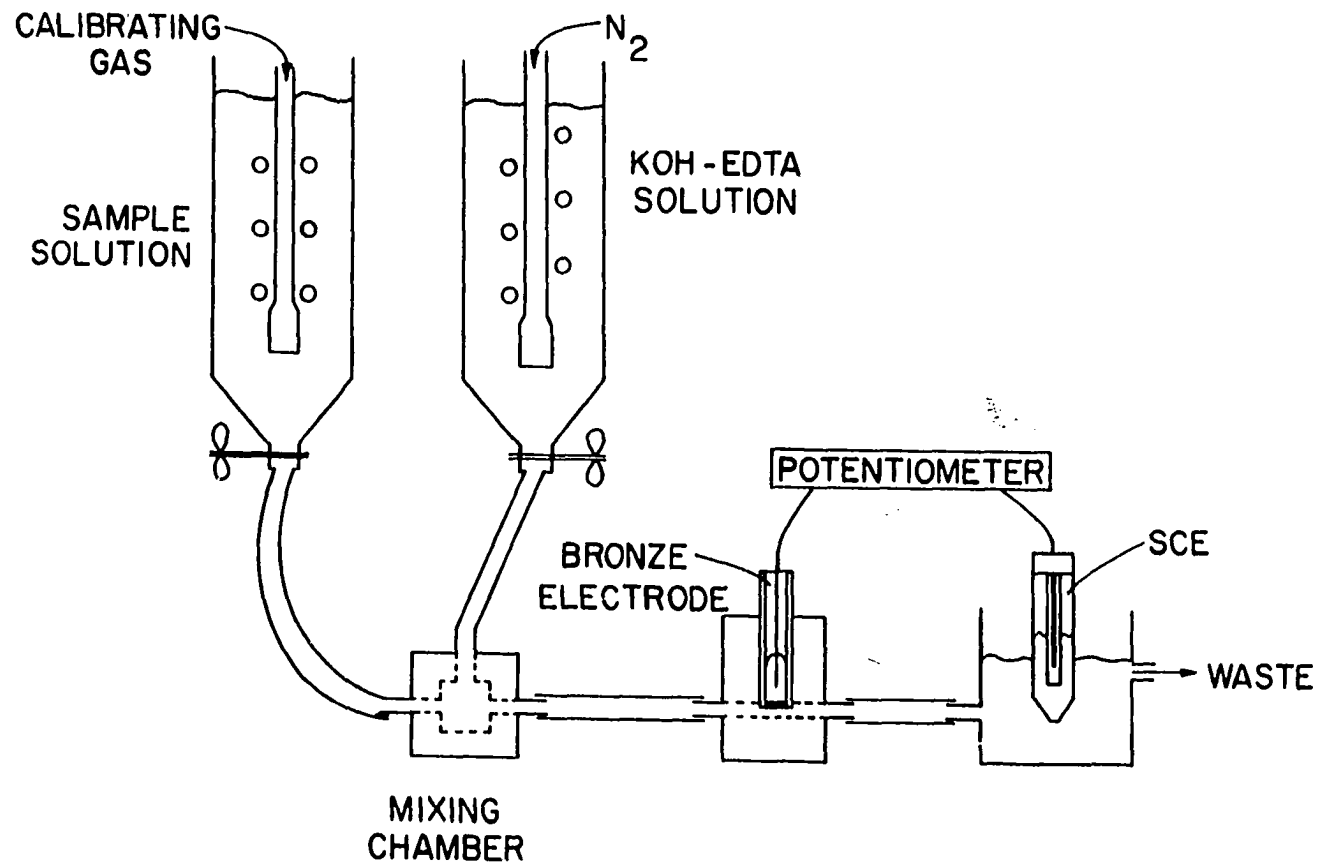
Figure 2. Flow-through system for dissolved oxygen analysis

(0.16M NH_4OH, 0.025M NH_4Cl). The metal solutions used in the quantitative determinations (Mg, Zn, Cu, and Fe) were made by dissolving a precisely weighed quantity of metal in a minimum volume of 6N HNO_3 and diluting to 0.1M with deionized water. The EDTA solutions used in the quantitative measurements were standardized potentiometrically using a $Na_{0.65}WO_3$ electrode against a calcium solution prepared by dissolving dried $CaCO_3$ in a minimum of HNO_3. The other metal solutions, used primarily to determine the general shapes of the titration curves, were made by dissolving the appropriate reagent grade chemical in deionized water.

All titrations were performed in 100-150 ml of solution which was stirred magnetically. The potential between the bronze and SCE electrodes was monitored as a function of the titrant volume. Equivalence points in the quantitative measurements were determined by the second derivative method.

The simultaneous titration of Ca^{2+} and Mg^{2+} was performed by first adjusting the pH to greater than 13 with 8M NaOH to precipitate $Mg(OH)_2$ and titrating for the Ca^{2+} end point. The precipitate was then dissolved with 6M HCl, the solution buffered to pH 10 and titrated to the Ca^{2+} + Mg^{2+} end point.

In the reverse titrations, excess EDTA was added to the solution containing the metal ion and the excess EDTA was titrated with a 0.1M $CaCl_2$ solution.

The Fe(III) titration differed from the others in that it was performed in acid solution (pH 2-3).

Metal ion response

The potentiometric response of the various bronze electrodes to a number of metals was determined in 1M NH_4OH solution. In these measurements $5\mu l$ to 10 ml aliquots of the 0.01 or 0.1M metal solution were diluted to 100-200 ml establishing formal concentrations in the range of 10^{-6} to 10^{-2}M. As in the case of the chelometric titrations all solutions were stirred magnetically.

Voltammetric studies

Voltammetric curves were obtained for the bronze electrodes using an assembly to rotate the electrode at a speed of 300 rpm. The voltage between the bronze electrode and the large area SCE electrode was scanned at a rate of 0.200 V/min. Voltage scans were generally carried out in both directions (+ to - and - to +) for each individual situation to check for significant differences in the polarization curves. The current was monitored in the $-50\mu A$ (anodic) to $+50\mu A$ (cathodic) range as a function of potential. As described earlier, the oxygen concentrations of the solutions were established by purging nitrogen, oxygen or one of the premixed gas mixtures into the system.

RESULTS AND DISCUSSION

Potentiometric Response of Cubic Na_xWO_3 to Dissolved Oxygen

Cubic sodium tungsten bronze $0.5 < x < 0.9$ was found to have a remarkable potenti-metric response to dissolved oxygen in basic solution (pH>12). Potential shifts as large as 500-550 mV were observed upon transferring Na_xWO_3 electrodes between oxygen-saturated and oxygen-free (nitrogen-saturated) solutions. Figure 3 illustrates this response in 0.1M KOH-1mM EDTA for several x values as a function of time after transfer. The potentiometric response to dissolved oxygen was found to be Nernstian-like over a concentration range of approximately two orders of magnitude from $P_{O_2} = 0.209$, $C_{O_2} = 8.3$ ppm (air saturation) to $P_{O_2} = 0.0035$, $C_{O_2} = 0.14$ ppm or lower. Analytically useful response extended from oxygen saturation $(C_{O_2} = 39$ ppm) to $P_{O_2} = 0.001$ atm (0.04 ppm). The slopes of potential-log C_{O_2} plots at $25°C$, Figures 4-6, are extremely large at pH 12-13, ranging from 90 to more than 150 mV/decade. Figure 4 illustrates the response of two $Na_{0.63}WO_3$ and two $Na_{0.81}WO_3$ electrodes to dissolved oxygen in a pH 12 solution as determined using the dilution technique. Figure 5 illustrates the response of a $Na_{0.71}WO_3$ electrode at pH 12.0, 10.5 and 9.2 as a function of oxygen concentration measured independently by voltammetry. A typical response curve for an annealed flat-surfaced crystal (x = 0.65) in 0.1M KOH-1mM EDTA using the premixed gases to establish the O_2 concentration is shown in Figure 6.

A series of time response curves for a $Na_{0.65}WO_3$ electrode at different oxygen concentrations is shown in Figure 7. In this study the electrode was transferred from an air saturated KOH solution into one of
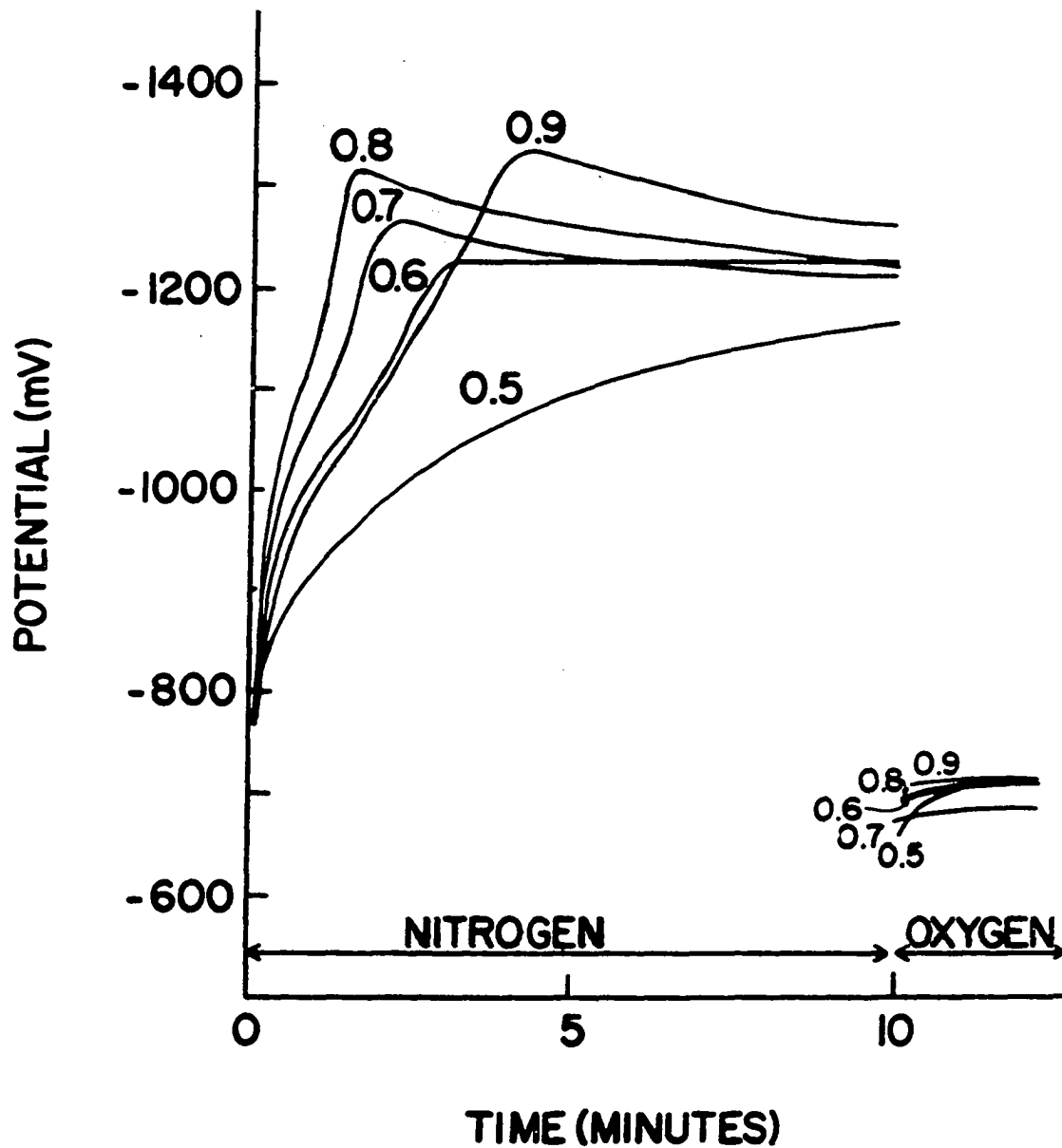
Figure 5. Time response of Na_xWO_3 electrodes in nitrogen and oxygen-saturated 0.1M KOH-1mM EDTA solutions as a function of x value
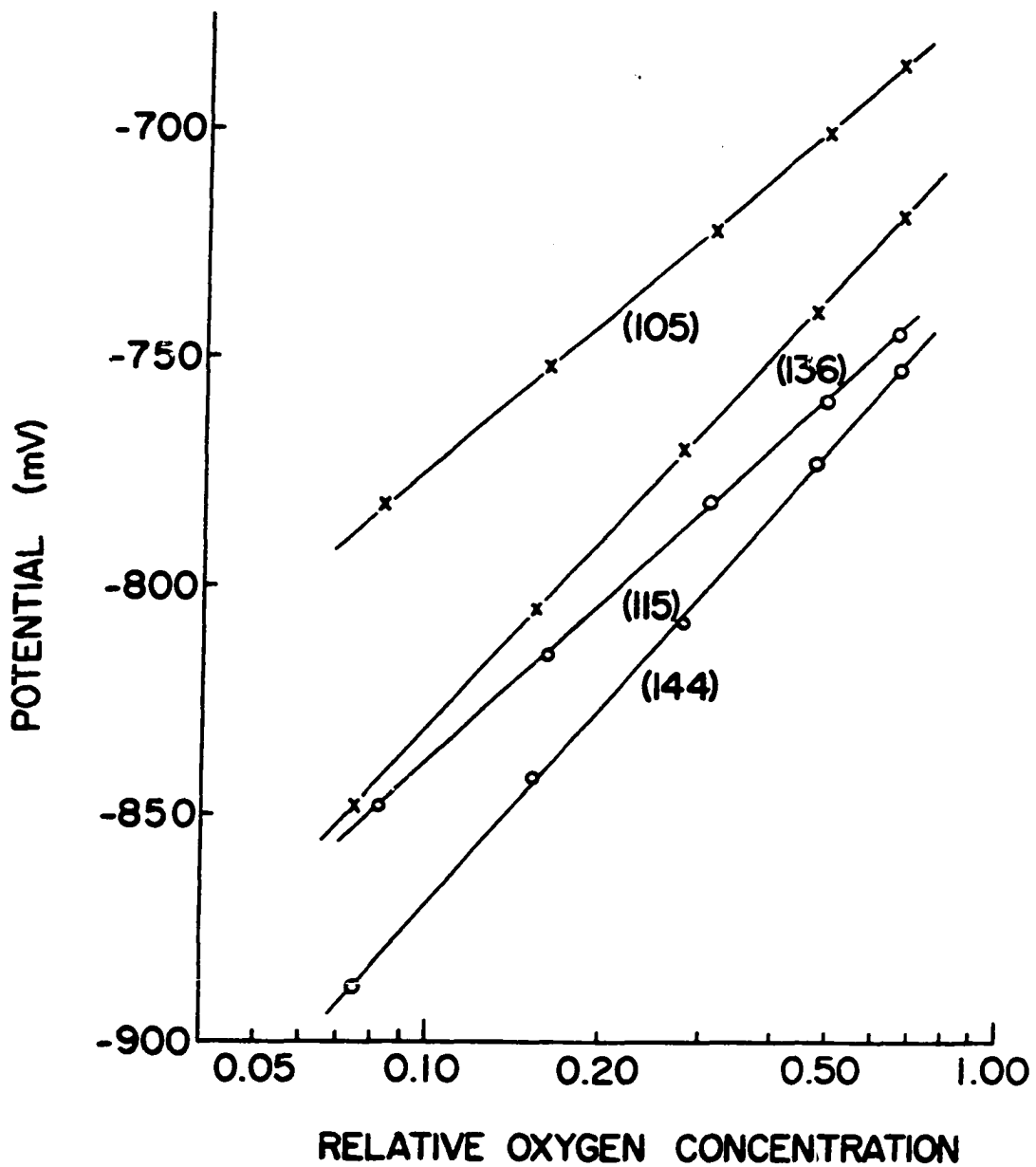
Figure 4. Oxygen response at pH-12 by dilution technique. Values in
parentheses are slopes in mV/decade. Concentration relative
to saturation with pure O_2

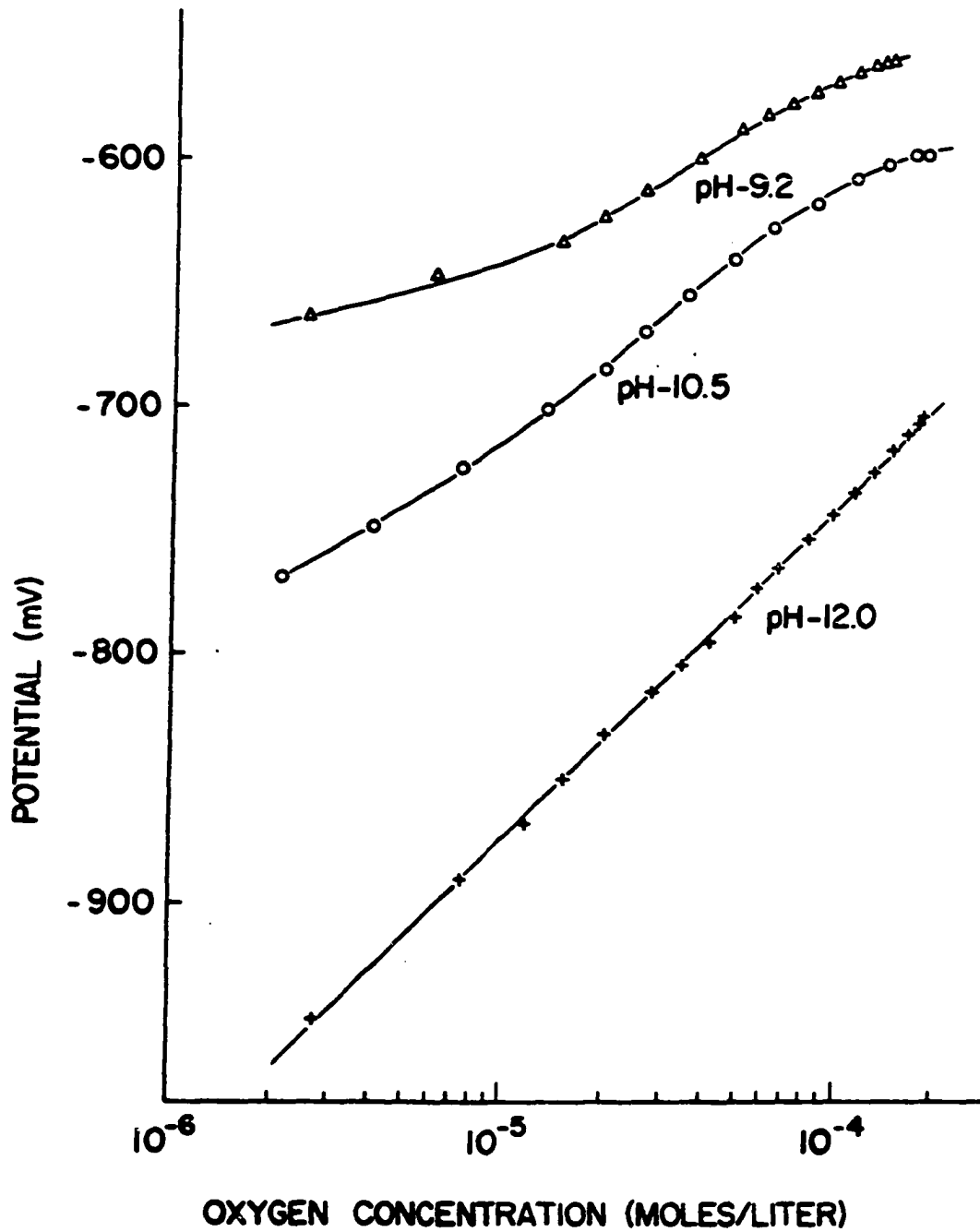(x) $Na_{0.63}WO_3$ electrodes   (o) $Na_{0.81}WO_3$ electrodes

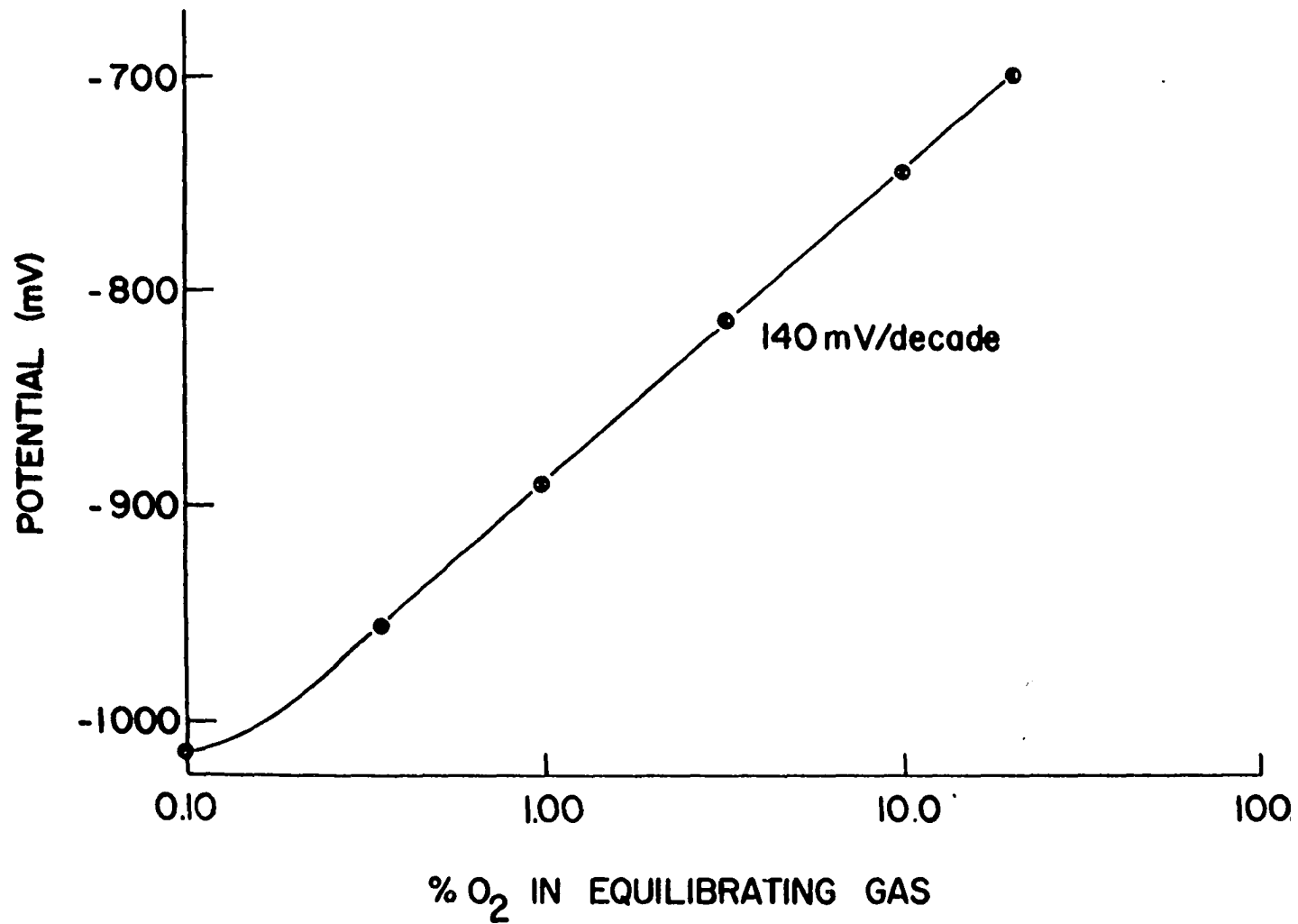Figure 5. Oxygen response of the $Na_{0.71}WO_3$ electrode at several pH values

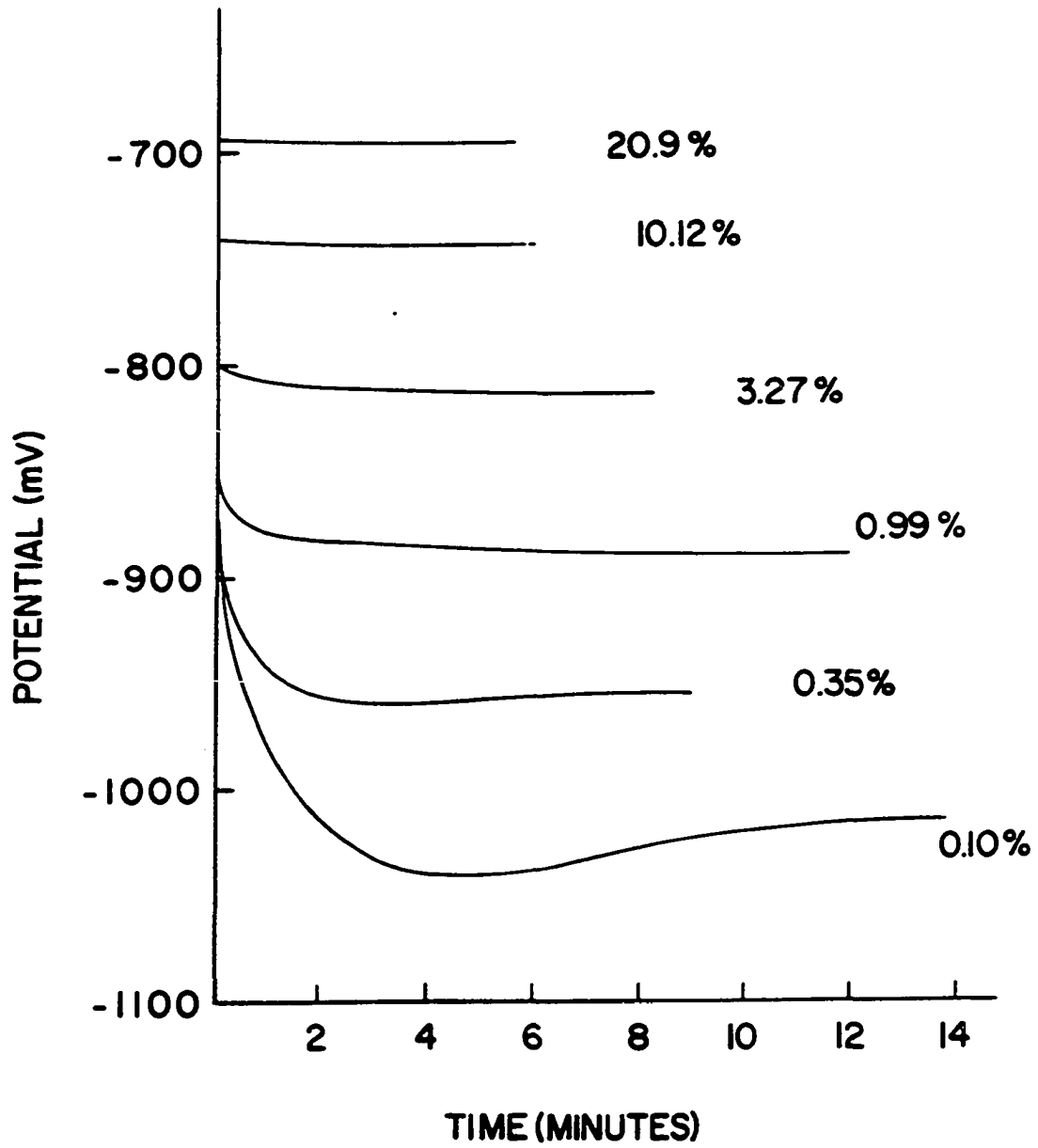Figure 6. Oxygen response of $Na_{0.65}WO_3$ electrode in 0.1M KOH-1mM EDTA using N_2-O_2 mixtures

Figure 7. Time response of $Na_{0.65}WO_3$ electrode

lower O_2 concentration equilibrated with one of the premixed N_2-O_2 gases. At the higher O_2 concentrations (P_{O_2} >0.01 atm) a stable potential was reached in 2-3 minutes but at lower concentration significantly longer time was required and a minimum was observed before the equilibrium potential was reached. Consistent and rapid stirring was found to be an essential factor both in maintaining a stable potential at a given O_2 concentration and in obtaining linear potential vs. log-C calibration plots. The bronze electrode potential in unstirred solutions drifted in a negative direction, and in very dilute oxygen solutions the potential stabilized at a value corresponding to a completely deoxygenated system indicating a depletion of oxygen in the vicinity of the electrode surface.

Variations in the slopes of the response curves and the potential established in an air-saturated solution (referred to as the "air potential") were found to be considerable. These variations were apparent not only between cubic sodium tungsten bronzes of differing x values but also between electrodes cut or chipped from the same parent crystal. In fact, the day-to-day response of a given electrode could exhibit variations as wide as those between electrodes of different x values. As an example, a $Na_{0.65}WO_3$ electrode exhibited response slopes of 163, 116, 131 and 105 mV/decade over a three day period. The corresponding potentials in air-saturated solution were 641, 701, 702 and 678 mV. These variations are considered to be due to changes in the bronze surface characteristics from repeated contact with the basic solutions. Visible etching and pitting of the electrode surface was generally encountered after prolonged use.

Somewhat less electrode to electrode variability was encountered

with a series of electrodes which had been annealed at 650°C in an argon atmosphere to insure homogeneity and cut with flat regular surfaces. A comparison between these and a series of non annealed crystals with irregular surfaces is shown in Table 3. The only apparent difference

Table 3. Comparison of electrode variability

	Annealed, flat surface	Not annealed, irregular surface
x value	0.65	0.63
No. of electrodes	16	8
No. of observations	20	15
Average air potential (mV)	-695 ± 22^a	-712 ± 42
Average slope (mV/decade)	120 ± 13	124 ± 14

[a]One standard deviation

in this comparison was the significantly lower variability of the air potential for the annealed, flat-surfaced electrodes. The annealed, flat-surfaced electrodes, moreover, were found to respond more rapidly to a change in O_2 concentration and Nernstian-like response generally extended to lower oxygen concentration.

Sodium tungsten bronzes having x values in the range 0.60-0.70 appeared to show the best response to dissolved oxygen. Electrodes of lower x value (0.5) usually responded extremely slowly and for those of higher x value (0.8) the calibration plots were often nonlinear.

The addition of EDTA at a concentration of 0.5 to 1mM was found to be necessary to complex traces of easily reducible metals which interfere with the oxygen response. Without the EDTA, the response would hardly extend to 1 ppm dissolved oxygen. Figure 8 shows the response of a $Na_{0.62}WO_3$ electrode when transferred between O_2-saturated and O_2-free 0.1M KOH solutions, illustrating the effect of EDTA at a concentration of 1mM. The EDTA extended the potentiometric range approximately 200 mV which corresponds to a factor of nearly 40 in oxygen concentration.

The temperature coefficient, dE/dT, for an annealed flat-surface $Na_{0.65}WO_3$ electrode in 0.1M KOH-1mM EDTA at P_{O_2} = 0.0327 atm (3.96 X 10^{-5}M dissolved O_2) was found to be -7.04 mV/$^\circ$C over a temperature range of 3-35°C (Figure 9). Only a small portion (-0.98 mV/$^\circ$C) of this temperature coefficient may be attributed to the change in oxygen solubility as a function of temperature. This value was estimated from the expression

$$\frac{0.1984T}{n} \left(\frac{d \log a_i}{dT}\right)$$

in which T is the temperature, n a constant depending on the slope of potentiometric response, and a_i the activity of the dissolved oxygen (83). Based on the observed 120 mV/decade oxygen response 0.5 was chosen for n. The value for $d(\log a_i)/dT$ was calculated from oxygen solubilities at 20°C and 30°C, 43.39 and 35.88 ppm respectively (84).

Analytically useful dissolved oxygen response was limited to strongly basic solution. At pH 10.5 or less, the response deteriorated and the potential-log C relationship became nonlinear (Figure 5). In acid solution (0.1M $HClO_4$) only minimal response was observed (20-30 mV/decade) for 0.01 atm<P_{O_2}<1 atm. Potassium hydroxide solutions appeared superior
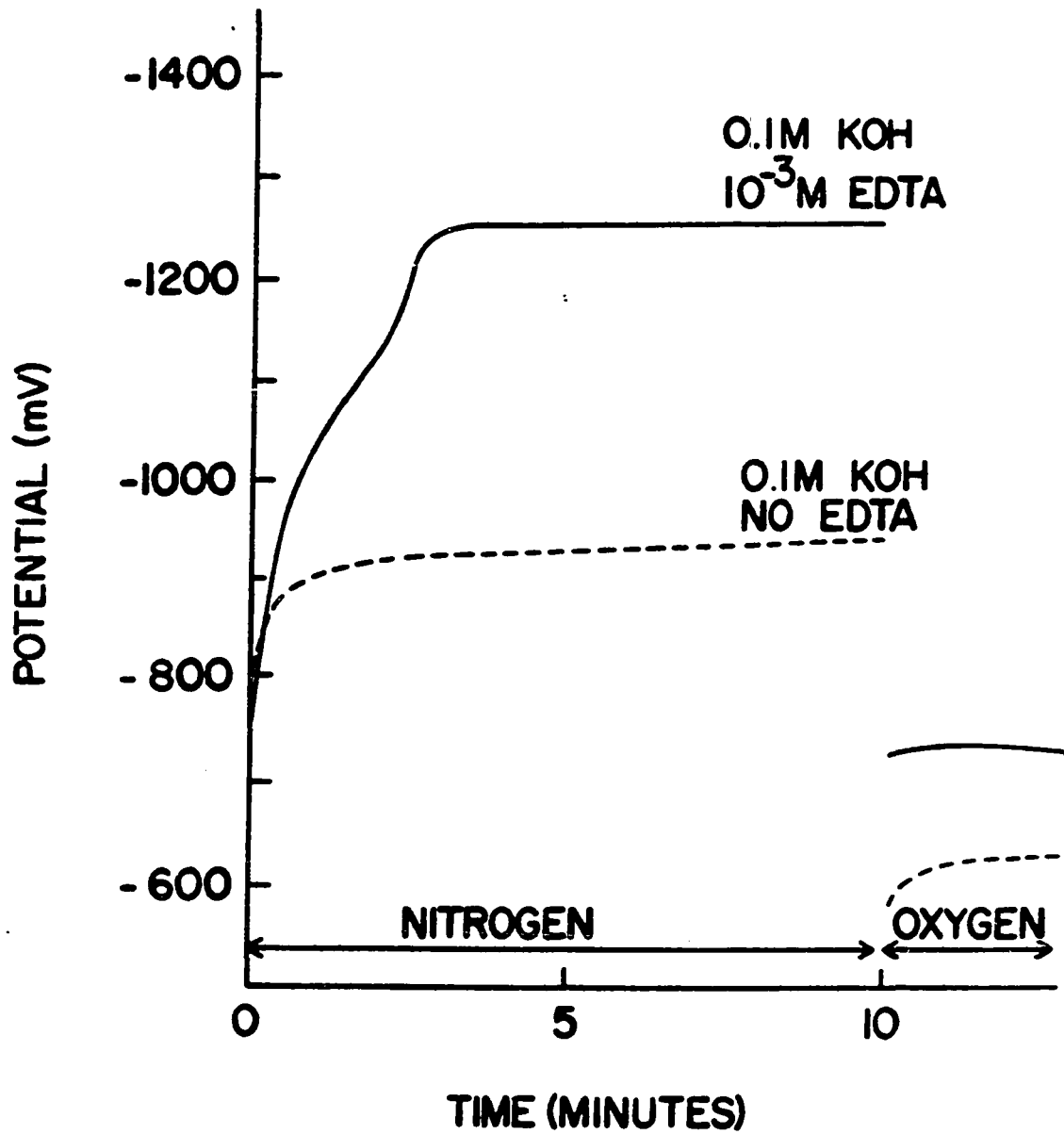
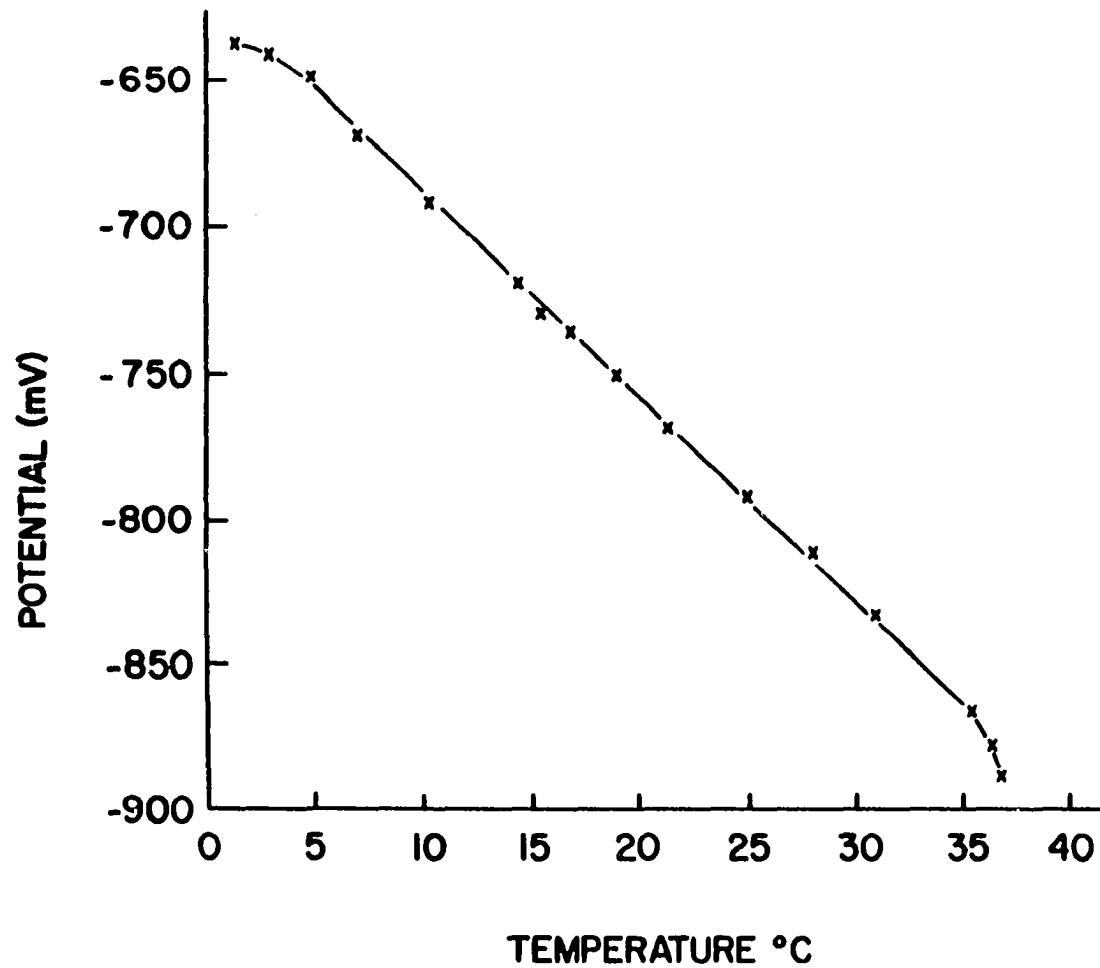Figure 8. Effect of EDTA on the response of $Na_{0.63}WO_3$ electrode in nitrogen and oxygen-saturated 0.1M KOH solution

Figure 9. Effect of temperature on response of $Na_{0.65}WO_3$ electrode

to both NaOH and LiOH. The electrode response in NaOH was often found
to be sluggish and the linear dependence did not extend to as low oxygen
concentrations as in KOH. In LiOH little response to dissolved oxygen
was found for electrodes having x values of 0.6 or less (compare Figures 3
and 10).

<div align="center">

Application of the Na_xWO_3 Electrode

to the Determination of Dissolved Oxygen

</div>

The cubic sodium tungsten bronze electrode was found to perform very
well as a selective-potentiometric electrode for the determination of
dissolved oxygen in basic solution. The results of 20 series of analyses
using 16 annealed, flat-surface $Na_{0.65}WO_3$ electrodes are presented in
Table 4. For each series the electrode potentials were measured in
0.1M KOH-1mM EDTA saturated sequentially with the N_2-O_2 gas mixtures listed
in Table 2. The potentials established in air-saturated and 0.99% satu-
rated solutions were used to provide a two-point calibration of the form,
log C = m(mV) + constant, from which the partial O_2 pressures of the other
four gases were determined.

Analyses at 10.12 and 3.27% oxygen partial pressure exhibited no
systematic error and had relative standard deviations of approximately
±5%. Analyses at 0.35 and 0.10% appeared to be systematically low with
deviations of 14 and 21% from the reported value and relative standard
deviations of similar magnitude. Significant improvement in accuracy in
this lower concentration range was achieved when calibrations were made
at the same order of magnitude as the unknown. Also presented in Table 4
are the results of the analyses performed on the 0.35% O_2 gas mixture when
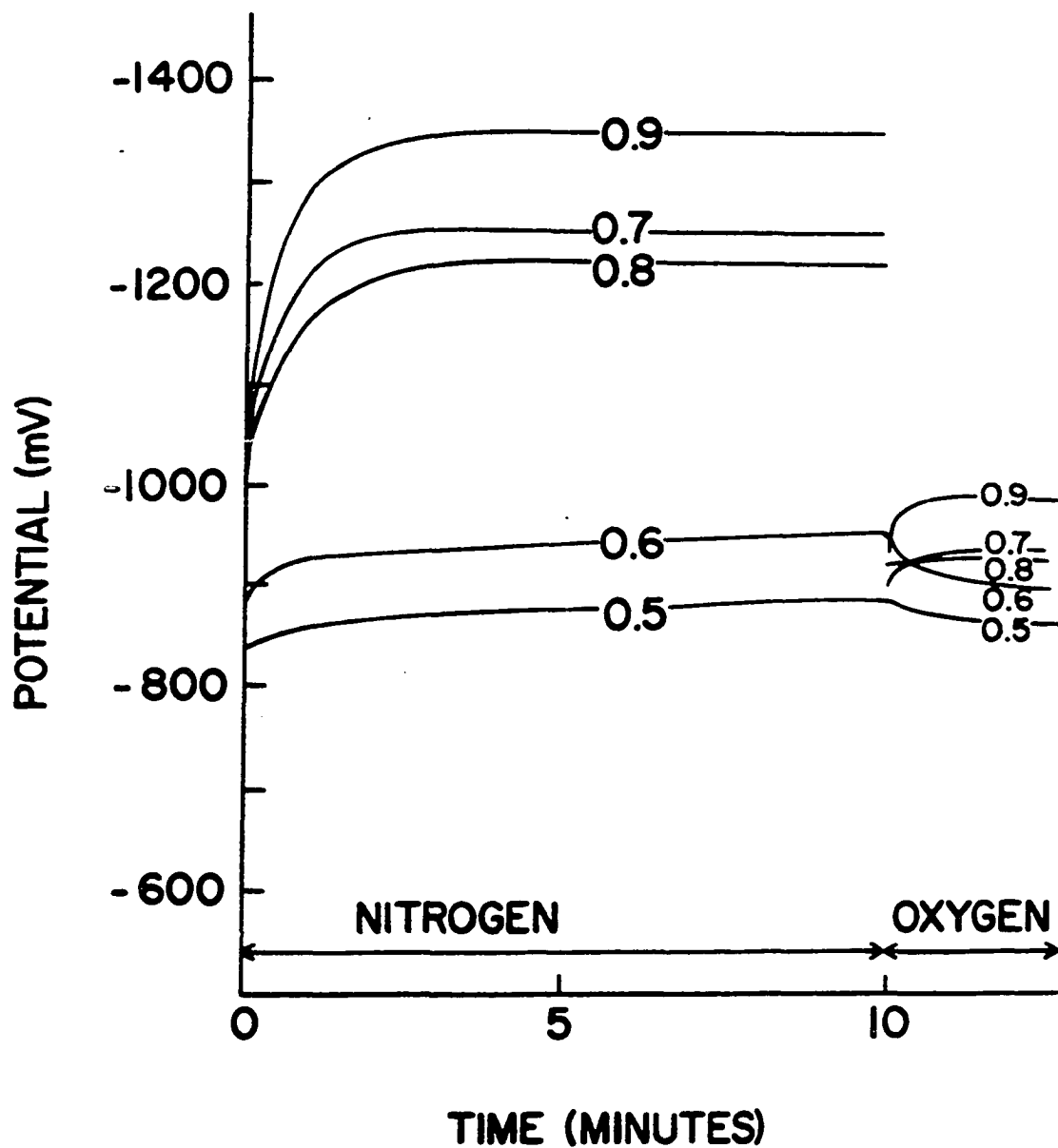the two-point calibration was done with the 0.99 and 0.10% O_2 gas mixtures.

Figure 10. Time response of Na_xWO_3 electrodes in nitrogen and oxygen-
saturated 0.1M LiOH-1mM EDTA solutions as a function of
x value

Table 4. Results of oxygen determinations using the $Na_{0.65}WO_3$ electrode

Electrode	Date	Air potential (mV)	Slope (mV/decade)	Measured O_2 partial pressure (% O_2 saturated)				
				10.12[a]	3.27[a]	0.35[a]	0.10[a]	0.35[b]
680	7/26	-689	119	9.76	3.40	0.295	0.068	0.351
681	7/26	-689	105	9.54	3.21	0.306	0.087	0.328
681	7/27	-718	116	9.81	3.55	0.295	0.081	0.327
682	7/26	-690	118	9.95	3.30	0.286	0.072	0.335
683	7/26	-705	110	10.07	3.06	0.283	0.106	0.305
685	7/26	-678	118	10.91	3.22	0.317	0.092	0.330
686	7/27	-700	123	10.91	3.22	0.281	0.072	0.329
690	8/03	-698	116	10.05	3.73	0.397	0.061	0.469
690	8/03	-708	126	10.80	3.50	0.303	0.064	0.367
690	8/04	-711	117	9.85	3.27	0.255[c]	0.029[c]	-

[a]Calibration at 20.9 and 0.99% O_2 partial pressure

[b]Calibration at 0.99 and 0.10% O_2 partial pressure

[c]Result discarded from statistical analysis

35

Table 4. (Continued)

Electrode	Date	Air potential (mV)	Slope (mV/decade)	Measured O_2 partial pressure (% O_2 saturated)				
				10.12^a	3.27^a	0.35^a	0.10^a	0.35^b
691	8/04	-717	159	9.65	3.05	0.384	0.108	0.371
691	8/08	-664	131	9.76	3.25	0.253	0.067	0.310
692	8/08	-622	96	9.81	3.12	0.323	0.077	0.363
693	8/07	-695	133	9.88	3.36	0.283	0.086	0.305
694	8/07	-678	128	9.84	3.24	0.258	0.065	0.319
695	8/07	-712	111	9.55	3.04	0.425^c	0.272^c	-
696	8/07	-717	123	10.73	3.69	0.298	0.065	0.361
697	8/07	-700	108	9.86	3.23	0.273	0.084	0.308
698	8/08	-696	112	10.26	3.50	0.249	0.053	0.335
699	8/07	-707	119	10.14	3.40	0.325	0.103	0.321
Average		-694.7	119.5	10.056	3.317	0.301	0.078	0.341
1 std. deviation		±22.3	±12.9	±0.439	±0.199	±0.039	±0.016	±0.038
				(4.4%)	(6.0%)	(13.1%)	(20.7%)	(11.3%)

The systematic error was reduced from 14 to 2.5 per cent but the precision of analysis was not significantly improved.

The wide variation in response slopes between electrodes had little or no bearing on the success of an oxygen determination; results were similar for electrodes 691 and 692 with slopes of 159 and 96 mV/decade as well as for electrodes having intermediate values. The variability of the response of a given electrode over a period of time, however, could cause considerable analytical error if the electrode was not calibrated soon after sample measurement. The effects of temperature variation and stirring have already been discussed, and a successful analysis would also depend upon the control of these variables.

Excellent oxygen response was also obtained in both tap water and lake water when adjusted to 0.1M in KOH and 1mM in EDTA (Figure 11). The impurities normally found in such samples are not expected to cause any problems in the determination of dissolved oxygen. Calcium and Fe(III) at concentrations below that of the EDTA (1mM) cause little interference in the oxygen response. The only effect noted was a slight shift in potential in the positive direction (Figures 12 and 13). The oxygen calibration curves remained linear for 0.001 atm$<P_{O_2}<0.10$ atm. At calcium concentrations in excess of that of the EDTA however, an excessive positive shift was noted and the calibration curve lost its linearity. This shift is not considered to be due to the calcium ion itself but to the reaction of calcium with the EDTA thereby decreasing its concentration to a level insufficient to adequately chelate traces of reducible metals which cause the shift. Increasing the EDTA concentration above that of the Ca^{2+} should eliminate this problem. Copper(II) and silver(I) were found to
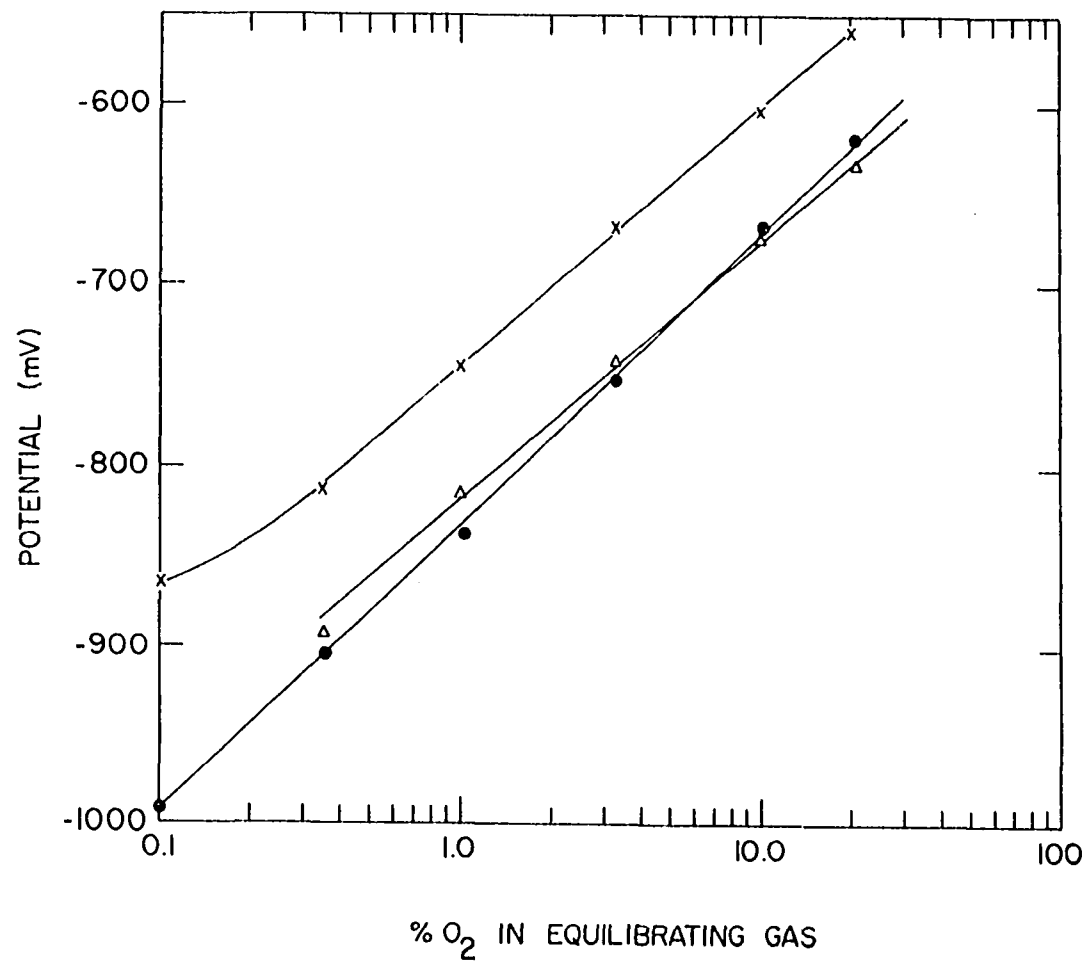
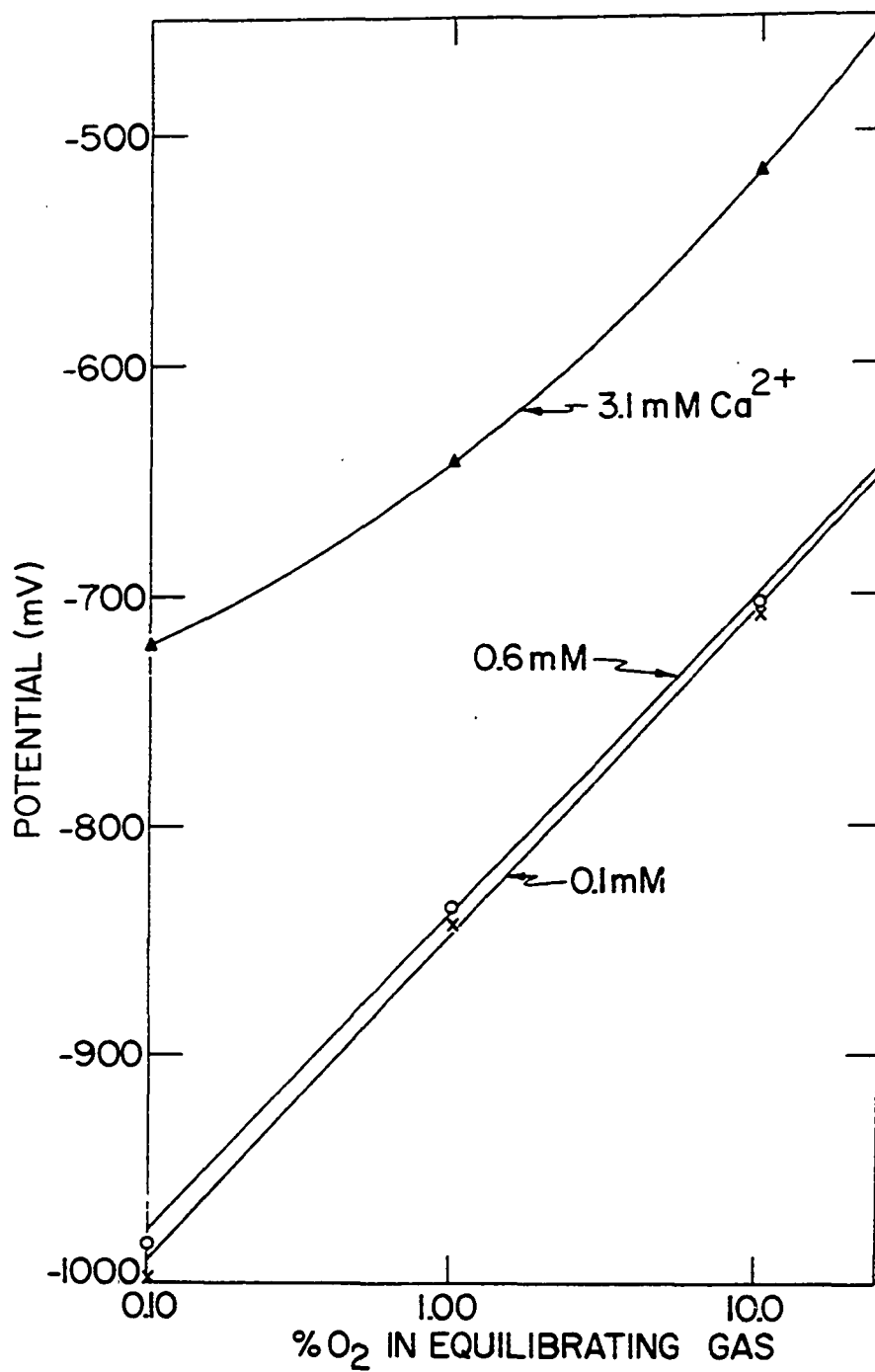Figure 11. Oxygen response in tap (△) and lake (x) (●) water when adjusted to 0.1M KOH-1mM EDTA

Figure 12. Effect of Ca^{2+} on the oxygen response of the $Na_{0.65}WO_3$
electrode in 0.1M KOH-1mM EDTA

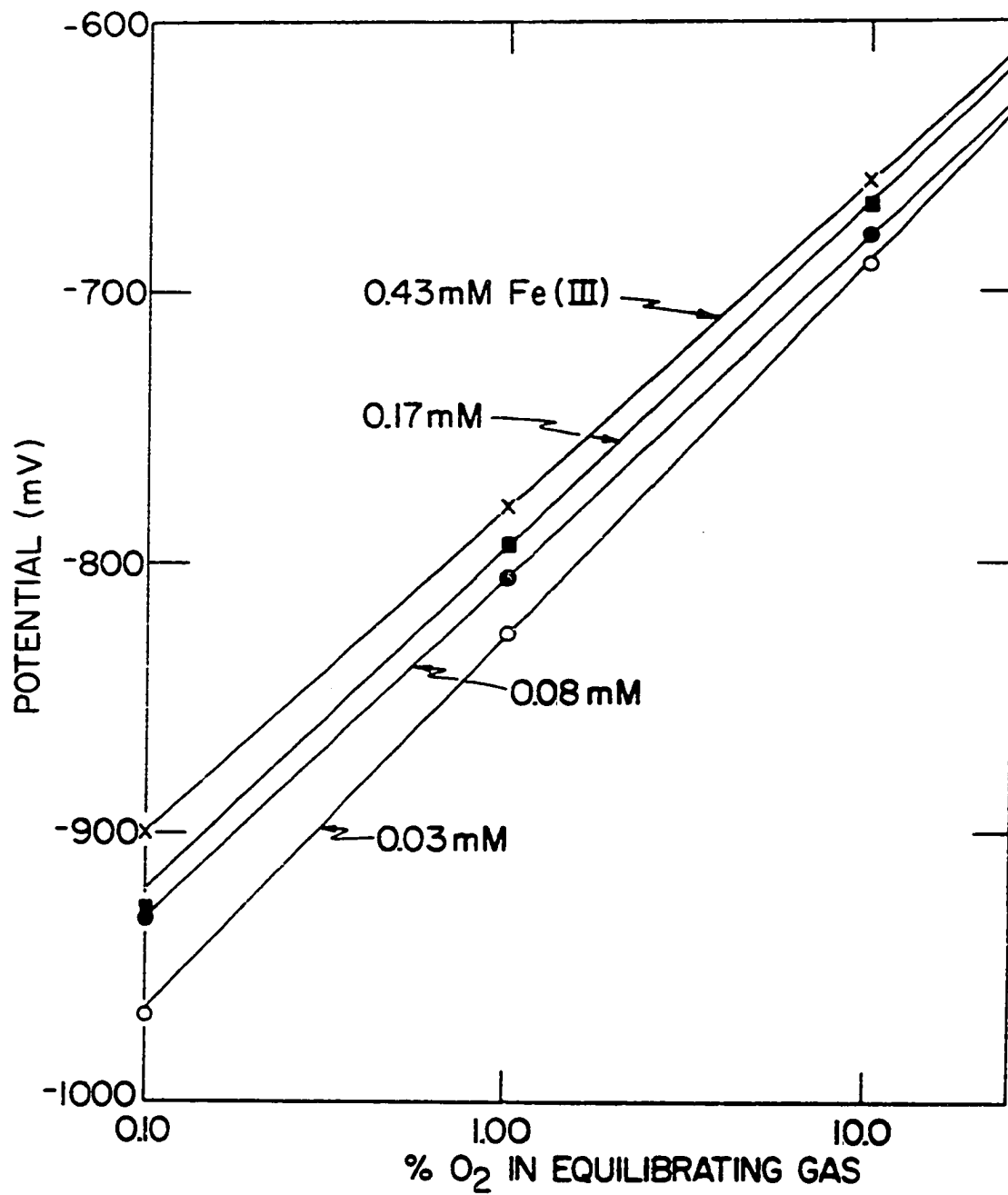Figure 13. Effect of Fe(III) on the oxygen response of the $Na_{0.65}WO_3$ electrode in 0.1M KOH-1mM EDTA

interfere much more seriously (Figures 14 and 15). As little as

0.03mM Cu(II) caused enough positive potential shift to destroy the

linearity of response below P_{O_2} = 0.01 atm. The oxygen response above

P_{O_2} = 0.01 atm however, was not seriously affected at copper concentra-

tions below 0.02mM. Trace silver (0.008mM) resulted in very large

positive potential shifts and non-linear response and actually enhanced

the oxygen response from approximately 120 mV/decade to 150-220 mV/decade.

Visible deposits of metallic silver were observed on the Na_xWO_3 electrode,

and the radical change in oxygen response is attributed to the subsequent

change in the electrode surface characteristics.

The application of the Na_xWO_3 electrode for the determination of

dissolved oxygen in a flow-through system was demonstrated using several

modifications of the apparatus shown in Figure 2. System specifications

are listed in Table 5 and the dissolved oxygen responses are illustrated

in Figure 16. Linear calibration curves with slopes between 100-130

mV/decade were generally realized for 0.01 atm$<P_{O_2}<$0.209 atm. The

10^3 cm/min linear flow past the bronze electrode appeared to provide

sufficient agitation to establish a potential representative of the oxygen

concentration. Attempts to measure dissolved oxygen below P_{O_2} = 0.01 atm

however, were generally unsuccessful, probably due to the diffusion of

atmospheric oxygen into the system. Improved system design should correct
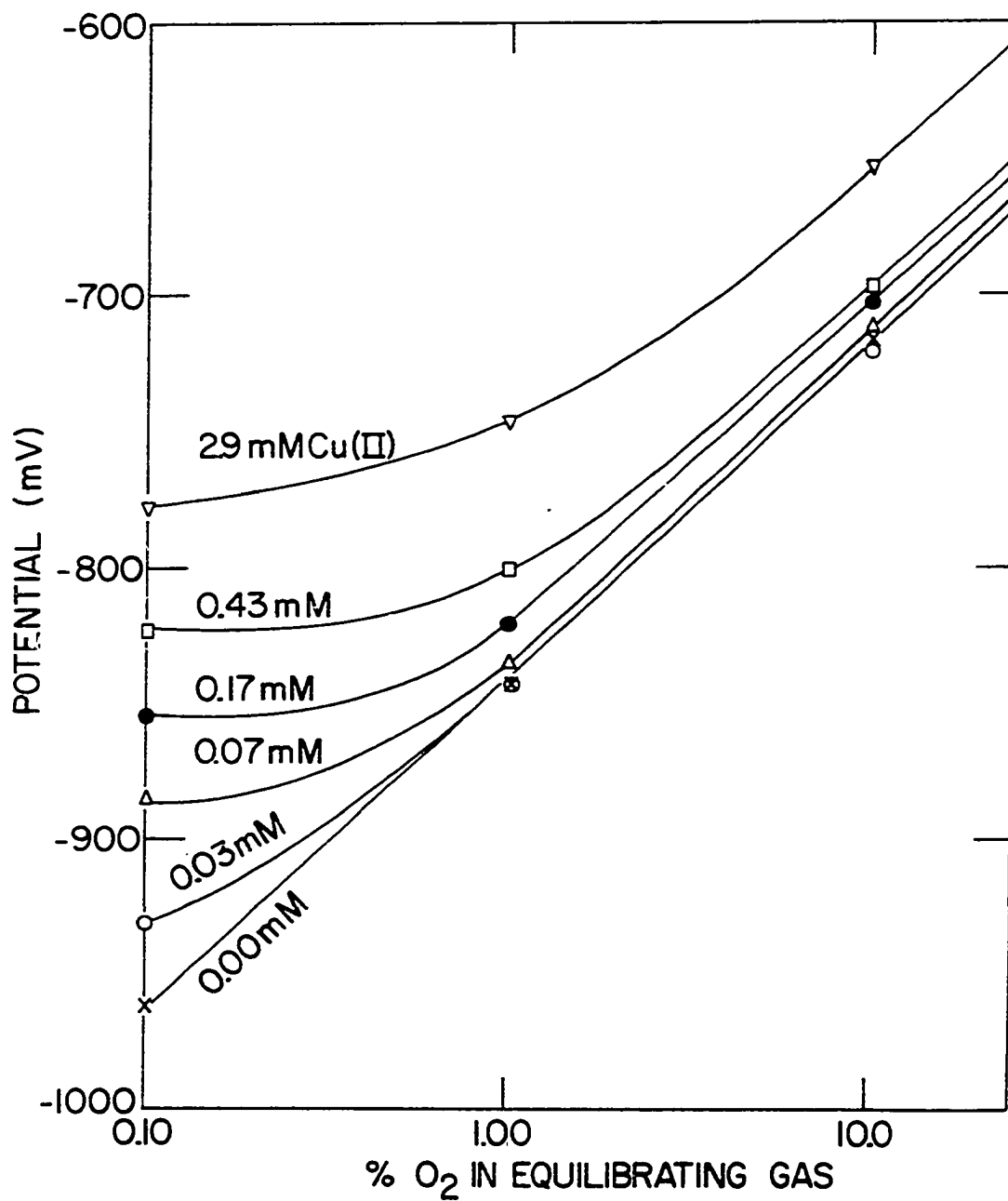
this limitation.

Figure 14. Effect of Cu(II) on the oxygen response of the $Na_{0.65}WO_3$ in 0.1M KOH-1mM EDTA
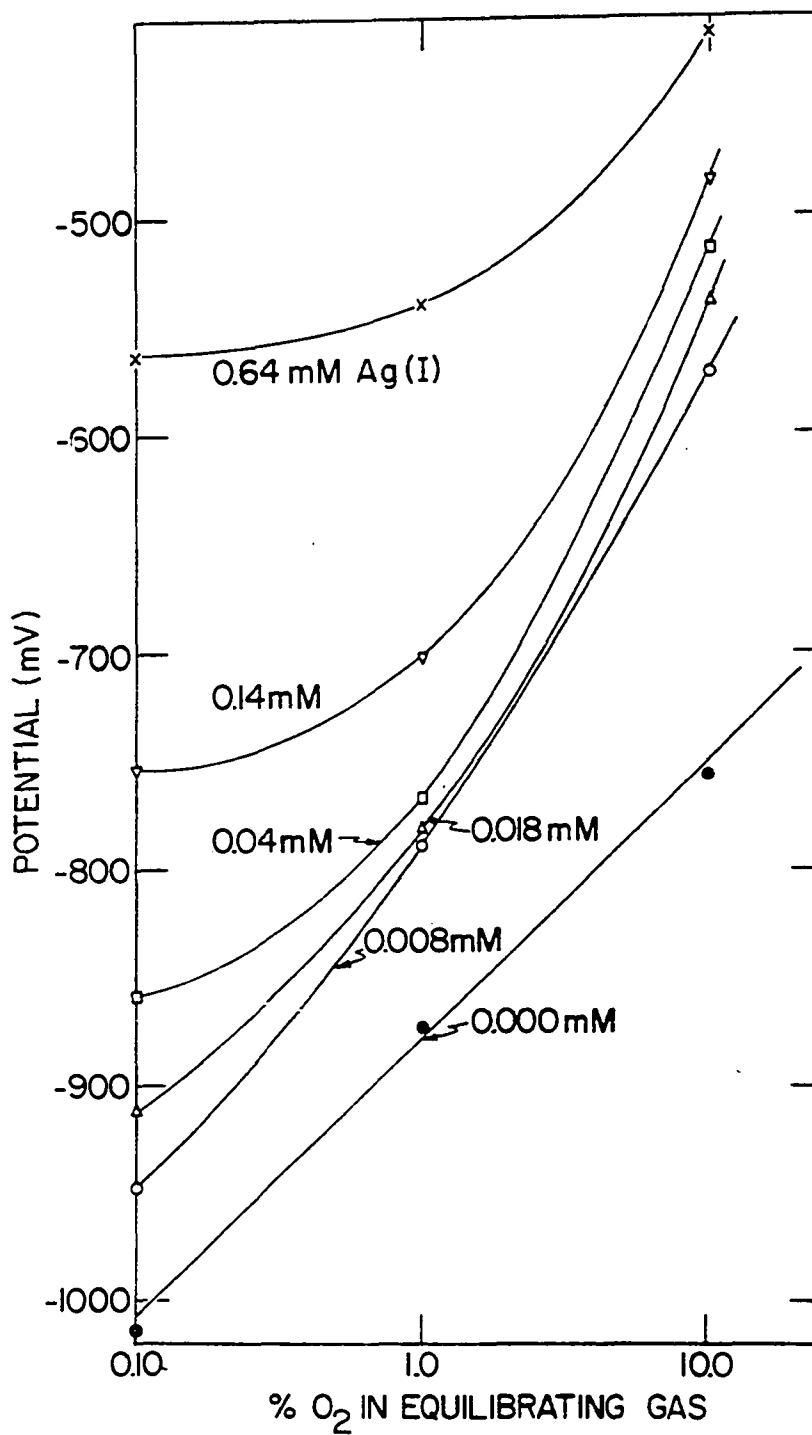
Figure 15. Effect of Ag(I) on the oxygen response of the $Na_{0.65}WO_3$ in 0.1M KOH-1mM EDTA

Table 5. Flow-through system specifications

System	Reagent	Flow rate (ml/min) Reagent	Sample	Mixing chamber volume (ml)	Linear flow past electrode (cm/min)
I	1M KOH 10mM EDTA	10^a	20	30	10^3
II	1M KOH 10mM EDTA	10^a	20	10	10^3
III	0.5M KOH 5mM EDTA	13^b	47	1	10^3

[a] Gravity feed

[b] Pressure feed

Response of Other Tungsten Bronzes

to Dissolved Oxygen

The excellent oxygen response appears quite unique to the cubic sodium tungsten bronzes. The dissolved oxygen responses of a number of other highly conducting alkali metal tungsten bronzes in 0.1M KOH-1mM EDTA are presented in Figure 17. Little or no response was observed for the hexagonal potassium and rubidium tungsten bronzes. The response of cubic lithium bronze was marginal (≈ 30 mV/decade) while significant responses were observed for tetragonal potassium bronze, $(K_{0.5}WO_3)$, (≈ 70 mV/decade) and hexagonal cesium bronze (≈ 80 mV/decade). These responses were much inferior to that of the cubic sodium tungsten bronze. They were extremely slow, much less reproducible, and exhibited nonlinear potential-log C relationships.
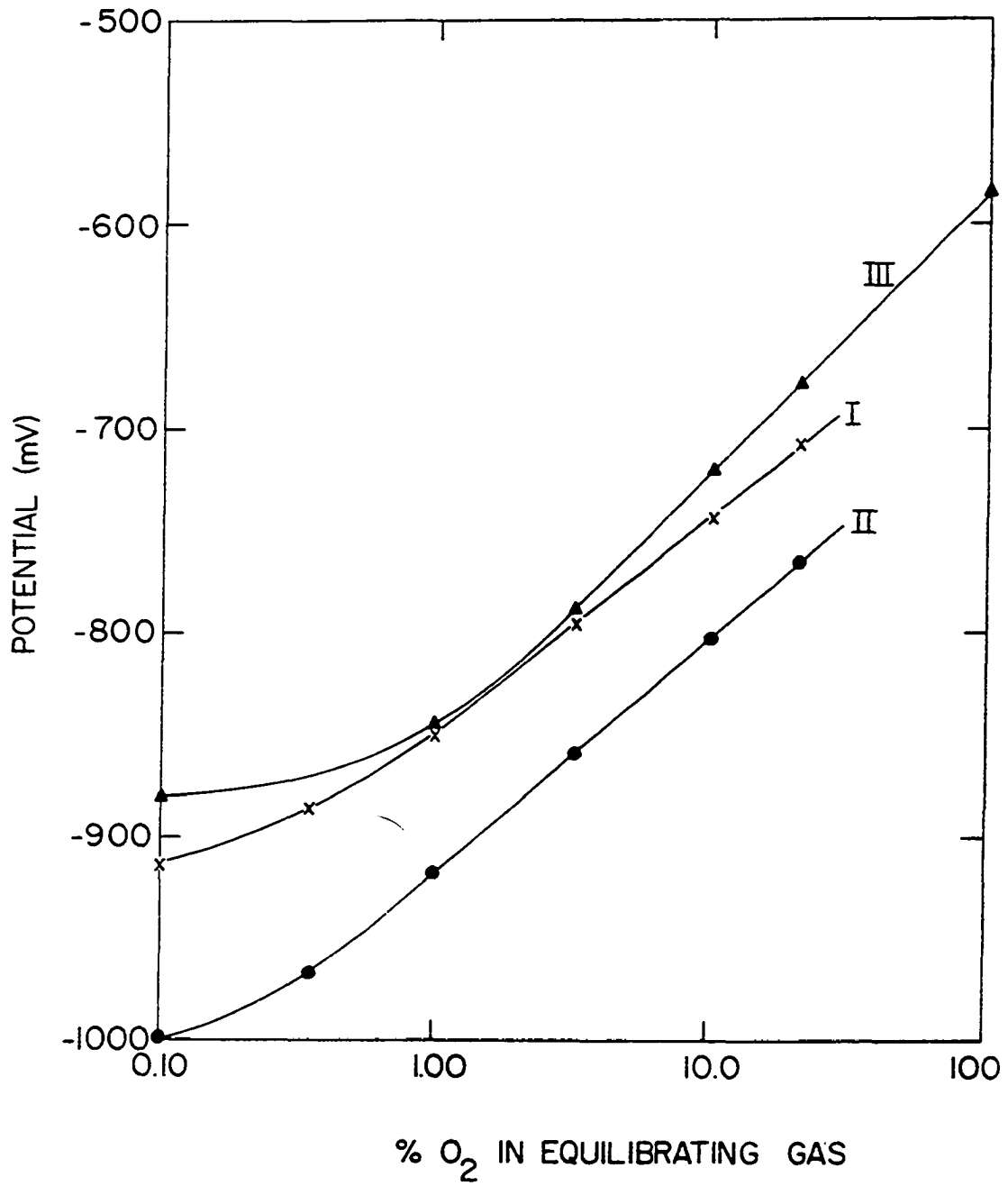
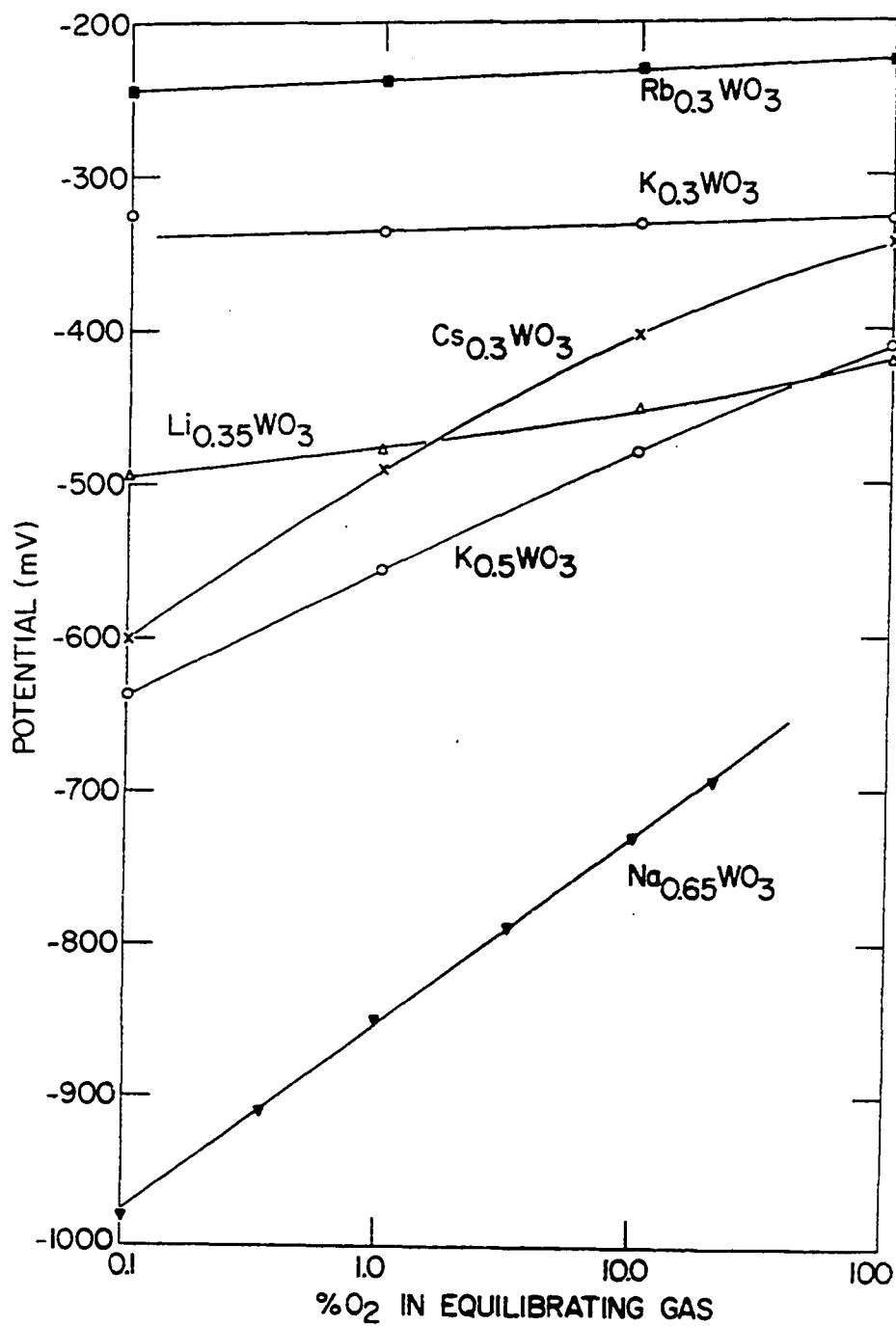Figure 16. Oxygen response in flow-through systems. See Table 5

Figure 17. Oxygen response of the hexagonal $M_{0.3}WO_3$, cubic $Li_{0.35}WO_3$, tetragonal $K_{0.5}WO_3$ and cubic $Na_{0.65}WO_3$ electrodes in 0.1M KOH-1mM EDTA

Application of the Na_xWO_3 Electrode

in Chelometric Titrations

The large negative potential shift observed for the Na_xWO_3 electrode

when EDTA was added to 0.1M KOH (Figure 8) suggested the possibility of

using the electrode to potentiometrically detect the end point in metal-

EDTA titrations in basic solution. Titrations involving a number of

metals with high metal-EDTA stability constants were performed in 0.1 to

1M NH_4OH (pH 10-11) and potentiometrically followed with a $Na_{0.65}WO_3$

electrode. Ammonium hydroxide was chosen as the titration medium over

an alkali metal hydroxide in view of the increased solubility of a number

of metal salts.

Direct titrations of Ca and Mg at pH 10 (0.16M NH_4OH-0.03M NH_4Cl)

are shown in Figures 18 and 19. End point-potential shifts of -50 to

-100 mV were realized when 2.5 millimoles of metal were titrated with

0.1M EDTA. Analytically useful curves were obtained for as little as 0.01

millimole of metal when titrated with 10^{-3}M EDTA. It was also found

possible to accurately determine both calcium and magnesium in a mixture

by titrating for Ca at pH 13 where Mg was precipitated as the hydroxide

and then titrating for Ca + Mg at pH 10 where Mg is soluble. Figure 20

illustrates this titration curve. Excellent titration curves were also

obtained for Ni(II), Mn(II), Cu(II), Cd(II) and Co(II) in ammoniacal

solution (Figures 21-23).

Back titrations of excess EDTA with calcium gave extremely good

potentiometric end points when monitored with a $Na_{0.65}WO_3$ electrode

(Figures 22-25). Reverse titrations involving Zn(II) and Pb(II) exhibited

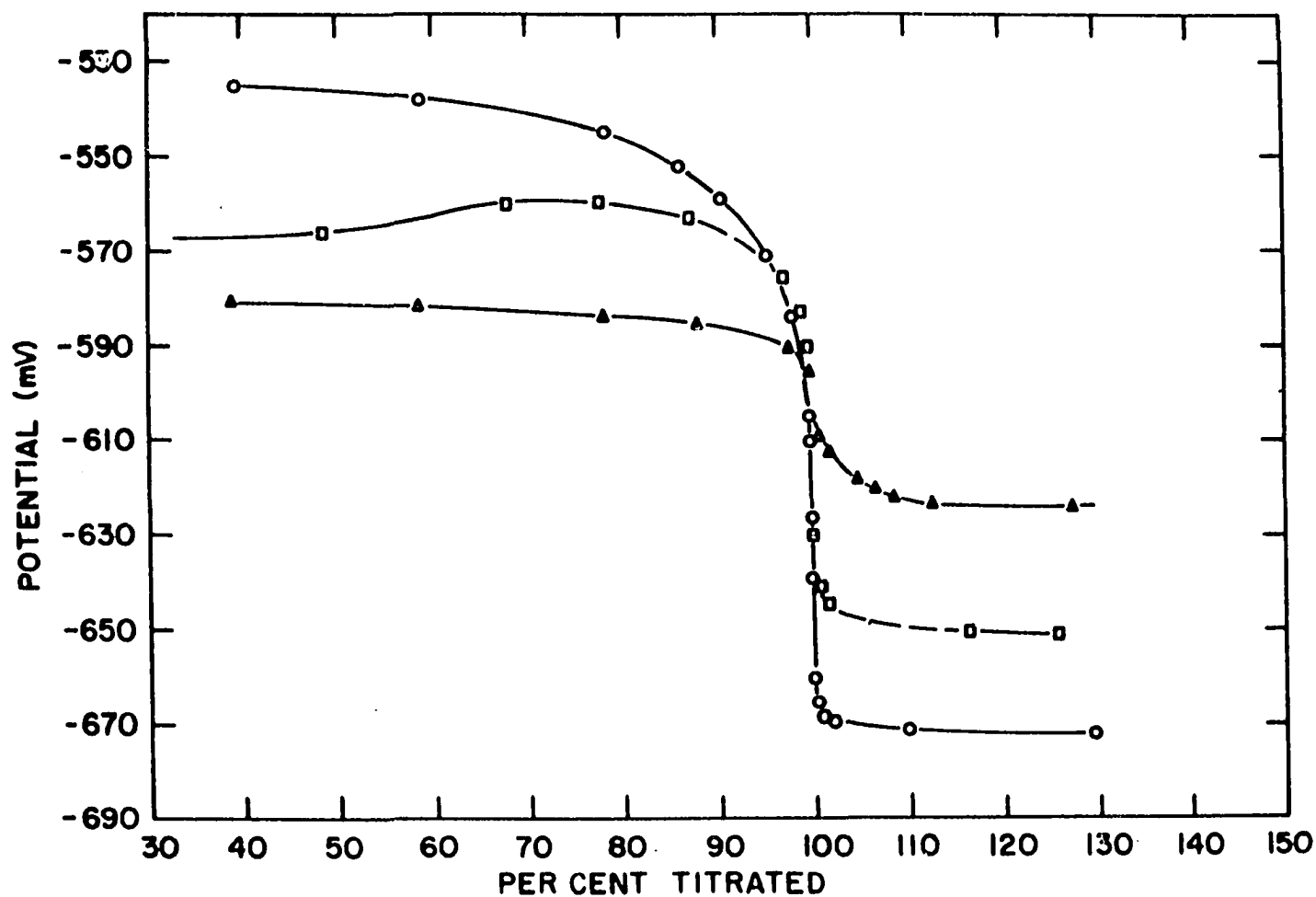significantly sharper potential breaks at the end point than the corres-

Figure 18. Calcium titrations with $Na_{0.65}WO_3$ electrode at pH 10. (O) 100 mg Ca(II) with 10^{-1}M EDTA

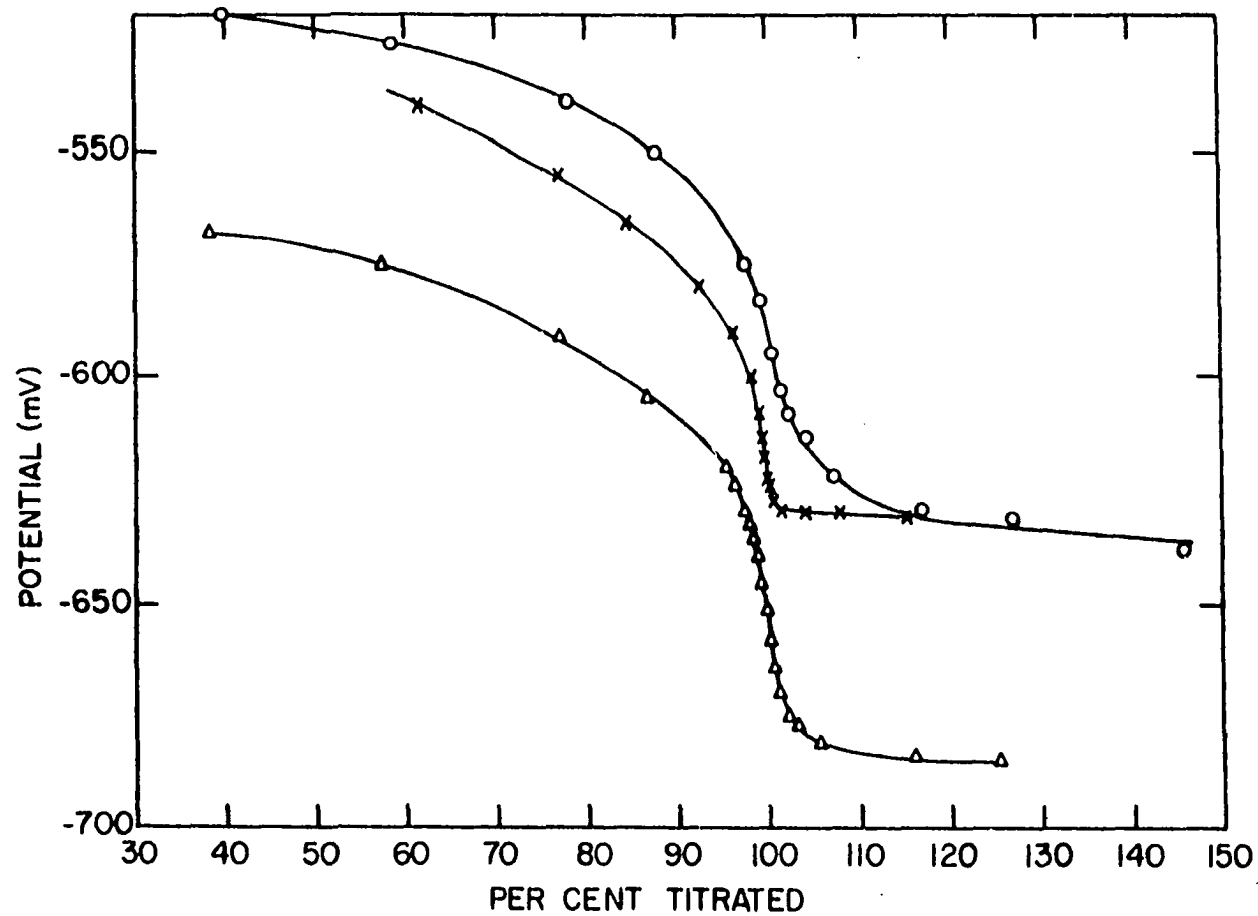(□) 4.10 mg Ca(II) with 10^{-2}M EDTA   (△) 0.41 mg Ca(II) with 10^{-3}M EDTA

Figure 19. Magnesium titrations with $Na_{0.65}WO_3$ electrode at pH 10. (X) 62.52 mg Mg(II) with $10^{-1}M$ EDTA   (△) 2.50 mg Mg(II) with $10^{-2}M$ EDTA   (O) 0.25 mg Mg(II) with $10^{-3}M$ EDTA
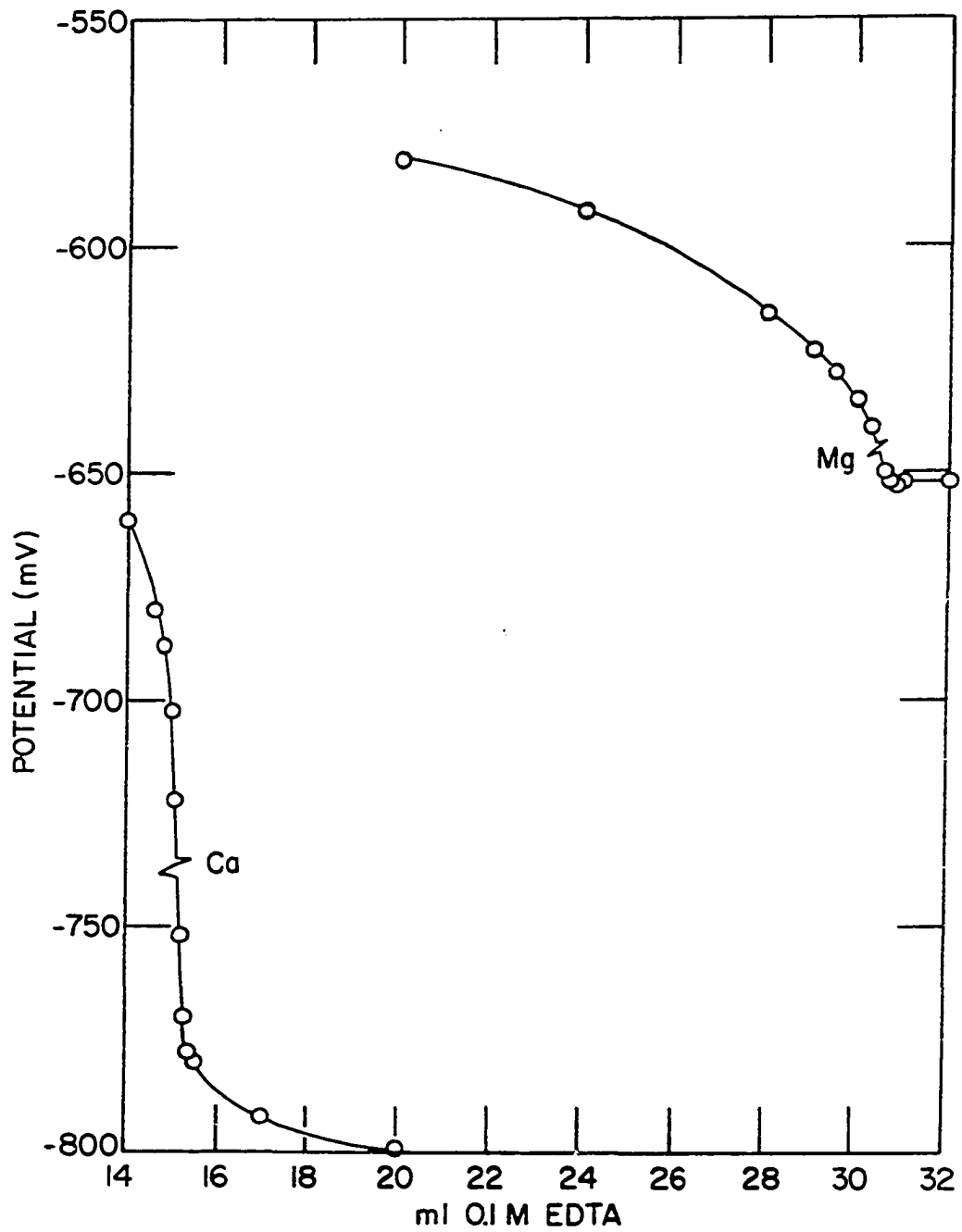
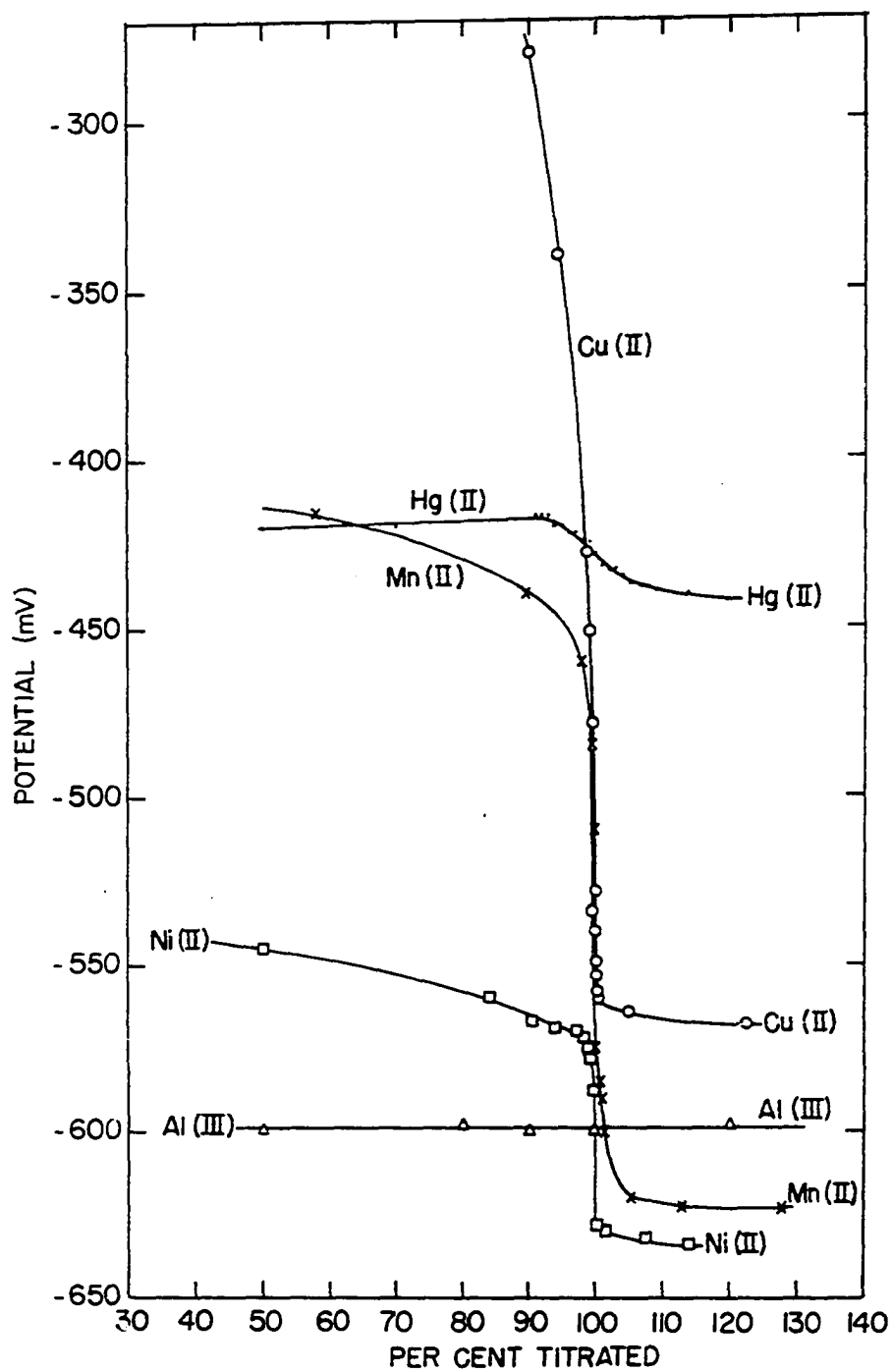Figure 20. Simultaneous titration of calcium and magnesium

Figure 21. Titration of 1.0-2.5 millimoles of several metals with
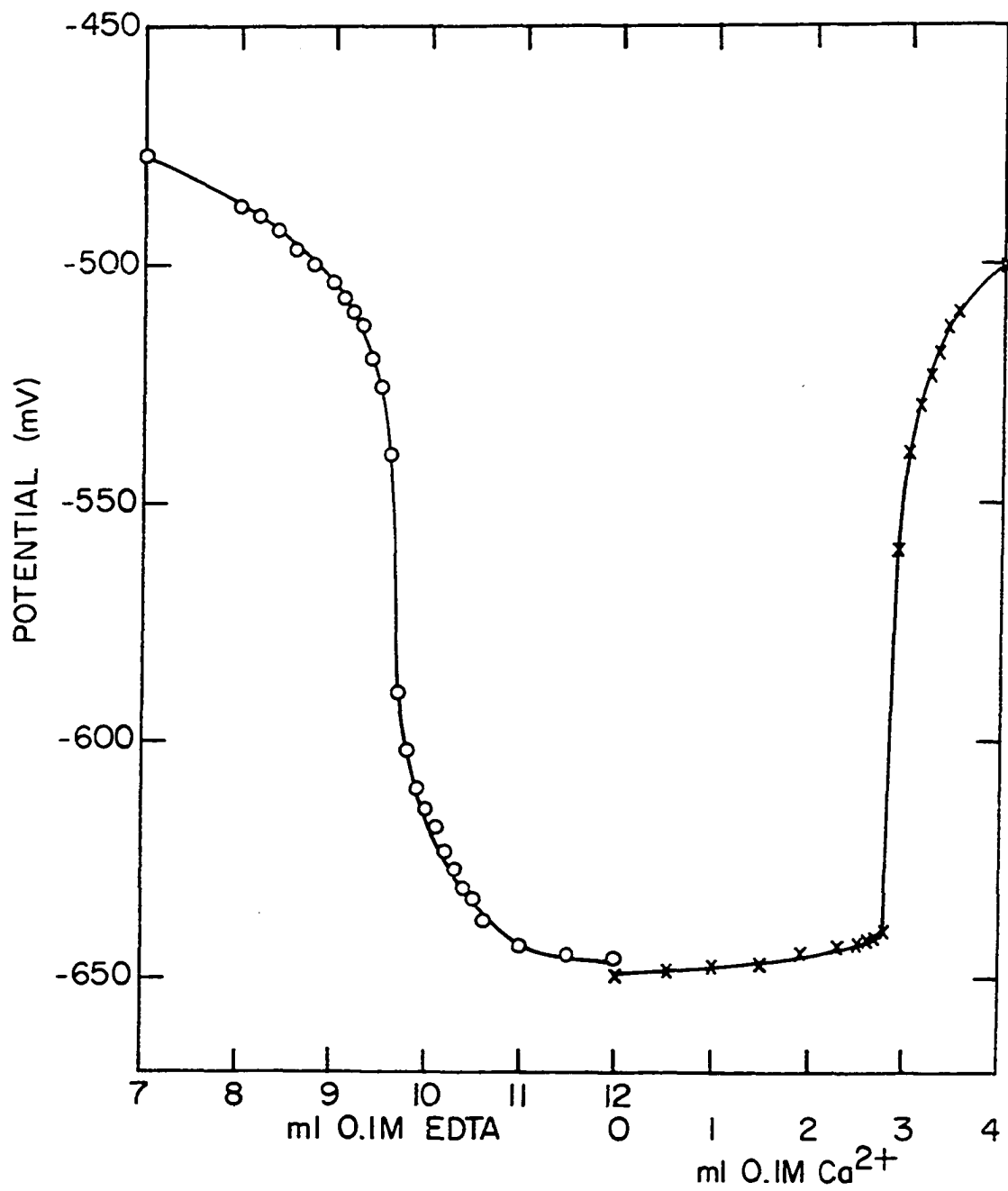0.1M EDTA electrode at pH 10

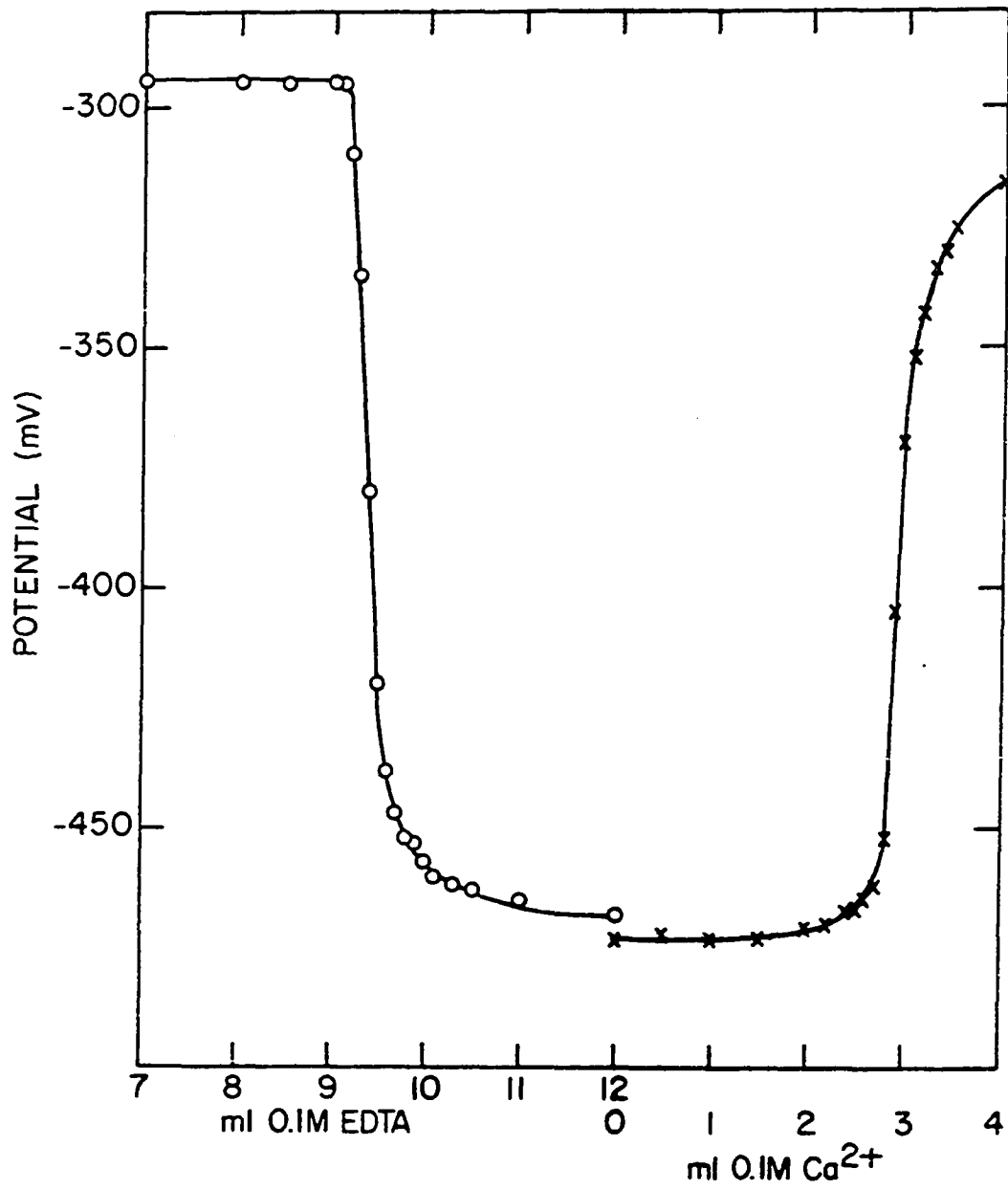Figure 22. Direct and reverse titrations of Cd(II) in 1M NH_4OH

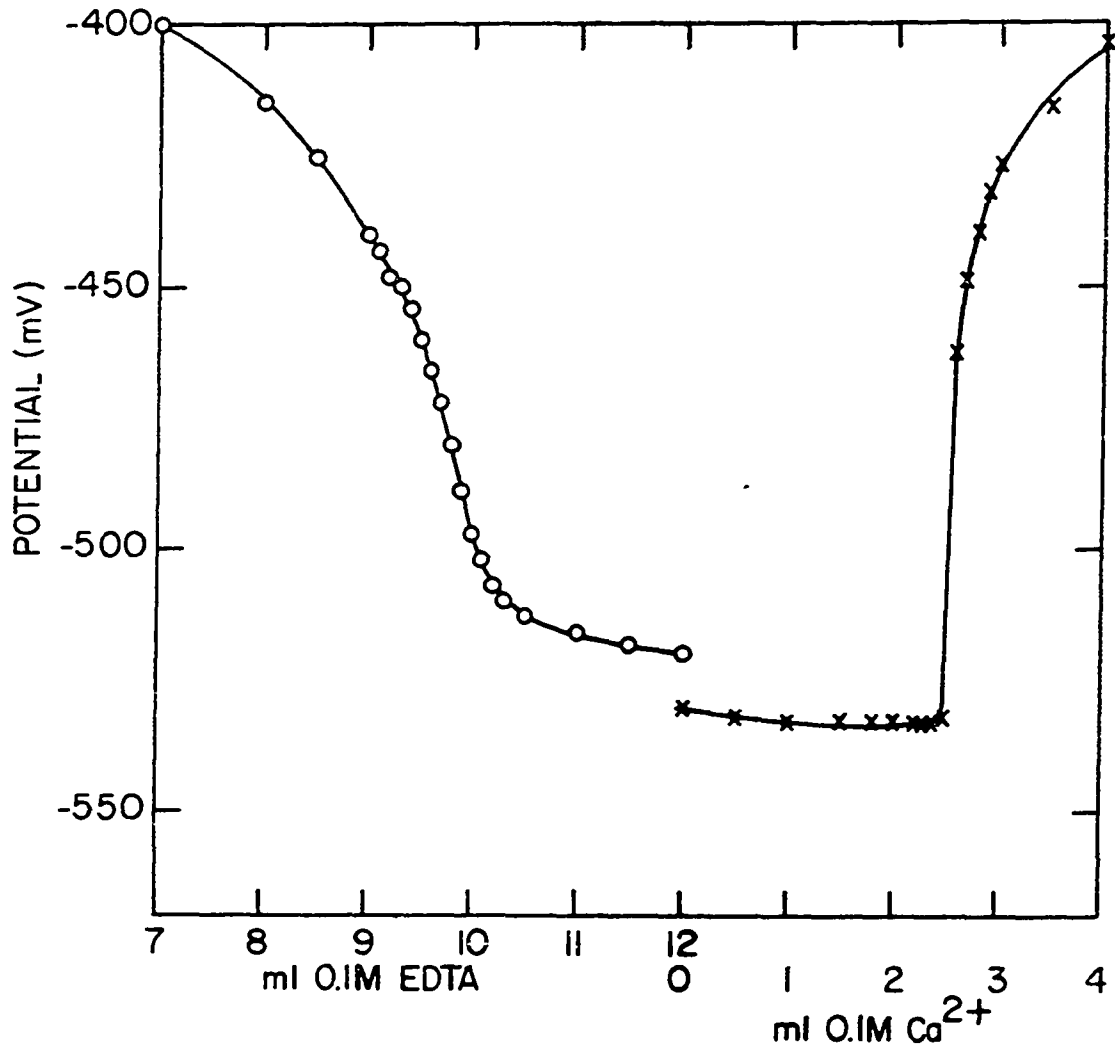Figure 23. Direct and reverse titrations of Co(II) at pH 10

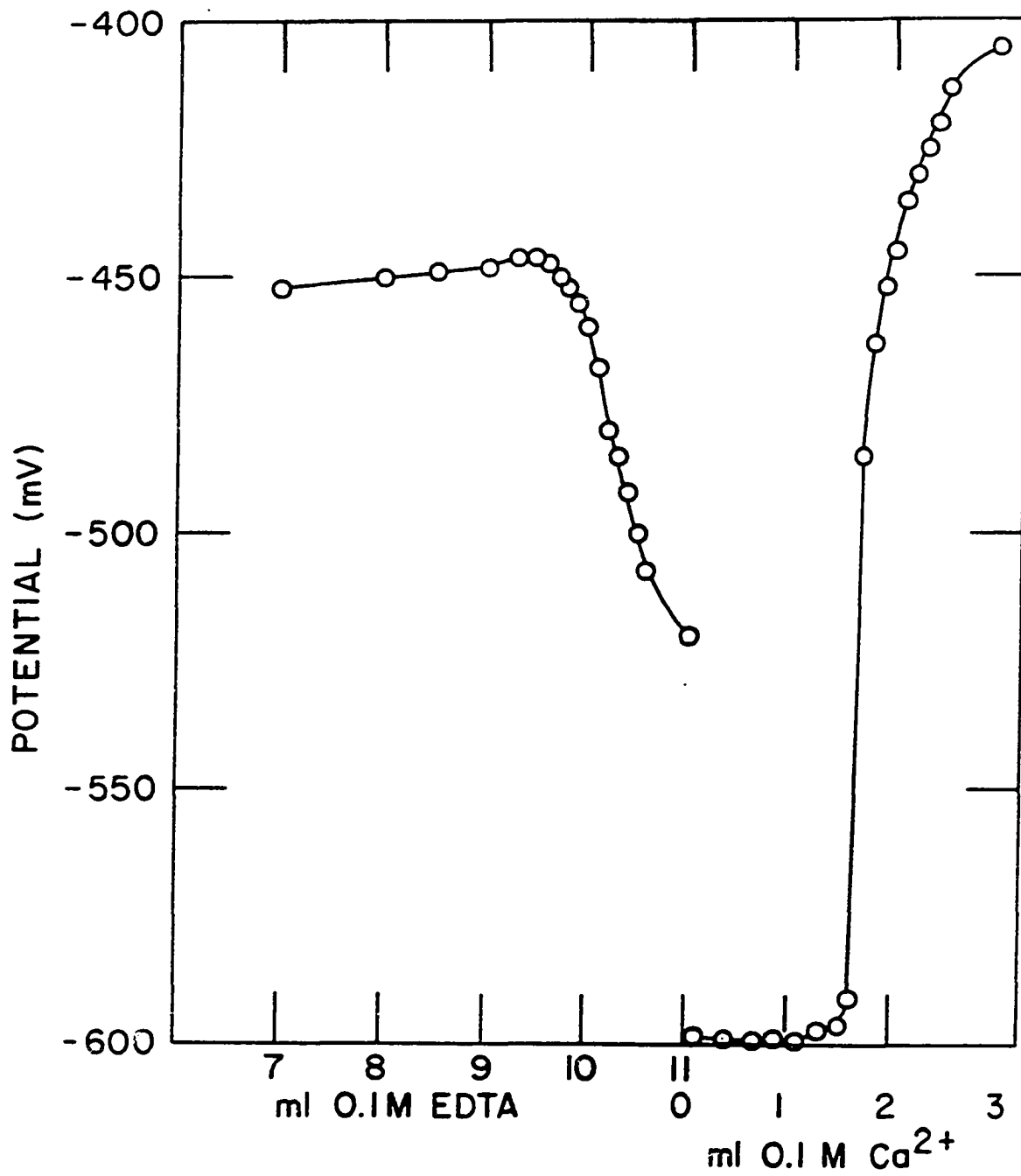Figure 24. Direct and reverse titrations of Zn(II) at pH 10

Figure 25. Direct and reverse titrations of Pb(II) in 1M NH_4OH

ponding direct titration. The poor end points in the direct titrations

of these metals are probably a result of slow reactions between the EDTA

and the $Pb(OH)_2$ precipitate or the strong $Zn(NH_3)_4^{2+}$ complex which exists

before the equivalence point. Aluminum(III) is an extreme example. No

potential shift was detected at the expected equivalence point in either

the direct or indirect titration. The shift was observed at the first

minute addition of EDTA indicating essentially no reaction between

Al(III) and EDTA at pH 10.

The titration of Cu(II) was unique. An extremely large potential

shift of 300-400 mV was observed at and near the equivalence point instead

of the usual 50-150 mV shift experienced with the other metals. Subse-

quent investigations showed the potentiometric response of the $Na_{0.65}WO_3$

and other cubic sodium tungsten bronzes to Cu(II) to be extremely large

(55-125 mV/decade) in ammoniacal solution (Figure 26). The Cu(II)

response extended down to a formal concentration of 10^{-6}M or lower suggest-

ing that trace copper may act as a redox indicator in the titration of the

other metals. A direct correlation was noted between the copper response

of a given electrode and the size of the potential break in a calcium titra-

tion (Figure 27). Low x value Na_xWO_3 electrodes which exhibited the largest

copper response (125 mV/decade) gave potential breaks of approximately

160-170 mV while higher x value electrodes with lower copper response

(55-75 mV/decade) gave potential breaks of 130-135 mV in identical calcium

titrations.

Further evidence that copper may be acting as a redox indicator in

the chelometric titrations of other metals was demonstrated in the signif-

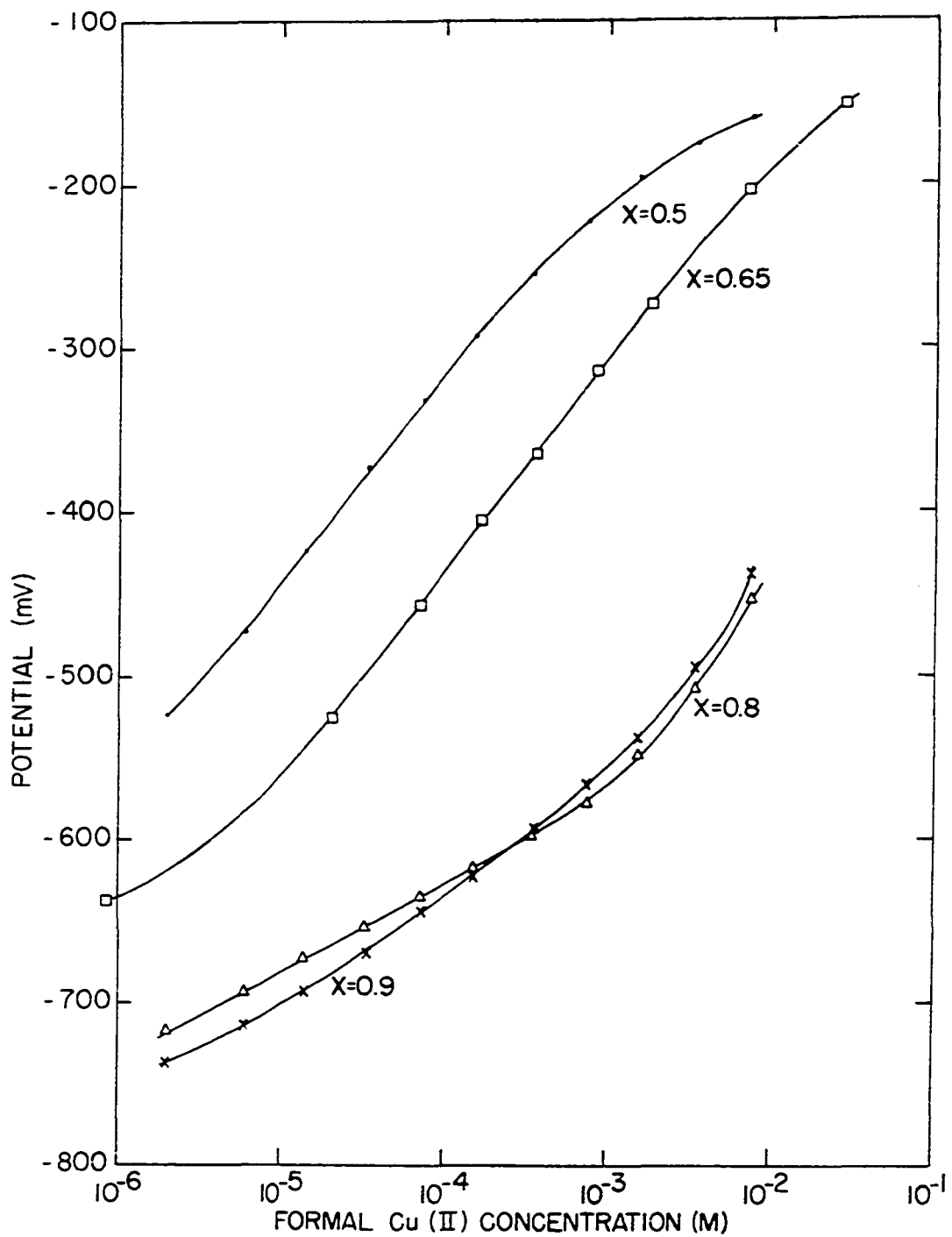icantly larger potential breaks obtained when Cu(II) was added to the

Figure 26. Potentiometric response of Na_xWO_3 electrodes to $Cu(II)$ in 1M NH_4OH as a function of x value
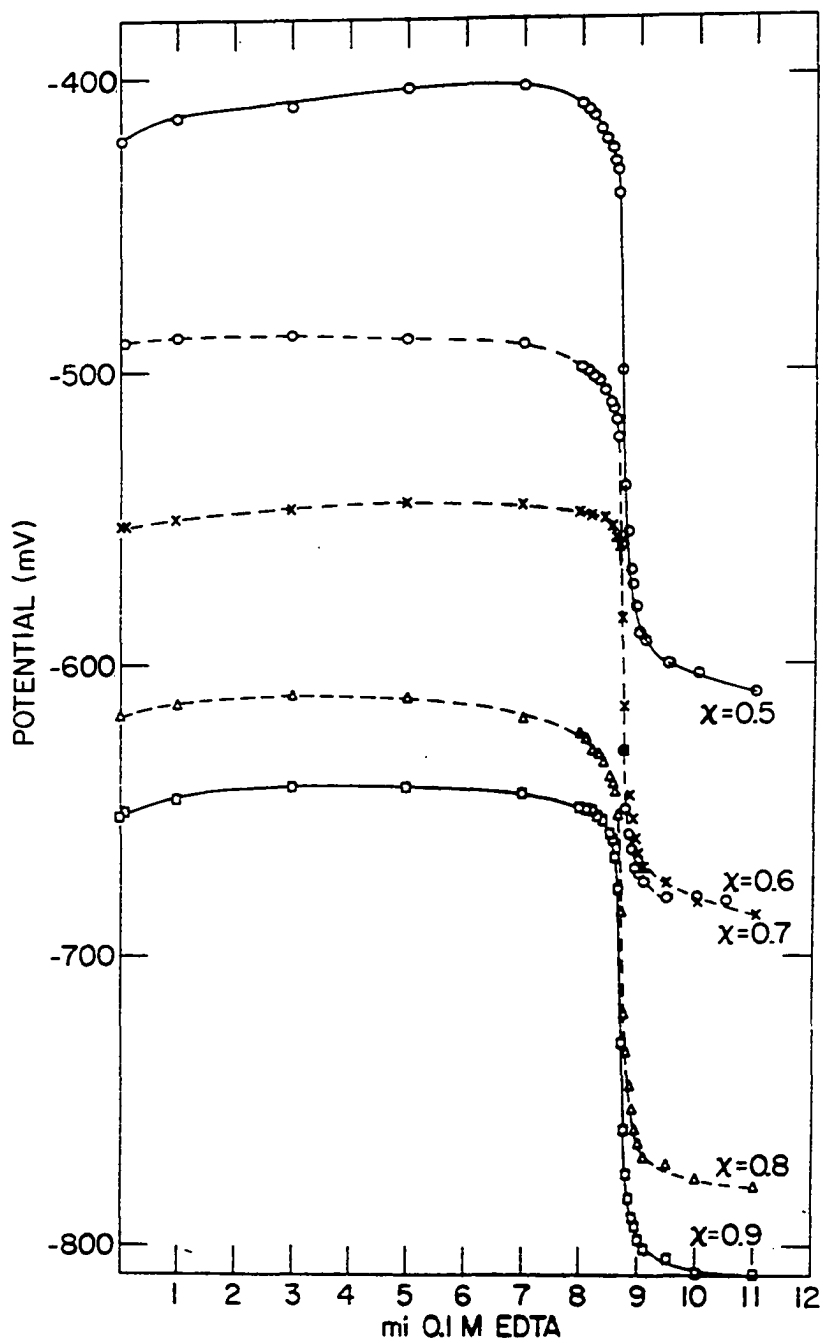
Figure 27.   Titration of calcium in 1M NH_4OH as a function of Na_xWO_3
electrode x value

titration mixture. Figure 28 presents curves for the titration of
1 millimole of Ca^{2+} with 0.1M EDTA and 0.3 millimole of EDTA with
0.1M Ca^{2+} at zero and 5×10^{-5}M added copper concentrations. The
additional copper was found to nearly double the potential break at the
end point in such titrations.

If trace copper is acting as a redox indicator in these titrations,
it is doing so at extremely low concentrations. A colorimetric method
employing bathocuproine (85) was used to analyze the deionized water
and the $CaCl_2$, NH_4OH and EDTA reagents for copper. The EDTA was first
wet ashed with nitric and perchloric acids. Results of these analyses
gave an upper limit of 1 to 5×10^{-7}M for the copper concentration in the
titration solution.

As in the case of the oxygen response, the cubic sodium tungsten
bronzes were found to perform significantly better than other alkali
metal tungsten bronzes in chelometric titrations. Figure 29 illustrates
potentiometric titrations of 1 millimole of Ca^{2+} with 0.1M EDTA in
1M NH_4OH using hexagonal Rb, K, and Cs, cubic Li, and tetragonal K
tungsten bronze electrodes. These electrodes were also found to have a
much lower response to $Cu(II)$ (30-40 mV/decade) than the cubic sodium
tungsten bronzes (Figure 30), consistent with the previously discussed
correlation between the titration potential break and the $Cu(II)$ response.

The unique properties of cubic Na_xWO_3 are further emphasized when
compared to some common metals as indicating electrodes. Potentiometric
titrations of calcium with EDTA using Pt, Cu and W as the indicating
electrodes are illustrated in Figure 31. Potential breaks using these
metals were much smaller, 10-30 mV, and generally much less sharp than the
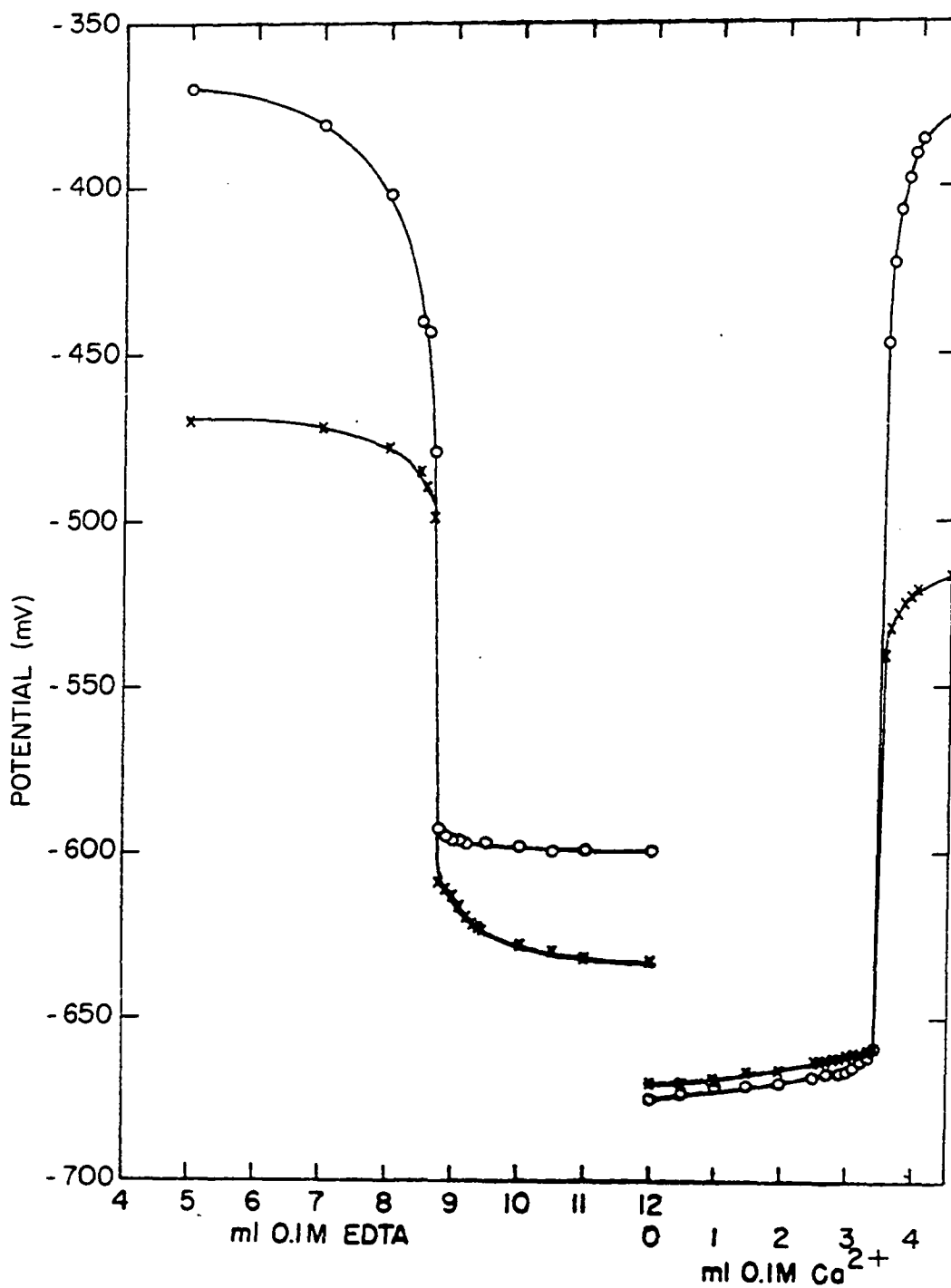
Figure 28. Titration of 1.0 millimole Ca^{2+} with 0.1M EDTA and 0.3 millimole EDTA with 0.1M Ca^{2+} at zero (x) and 5 X 10^{-5}M (o) added Cu(II)
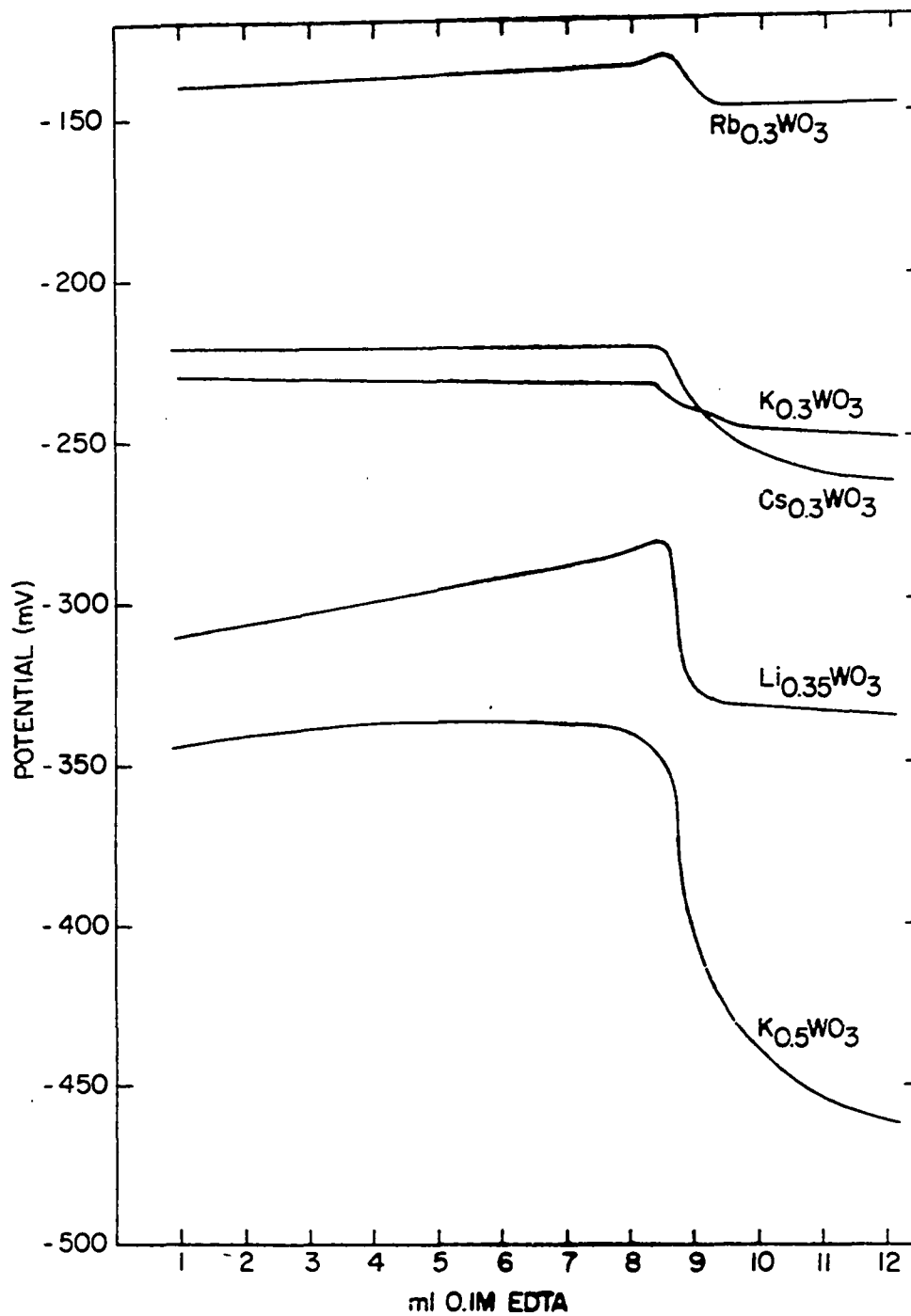
Figure 29. Titrations of 1.0 millimole Ca^{2+} in 1M NH_4OH using other alkali metal tungsten bronze electrodes
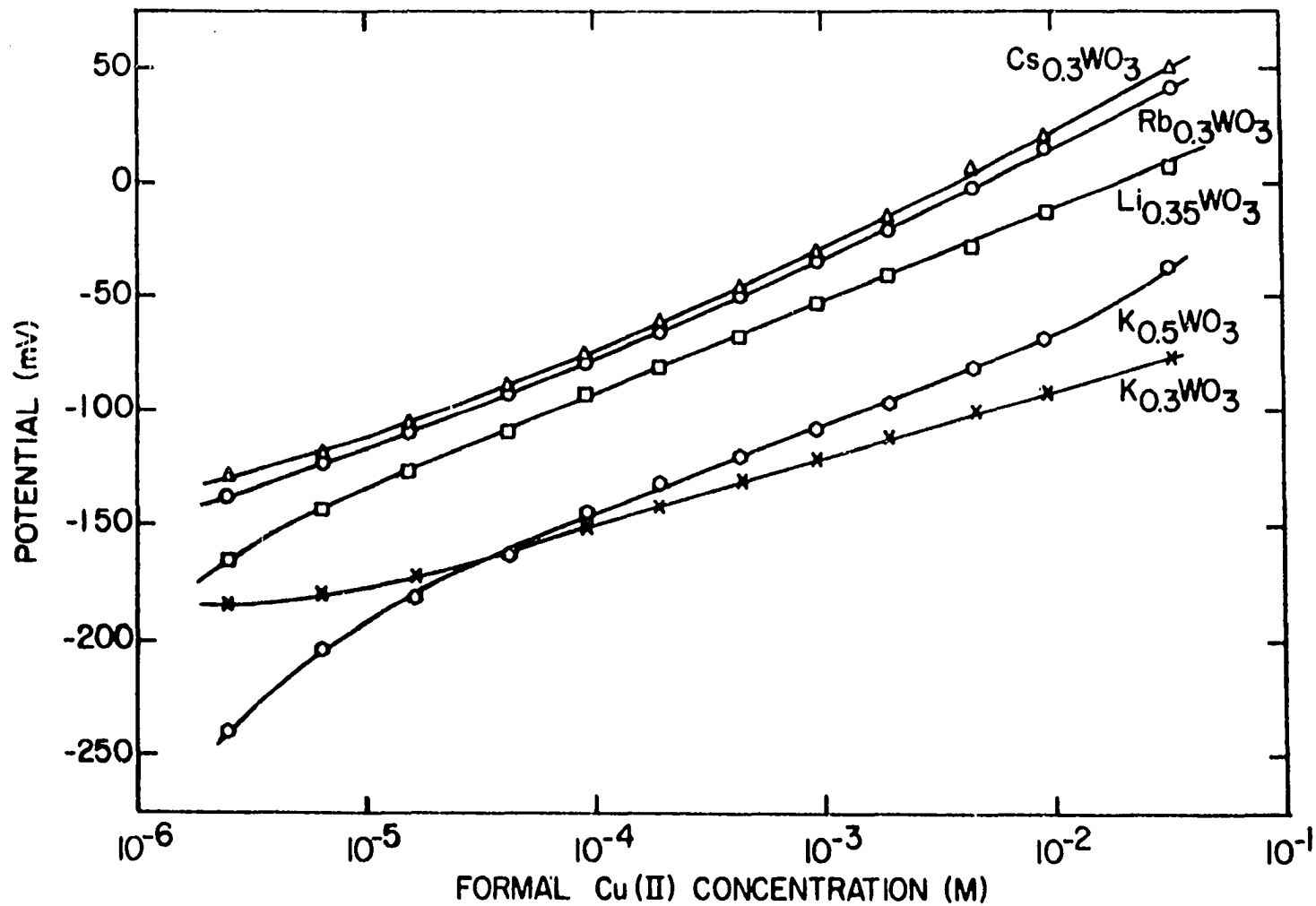
Figure 30. Potentiometric response of several alkali metal tungsten bronze electrodes to Cu(II) in 1M NH_4OH
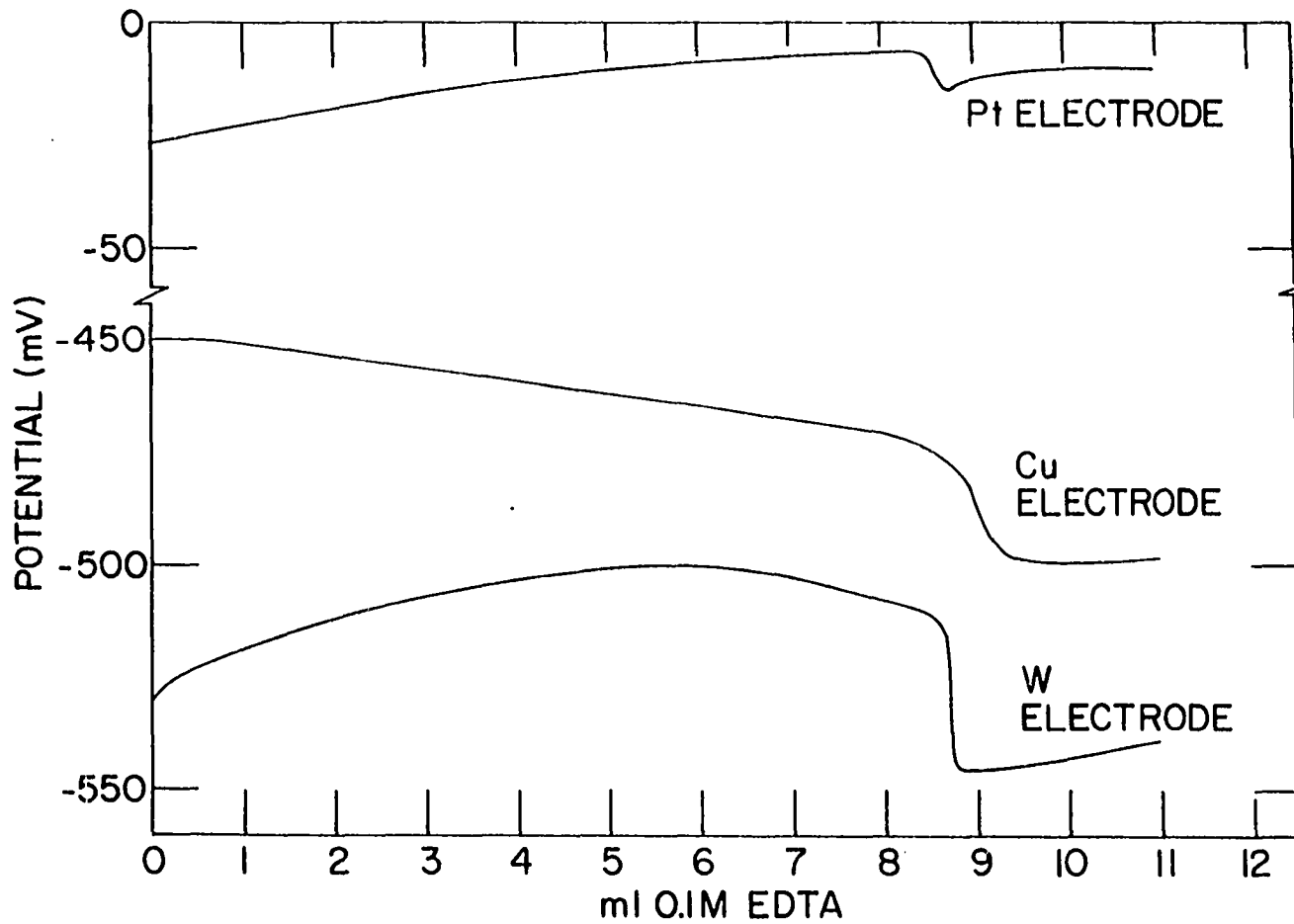
Figure 31. Titration of 1.0 millimole Ca^{2+} in 1M NH_4OH using Pt, Cu, and W electrodes

breaks obtained at the same concentration of reagents with Na_xWO_3.

In acid solution the response of the Na_xWO_3 electrode was typical of a highly conducting inert electrode. The titration of approximately 2.5 millimoles of $Fe(III)$ with $0.1M$ EDTA at pH 2-3 is presented in Figure 32. The large potential change (at positive potential) reflects the change in the concentration ratio of the $Fe(III)/Fe(II)$ redox couple and is much like that obtained with a platinum-indicating electrode (78).

Quantitative results from a number of titrations described in this section are presented in Table 6. All titrations were performed with an annealed, flat-surface cubic $Na_{0.65}WO_3$ indicating electrode and a SCE reference electrode. End points were determined by the second derivative method. Excellent agreement is seen between quantities taken and the measured value for even the most dilute titrations where 0.01 millimole of metal was titrated with $10^{-3}M$ EDTA. Excellent results were also obtained for the simultaneous titration of Ca and Mg in a mixture and for $Pb(II)$ by reverse titration.

Mechanism of Response

The extremely large oxygen response (120 mV/decade) made it appear doubtful that simple oxygen redox reactions played a major role in the response. The reduction of O_2 to OH^- or H_2O requires four electrons per molecule predicting a 15 mV/decade response slope by the Nernst Equation while reactions yielding peroxide require two electrons predicting a 30 mV/decade slope. The poisoning of the oxygen response for low x value Na_xWO_3 electrodes in LiOH and the potential shifts experienced in EDTA titrations of nonreducible cations without any apparent redox
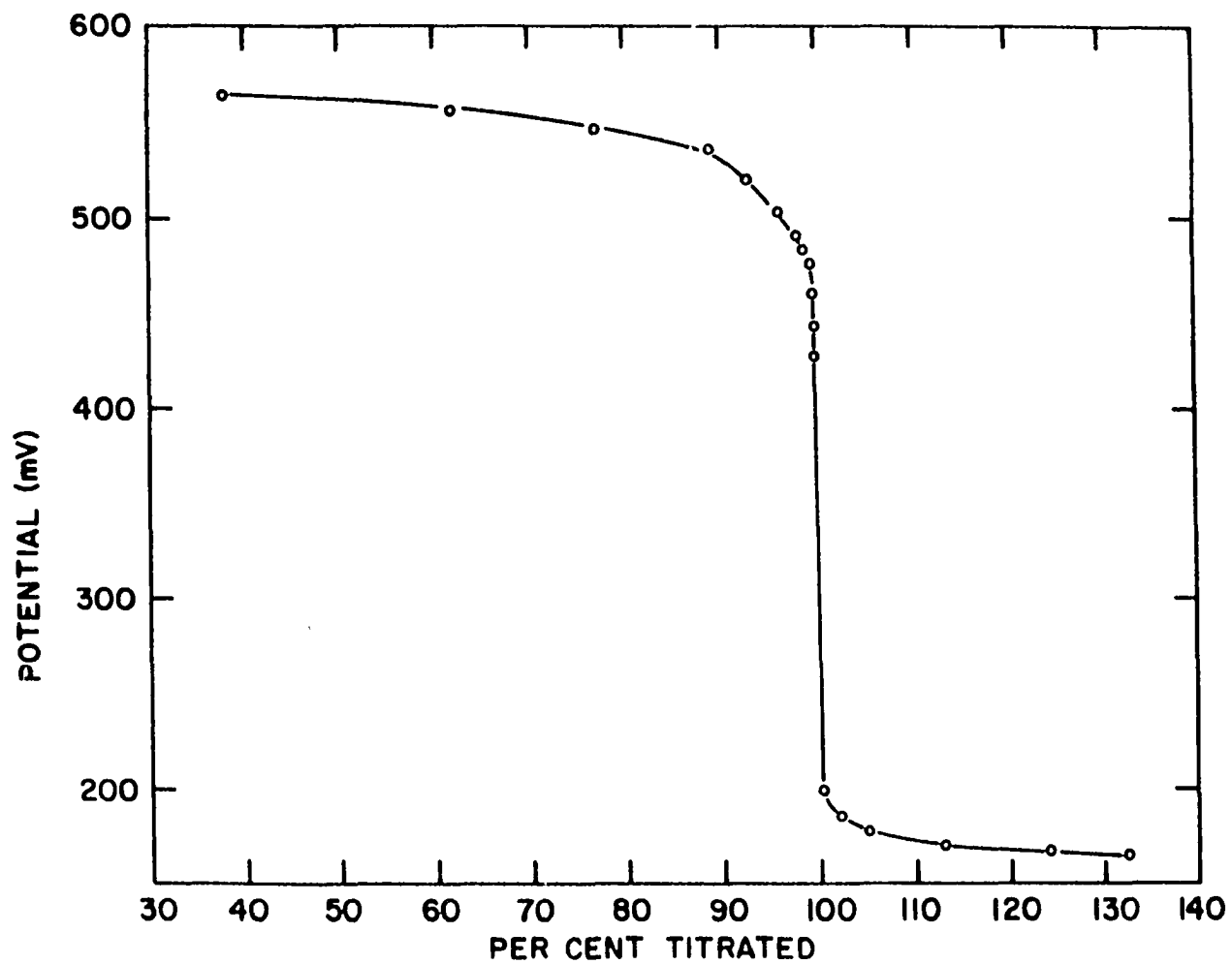
Figure 32. Titration of Fe(III) with 0.1M EDTA at pH 2-3 using the $Na_{0.65}WO_3$ electrode

Table 6. Results of metal-EDTA titrations

Metal detected	Log K_m (78)	pH	Approximate titrant (EDTA) concentration, M	Weight of metal titrated (mg) Taken	Found
Ca(II)	10.7	10	10^{-1}	100.4	100.4
			10^{-2}	4.10	4.10
			10^{-3}	0.41	0.41
Mg(II)	8.7	10	10^{-1}	62.52	62.56
			10^{-2}	2.50	2.50
			10^{-3}	0.25	0.25
Zn(II)	16.7	10	10^{-1}	162.3	161.1
			10^{-2}	6.49	6.56
Ca(II), Mg(II)		13.10	10^{-1}	61.50, 37.53	61.39, 37.38
Cu(II)	18.8	10	10^{-1}	146.9	146.5
Pb(II) (back titration)	18.0	10	10^{-1} (EDTA) 10^{-1} (Ca^{2+})	202	200
Fe(III)	25.1	3	10^{-1}	143.1	143.3

indicator were also difficult to explain in terms of conventional oxidation reduction reactions.

Very early in the course of this investigation the correlation was made between the unique response of the Na_xWO_3 electrode and the presence of the hydroxide ion. The oxygen response deteriorated and chelometric titrations of nonreducible metals became unsuccessful at lower hydroxide concentration.

Consequently a mechanism was proposed in which the adsorption and desorption of hydroxide ions at the Na_xWO_3 surface played an important role in establishing the potential of the electrode. The pH response of the Na_xWO_3 electrode (Figure 33) could be explained on this basis where adsorbed hydroxide ions form a charged double layer at the electrode surface and establish the negative potential. Numerous parallel examples may be cited among the ion-selective potentiometric electrodes developed in recent years. These include the glass electrodes for measuring pH and alkali and alkaline earth metals, the solid state rare earth fluorine membrane electrodes for F^-, and mixed sulfide membrane electrodes for S^{2-} and various cations, and the liquid and ion exchange resin membrane electrodes for anions and cations. The potentiometric response of these are all considered to arise from the specific adsorption of charged species at the electrode surface (86,87).

The oxygen response could be explained as follows: The strong adsorption of hydroxide ions in de-oxygenated 0.1M KOH establishes the large negative potential (-1200 mV or less). When O_2 molecules are introduced, they also are strongly adsorbed at the bronze surface, displacing the negatively charged OH^- ions and resulting in a positive
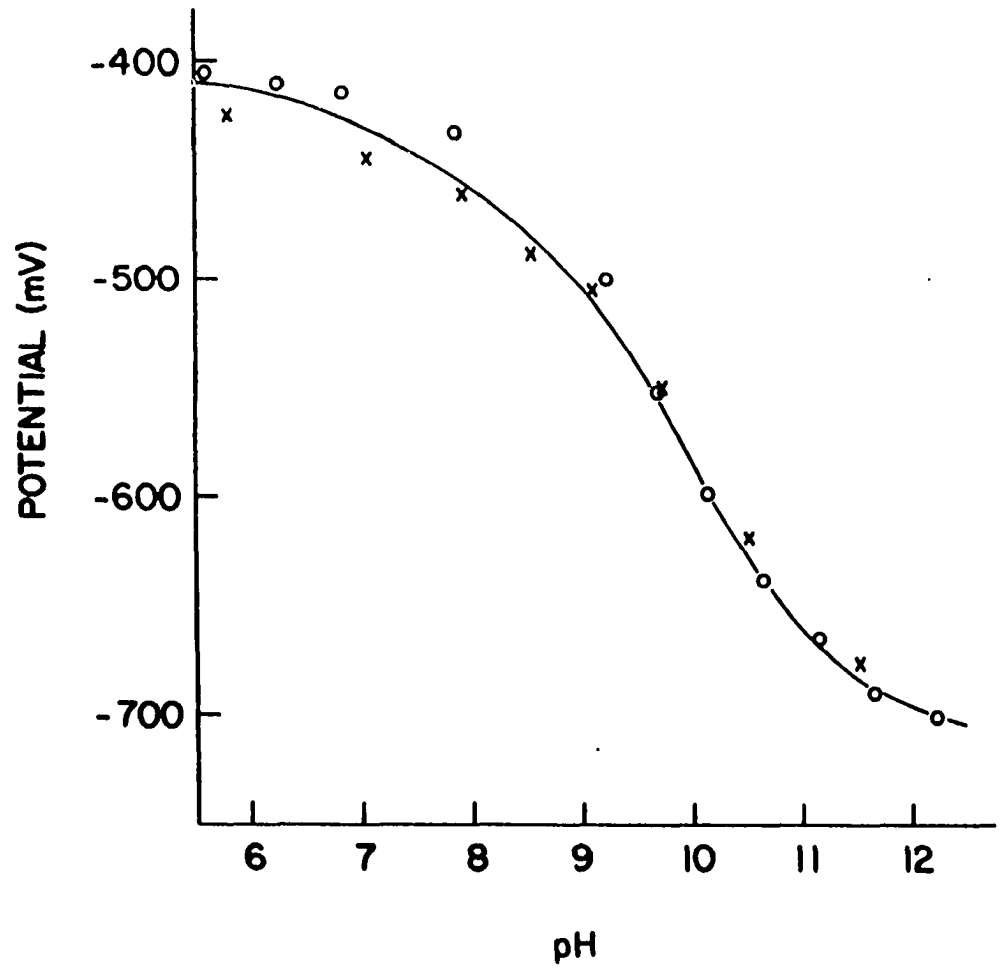
Figure 33. pH response of $Na_{0.65}WO_3$ electrode in air-saturated solution

        (o)   Increasing pH

        (x)   Decreasing pH

shift in electrode potential. The success of EDTA titrations in basic solution and the action of Li^+ on the oxygen response could similarly be explained if the positive ions act in a manner similar to the oxygen molecules in displacing adsorbed OH^-.

Subsequent observations and considerations however, place serious doubt on this adsorption mechanism. The potentiometric response to a number of species was determined in 1M NH_4OH and appeared to be limited to only those species which are easily reduced in aqueous solution (Figure 34). Response slopes for $Cu(II)$, $Ag(I)$ and $Fe(CN)_6^{3-}$ were found to be unpredictably large (80-300 mV/decade) paralleling the response to dissolved oxygen in 0.1M KOH. Response to difficultly reducible metals, $Cd(II)$, $Zn(II)$, $Ni(II)$, $Ca(II)$, was extremely small and the success of chelometric titrations of these species could no longer be explained on the basis of displacement of adsorbed OH^- ions as the cause of the substantial shift in potential. Further evidence that a redox reaction takes place at the Na_xWO_3 electrode in basic solution was seen during oxygen measurements in quiescent solutions when the electrode potential drifted in a negative direction indicating the depletion of dissolved oxygen in the vicinity of the electrode. This observation was consistent with those of other investigators (12,13) who demonstrated the slow dissolution of Na_xWO_3 in basic solution in the presence of oxygen and the rapid dissolution in the presence of very strong oxidizing agents such as sodium peroxide. The spontaneous plating of metallic silver from ammoniacal and 0.1M KOH-1mM EDTA solutions containing $Ag(I)$ provided additional evidence of the ability of Na_xWO_3 to act as a reducing agent in basic solution.
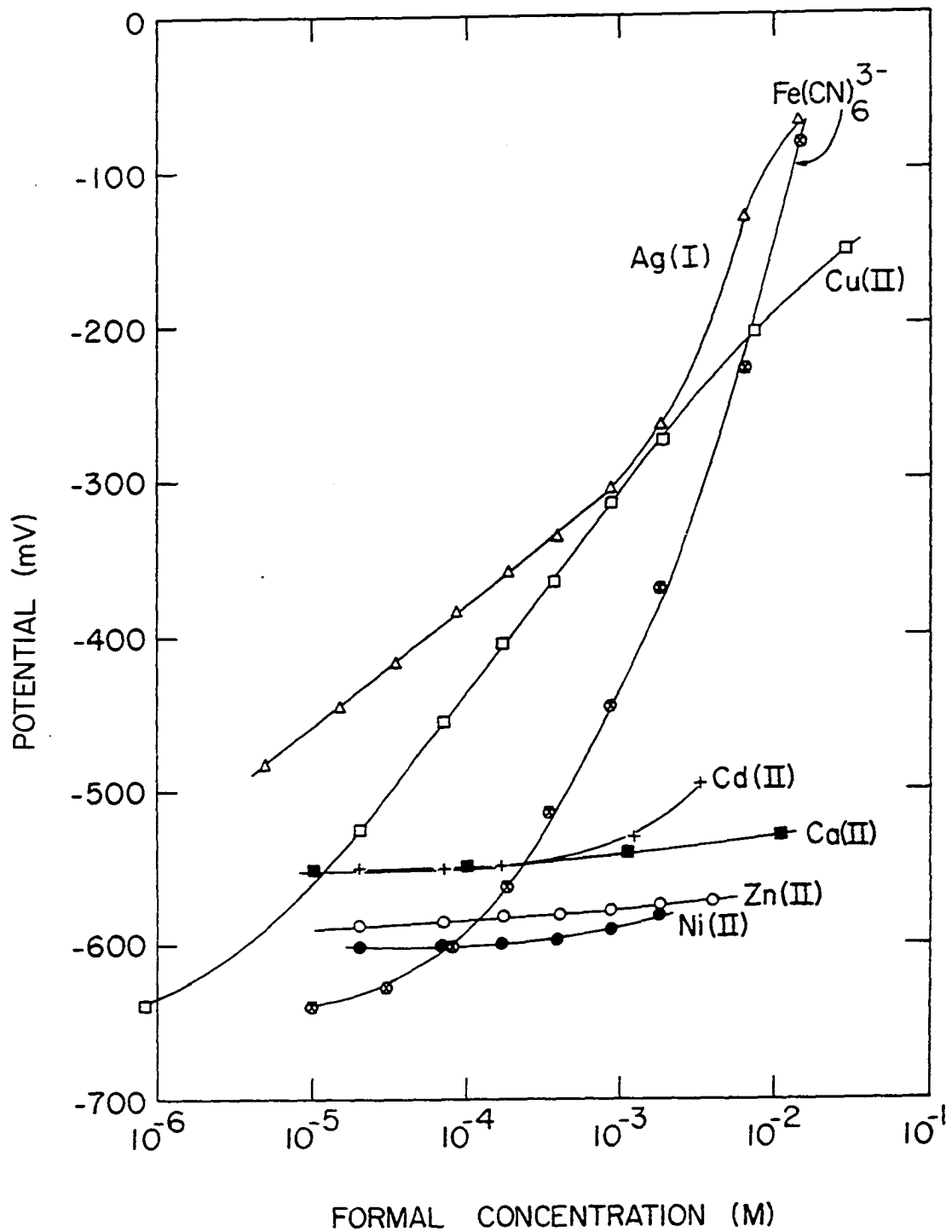
Figure 34. Potentiometric response of the $Na_{0.65}WO_3$ electrode to several species in 1M NH_4OH

Voltammetric measurements involving cubic Na_xWO_3 electrodes in 0.1M KOH-1mM EDTA demonstrated that both the reduction of dissolved oxygen and the oxidation of Na_xWO_3 were occurring in the same general potential range of the potentiometric oxygen response (-600 to -1200 mV vs. SCE). Figures 35 and 36 illustrate current vs. potential curves for Na_xWO_3 electrodes having x values of 0.65 and 0.79 in KOH solutions saturated with nitrogen, the 1%, 3.3% and 10% oxygen gas mixtures and pure oxygen.

In deoxygenated solution the voltammetric curves exhibited the expected cathodic wave for the reduction of H_2O to H_2 at approximately -1.5 V vs. SCE much like that observed with platinum electrodes (81). Also observed however, was an anodic wave beginning at -1.0 to -1.2 V vs. SCE (the open circuit potential) and becoming extremely large at potentials more positive than -0.5 to -0.6 V vs. SCE. The anodic wave was attributed to the oxidation of the Na_xWO_3 electrode to WO_4^{2-} (tungstate) for two reasons; the absence of other oxidizable species and the observation that dissolved oxygen (which establishes potentials between -0.6 and -1.2 V at the Na_xWO_3 electrode) is known to cause this reaction to take place (12,13). When oxygen was introduced into the 0.1M KOH-1mM EDTA solution, a cathodic wave representing the reduction of O_2 to H_2O was observed in the same general potential range (-0.6 to -1.2 V) where the Na_xWO_3 oxidation takes place.

The potentiometric response of the Na_xWO_3 electrode to dissolved oxygen in basic solution must therefore be considered to arise from a mixed potential established by the spontaneous oxidation of the Na_xWO_3 electrode by dissolved oxygen.

Figure 35. Voltammetric curves of $Na_{0.65}WO_3$ electrode in 0.1M KOH-1mM EDTA as a function of oxygen concentration. (*) Open circuit potential in N_2-saturated solution
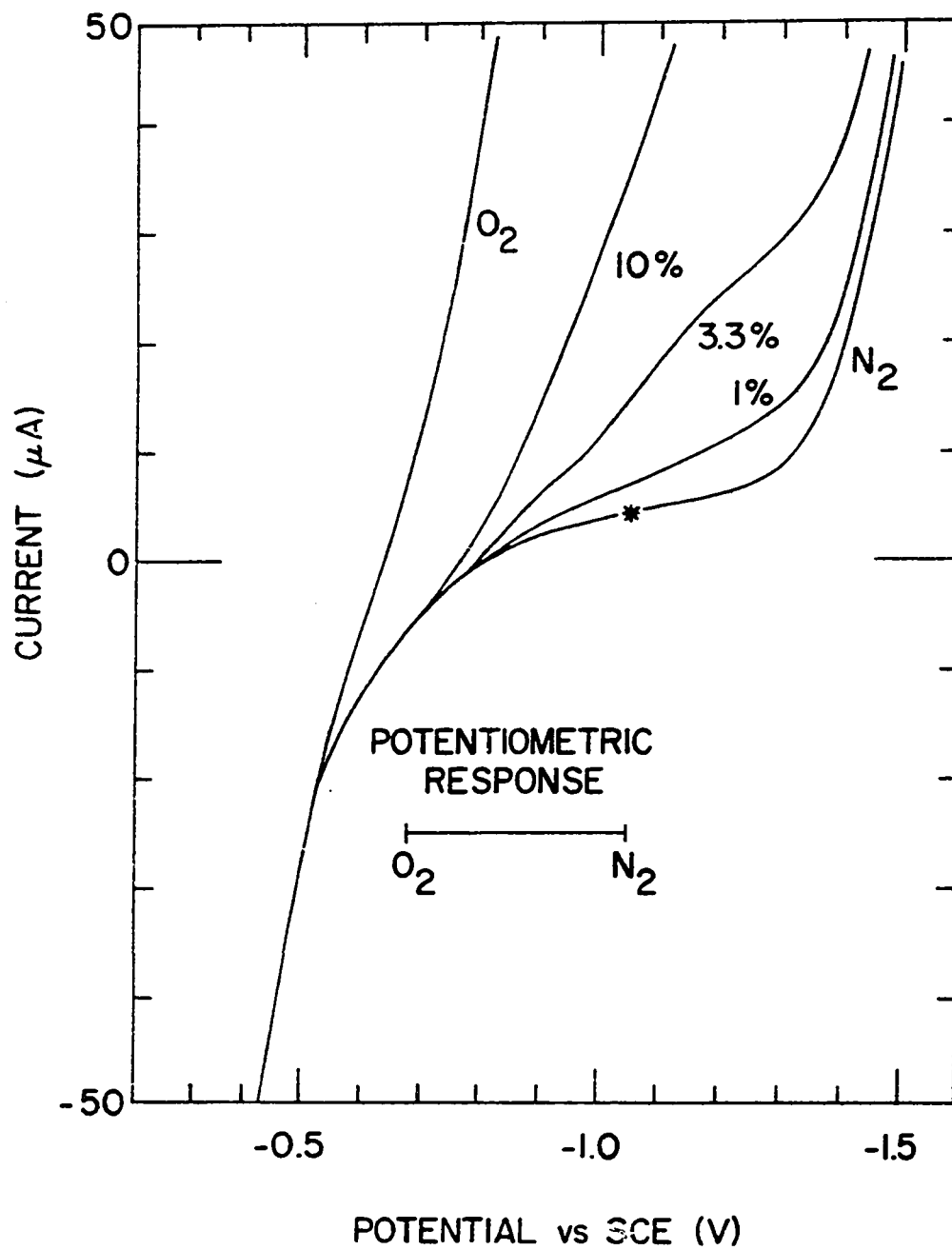
Figure 36. Voltammetric curves of Na$_{0.79}$WO$_3$ electrode in 0.1M KOH-1mM EDTA as a function of oxygen concentration. (*) Open circuit potential in N$_2$-saturated solution

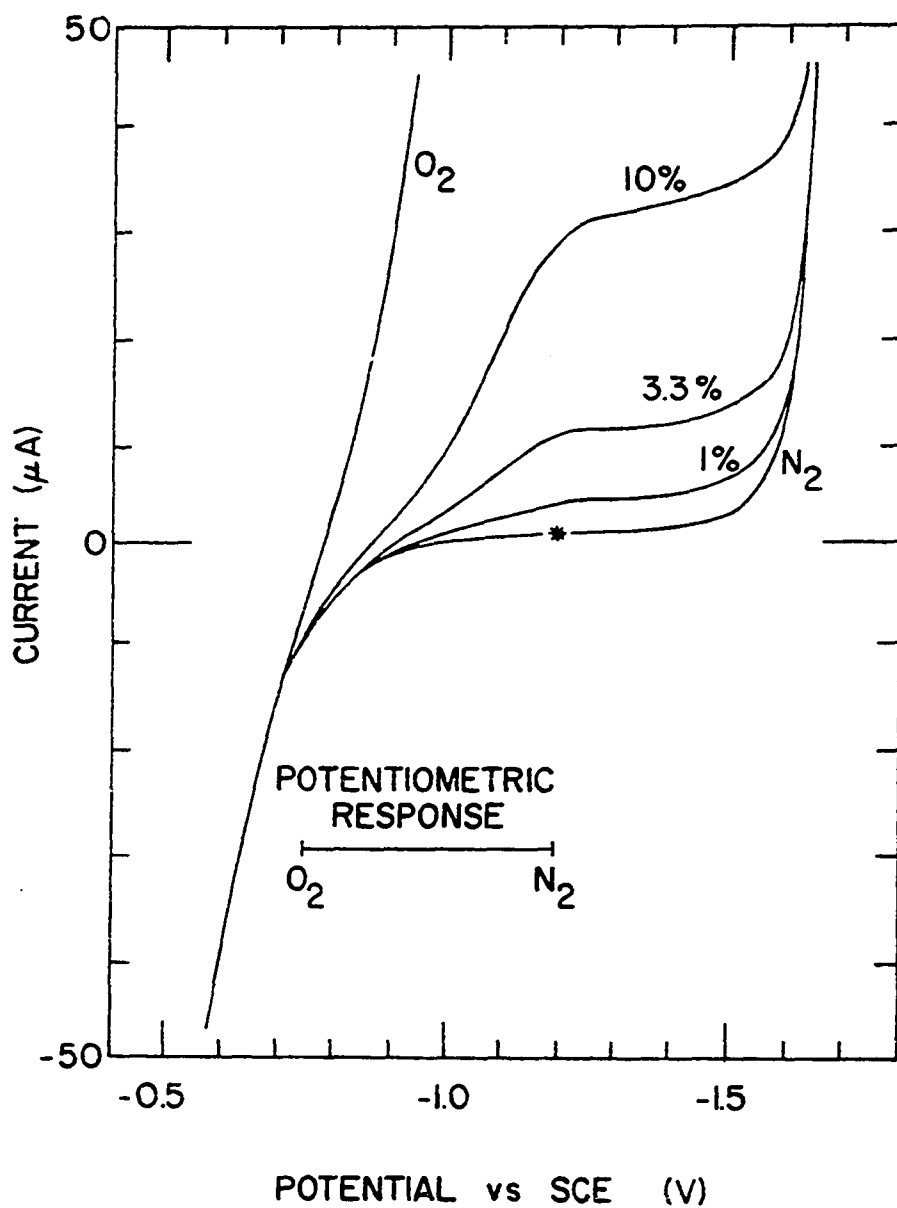Mixed potential phenomena have been discussed by a number of authors (88-93) and are considered to arise when a nonequilibrium state exists involving two or more different electrode processes. Such a state is connected with a spontaneous change at the electrode surface where simultaneous oxidation and reduction are occurring. The classic example is the reaction $Zn + 2H^+ \longrightarrow Zn^{2+} + H_2$ at a zinc electrode in acid solution which was first studied in terms of mixed potentials by Wagner and Traud (88).

The sum of the partial currents, $i_{cathodic} - i_{anodic}$, of such a reaction must be equal to zero and since the rate of each partial reaction is dependent on the electrode potential, the mixed potential satisfying the condition of zero net current is established. If the voltammetric polarization curves of cathodic and anodic processes can be individually determined the value of the mixed potential can be estimated schematically as shown in Figure 37. Represented in this figure are the anodic wave for the dissolution or oxidation of the $Na_{0.65}WO_3$ electrode in 0.1M KOH-1mM EDTA and a series of cathodic waves for the reduction of O_2 at different dissolved oxygen concentrations $(C_1 < C_2 < C_3 < C_4)$. The anodic Na_xWO_3 wave was determined directly in nitrogen-saturated solution while the cathodic oxygen waves were estimated by subtracting the anodic wave from the corresponding total voltammetric waves in Figure 35. The condition of equal and opposite anodic and cathodic currents (zero net electrode current) to establish the mixed potential is represented by the vertical dashed lines for the various dissolved oxygen concentrations. The shift of the mixed potential toward positive potentials with increasing dissolved oxygen concentration is clearly illustrated.
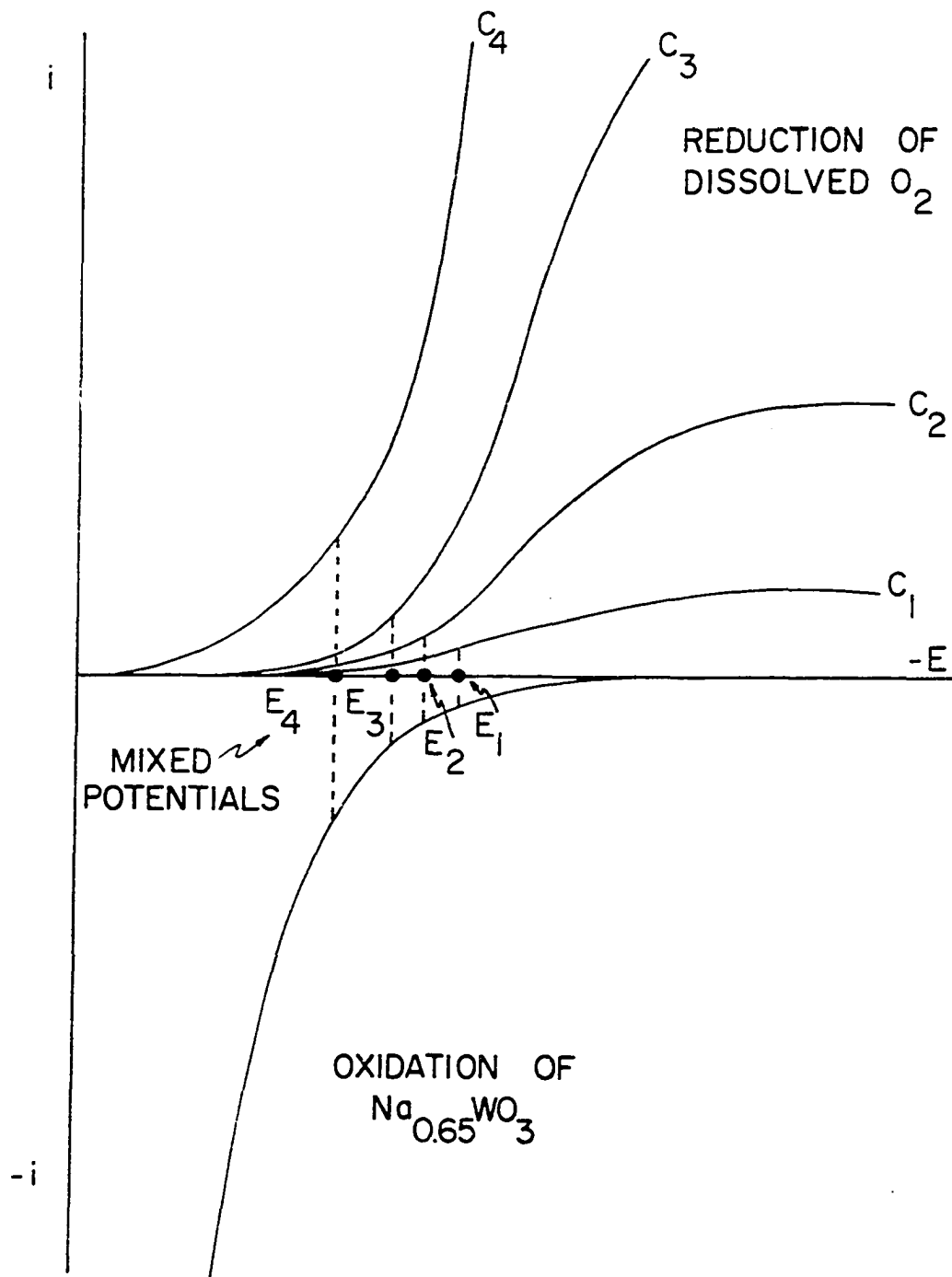
Figure 37. Schematic diagram illustrating the establishment of the mixed potential

The potentiometric response of the Na_xWO_3 electrode to $Cu(II)$ and other oxidizing agents in ammoniacal solution can be similarly explained. The only prerequisite for such response would be that the cathodic wave for the oxidizing agent exist over the same potential range where the Na_xWO_3 anodic wave occurs. Figure 38 presents voltammetric curves for various $Cu(II)$ concentrations in 1M NH_4OH. The similarity between these and the oxygen curves in 0.1M KOH (Figures 34 and 35) is apparent.

The extremely large potentiometric response slopes observed in the oxygen, $Cu(II)$, and $Fe(CN)_6^{3-}$ measurements are not totally unexpected. Herbelin et al. (93) encountered similarly large potentiometric response slopes (125-250 mV/decade) for $Ce(IV)$ and $Fe(II)$ when working in a mixed-potential system involving the $Ce(IV)/Ce(III)$ and $Fe(III)/Fe(II)$ redox couples.

Response slopes as high as 250 to 300 mV/decade could in fact be anticipated for the Na_xWO_3 electrode by the mixed-potential mechanism under certain conditions. Figure 39 is a logarithmic plot of the anodic wave for the oxidation of the $Na_{0.65}WO_3$ electrode in 0.1M KOH-1mM EDTA showing a ten-fold increase in anodic current for a 285 mV shift in potential. If the cathodic wave for the reduction of an oxidizing agent were completely diffusion limited in this general potential region the cathodic current would be directly proportional to the concentration and independent of the electrode potential. A ten-fold increase in the oxidant concentration would result in a similar ten-fold increase in the cathodic partial current. To balance this increase in cathodic current a ten-fold increase in the anodic partial current would be required which, in turn, would result in a 285 mV shift in the mixed potential of the Na_xWO_3
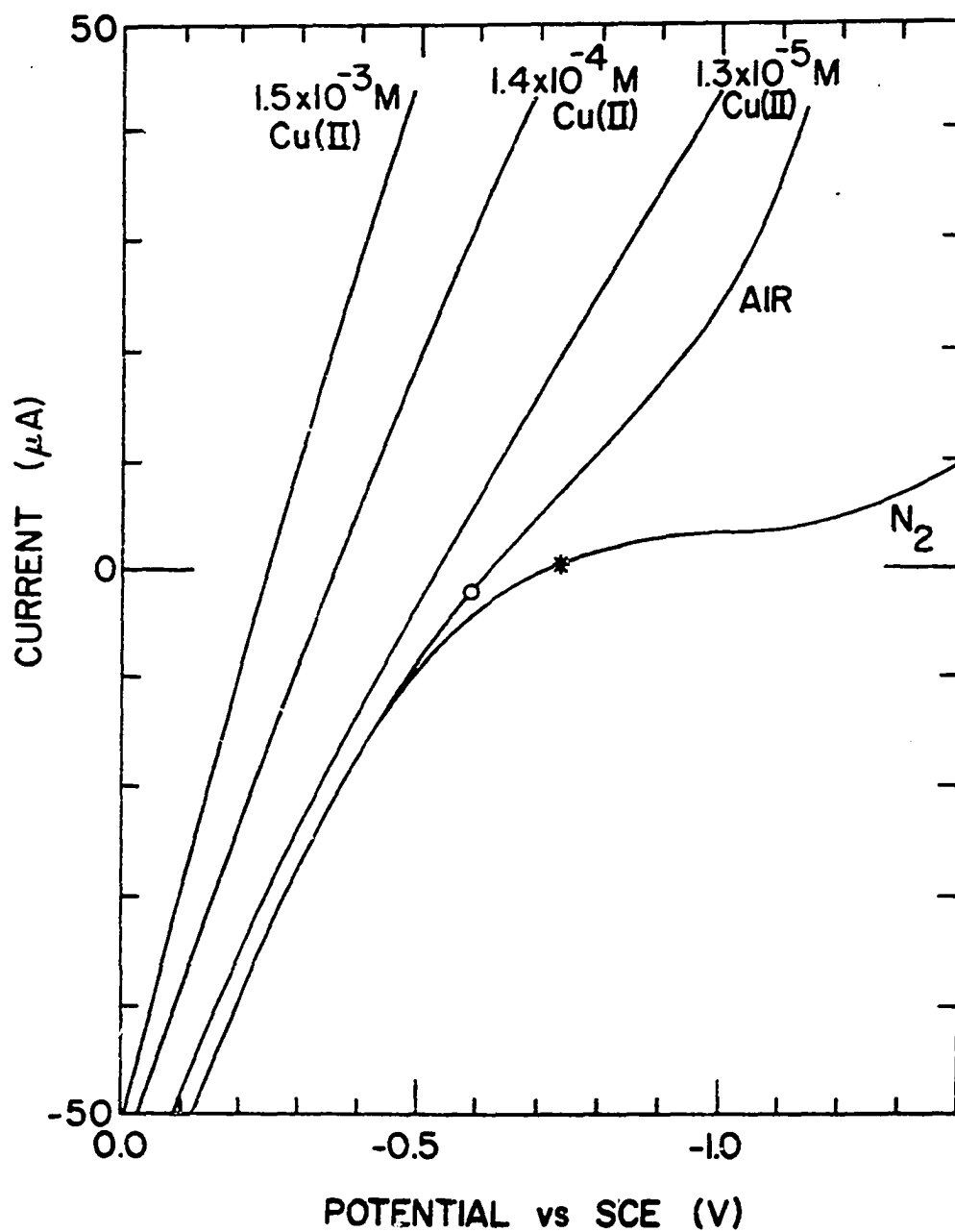
Figure 38. Voltammetric curves of $Na_{0.65}WO_3$ electrode in 1M NH_4OH as a function of Cu(II) concentration

(o) (x) Open circuit potentials
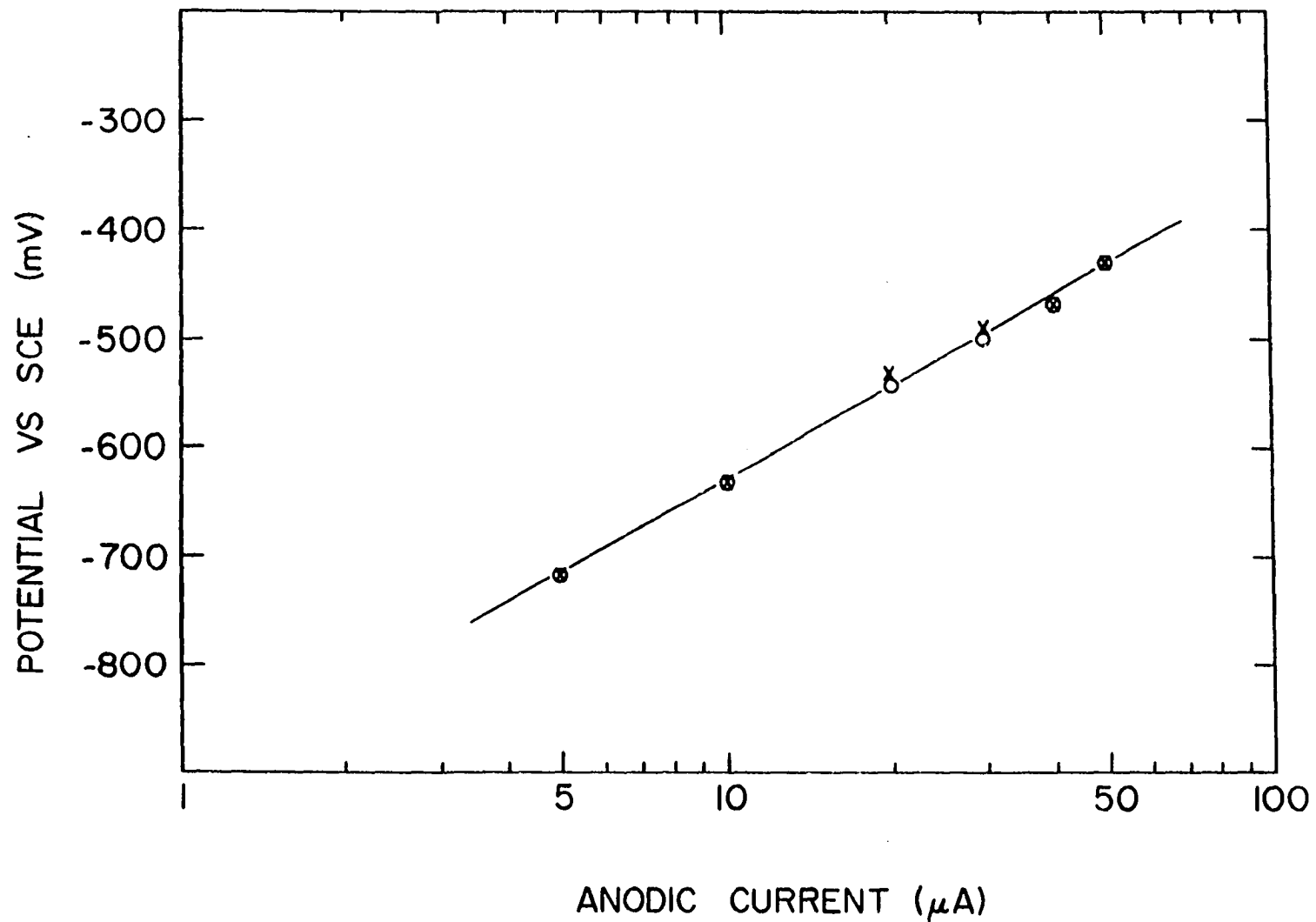
Figure 39. Anodic wave for the oxidation of the $Na_{0.65}WO_3$ electrode

(o) Positive to negative voltage scan   (x) Negative to positive voltage scan

electrode. Such a situation may exist for ferricyanide in 1M NH_4OH explaining the 300 mV/decade response slope observed at high $Fe(CN)_6^{3-}$ concentration (Figure 34).

The mixed-potential mechanism provides excellent explanations for several observations connected with the oxygen response of the Na_xWO_3 electrode. Any factor influencing either the rate of Na_xWO_3 oxidation or the rate of O_2 reduction reactions as a function of potential (polarization curves) will subsequently alter the mixed-potential response of the electrode.

The enhanced response to dissolved oxygen in the presence of trace Ag(I) (Figure 15) can be explained if the minute quantity of Ag metal depositing on the bronze electrode acts as a catalyst for the oxygen reduction reaction. A number of metals, including Ag, have been shown to catalyze the reduction of dissolved oxygen at a Na_xWO_3 electrode when present in the bronze as impurities (70). Such catalysis would shift the cathodic oxygen waves (Figure 37) to more positive potential and result in a larger mixed-potential response to dissolved oxygen.

The poor oxygen response for low x Na_xWO_3 electrodes in LiOH (Figure 10) may be rationalized on the basis of a change in the Na_xWO_3 anodic wave. The negative charge on the electrode and the small ionic size of the Li^+ ion suggests the possibility of lithium diffusing into the Na_xWO_3 crystal lattice forming a Li_xWO_3 or mixed Li_xWO_3-Na_xWO_3 layer at the electrode surface. This would be most apt to happen with low x value bronzes which have a greater number of available vacant lattice sites. Lithium tungsten bronzes and mixed sodium-lithium tungsten bronzes are known to be much more resistant to oxidation in basic solution than the

pure sodium bronzes (12,13,54). Under these circumstances the anodic wave for the bronze oxidation could be shifted far enough toward positive potentials to render the mixed-potential response to oxygen inoperative.

The day-to-day variations in electrode response and the dependence of the potential on stirring rate can also be understood in terms of the mixed-potential mechanism. Changes in the electrode surface will result from the slow dissolution of the electrode in oxygenated basic solution. If the bronze is not perfectly homogeneous preferential attack of the more active sites will occur. Such surface changes are certain to alter both the anodic and cathodic polarization curves and result in a change in the oxygen response. The rate of stirring will primarily affect the polarization curve for the diffusion controlled oxygen reduction. Increased stirring will result in a larger cathodic current for a given oxygen concentration and explain the shift of the mixed potential toward a more positive potential.

Voltammetric curves for several other highly conducting alkali metal tungsten bronze electrodes in $0.1M$ KOH-1mM EDTA are presented in Figures 40 to 43. Immediately apparent is the absence of any bronze oxidation wave at potentials between -0.5 and -1.0 V in deoxygenated (N_2 saturated) solution. The inability of these bronzes to undergo oxidation and establish a mixed potential with the oxygen or Cu(II) reduction couples is consistent with their poor performance in responding to dissolved oxygen and in detecting the equivalence point in chelometric titrations.

A number of these electrodes however, did exhibit some potentiometric response to dissolved oxygen in $0.1M$ KOH-1mM EDTA (Figure 17) and a 30-40 mV/decade response to Cu(II) in 1M NH_4OH (Figure 30). Other mixed-

Figure 40. Voltammetric curves of hexagonal $K_{0.3}WO_3$ electrode in oxygen
and nitrogen-saturated 0.1M KOH-1mM EDTA solutions

(*) Open circuit potential in N_2-saturated solution
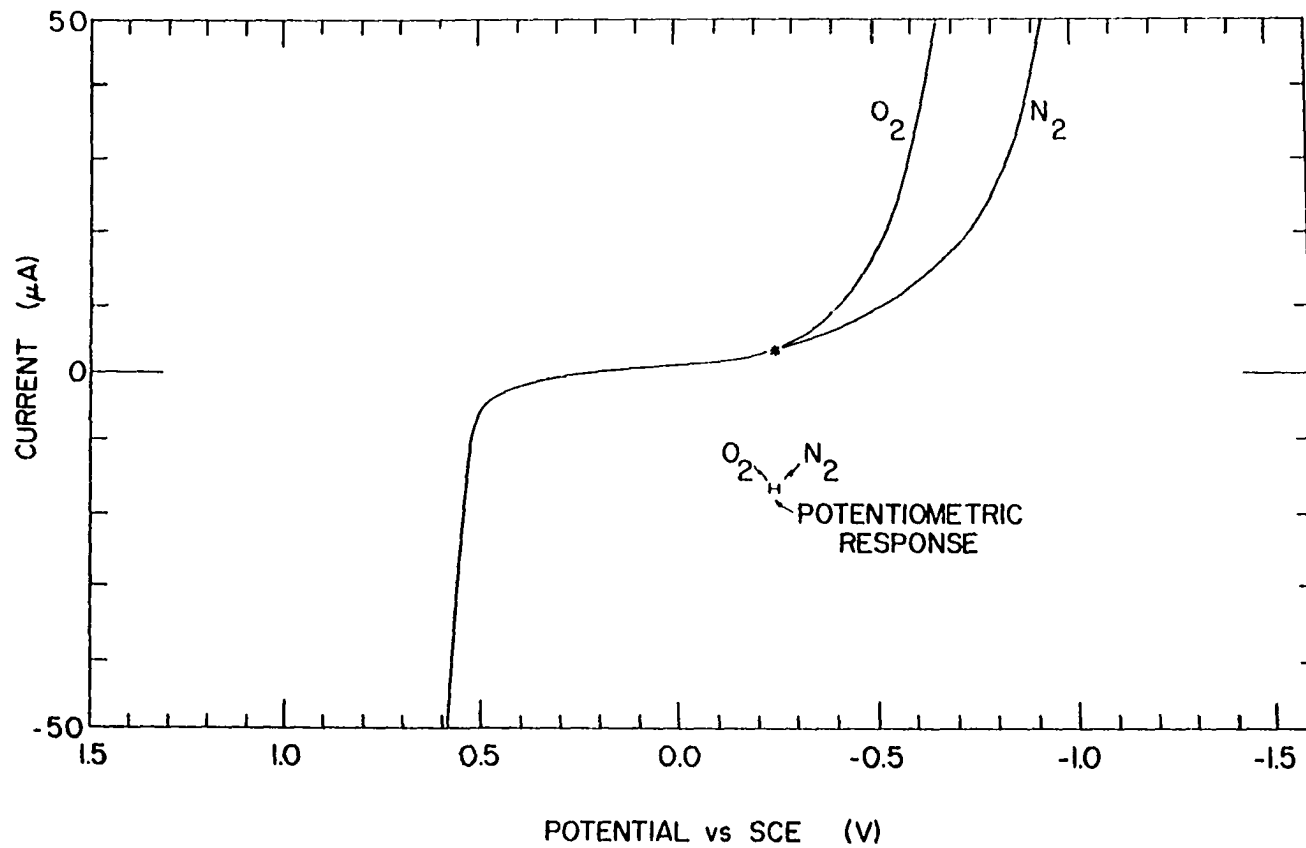
Figure 41. Voltammetric curves of hexagonal $Rb_{0.3}WO_3$ electrode in oxygen and nitrogen-saturated
0.1M KOH-1mM EDTA solutions

(*) Open circuit potential in N_2-saturated solution
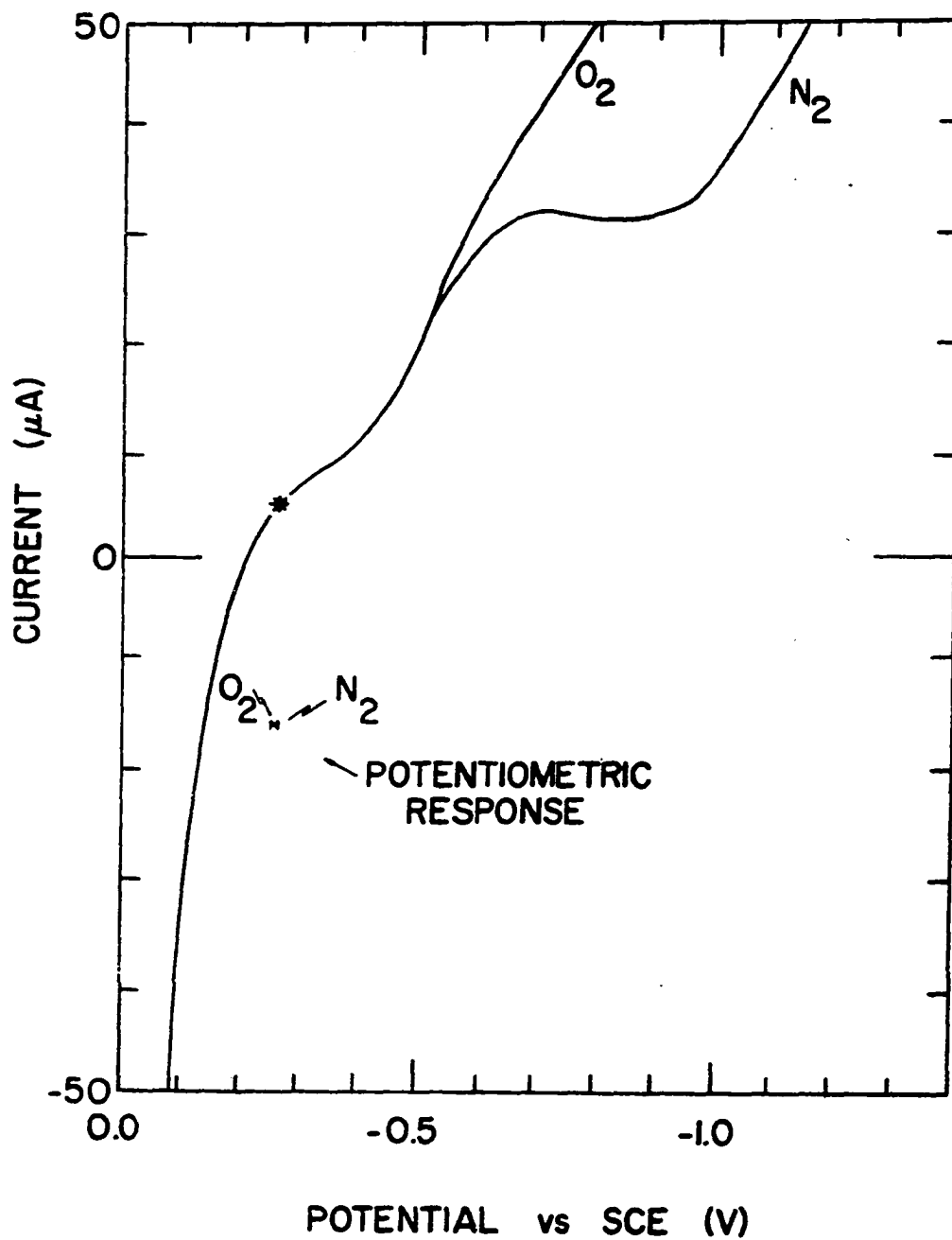
Figure 42. Voltammetric curves of hexagonal $Cs_{0.3}WO_3$ electrode in oxygen and nitrogen-saturated 0.1M KOH-1mM EDTA solutions

(*) Open circuit potential in N_2-saturated solution

Figure 43. Voltammetric curves of cubic $Li_{0.35}WO_3$ electrode in oxygen and nitrogen-saturated 0.1M KOH-1mM EDTA solutions

(*) Open circuit potential in N_2-saturated solution

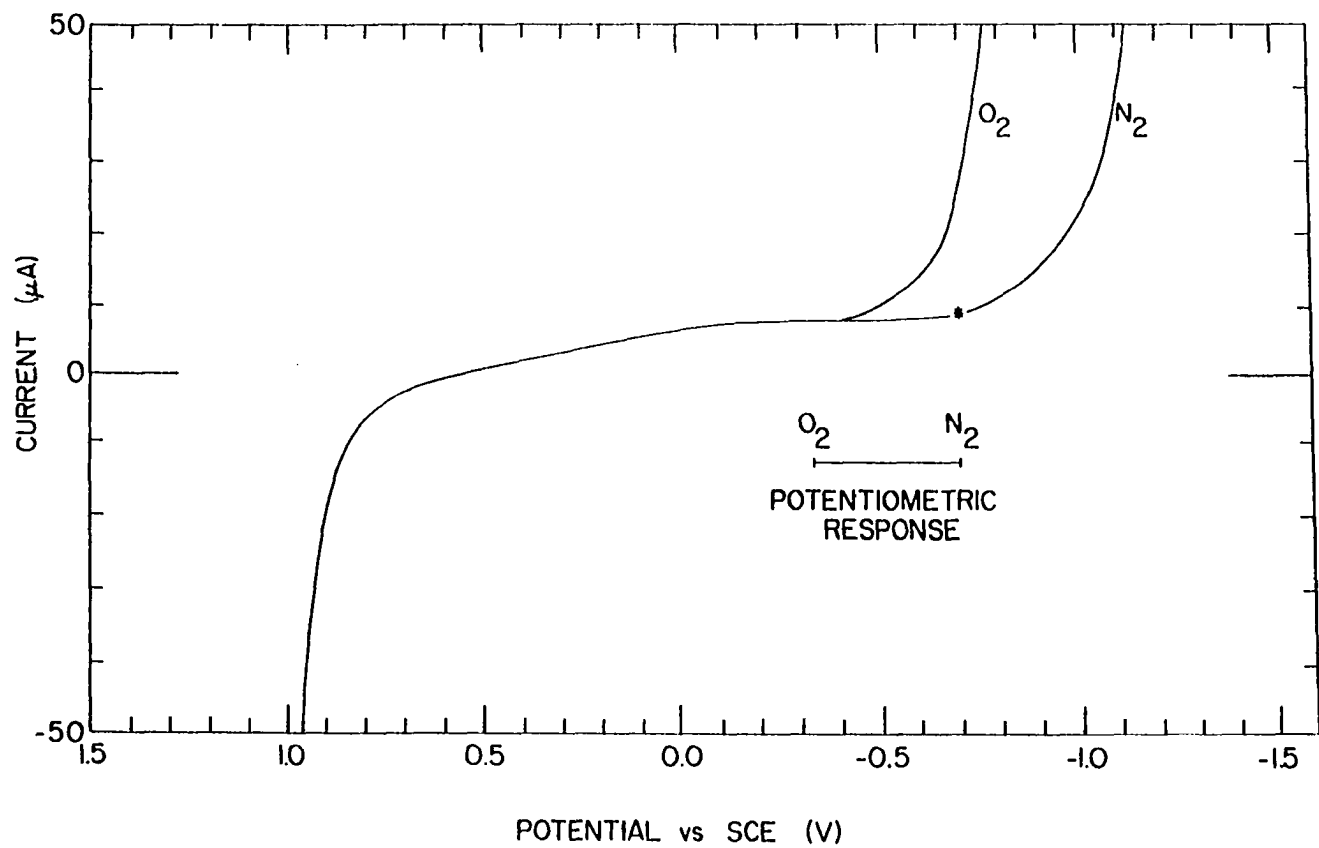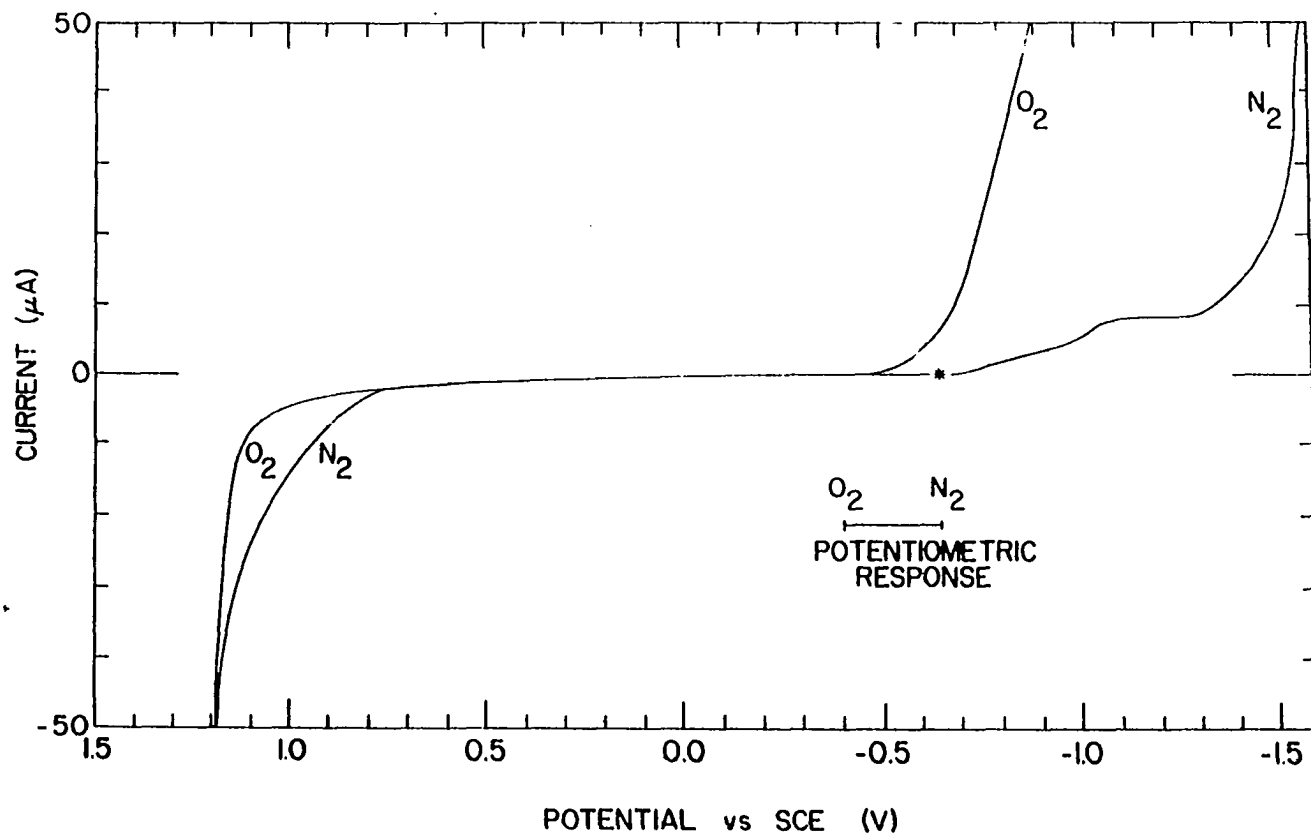potential phenomena are suspected as the cause of these observations.

The oxidation partial current here may involve the formation of an oxide layer at the electrode surface or the oxidation of water to O_2 or H_2O_2. The fact that the hexagonal $K_{0.3}WO_3$ and $Rb_{0.3}WO_3$ exhibited no response whatsoever to dissolved oxygen is an extremely strong argument for the mixed-potential response mechanism. The voltammetric curves for these electrodes (Figures 40 and 41) show that the O_2 reduction wave begins at more negative potentials than the open circuit potential in deoxygenated solution. In these instances, dissolved oxygen is not a strong enough oxidizing agent to participate in establishing a mixed potential.

The substantial shift in the potential of the Na_xWO_3 electrode in chelometric titrations of nonelectroactive species can also be explained by the mixed-potential mechanism. Copper or some other oxidizing agent complexed by EDTA would indeed act as a potentiometric indicator if it was present in the titration solution. The voltammetric curves for the $Na_{0.65}WO_3$ electrode in 1M NH_4OH (Figure 37) clearly demonstrate a negative shift in the mixed potential with decreasing $Cu(II)$ concentration. A similar shift would be expected if a given amount of $Cu(II)$ was complexed with excess EDTA making it more difficult to undergo reduction. In practice however, there does not appear to be enough $Cu(II)$ or other EDTA-complexable oxidizing agent present to cause this effect, especially in view of the large amount of reducible oxygen present during these titrations.

The shift in the mixed potential at the equivalence point is due to the presence of the EDTA itself instead of the effect of complexing a trace potentiometric indicator. Figure 44 presents voltammetric curves
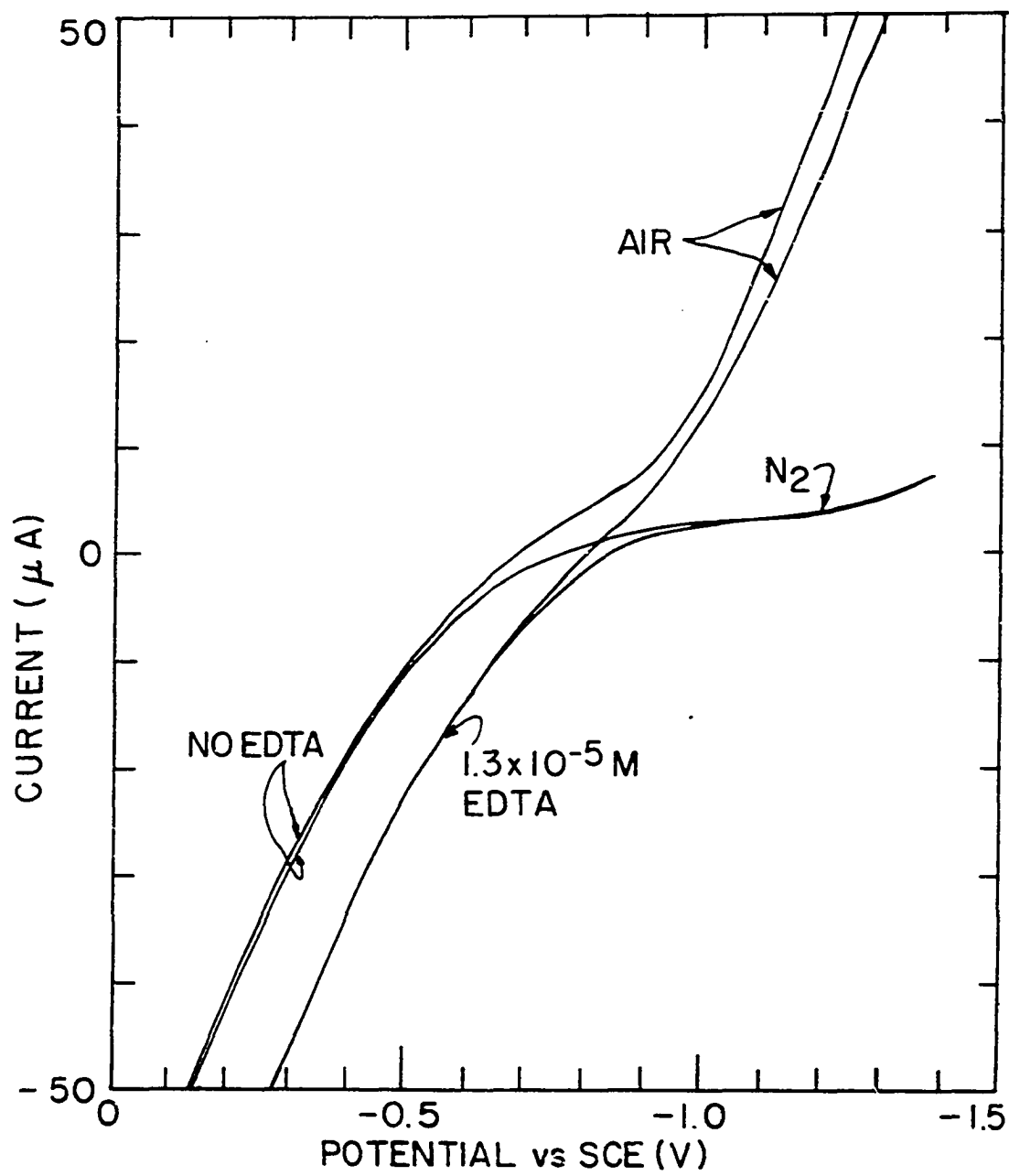
Figure 44. Voltammetric curves for the $Na_{0.65}WO_3$ electrode in 1M NH_4OH showing the effect of trace EDTA

for the $Na_{0.65}WO_3$ electrode in nitrogen and air-saturated 1M NH_4OH

solution showing the effect of EDTA at a concentration of 1.3 X 10^{-5}M.

The presence of trace EDTA was found to shift the anodic polarization wave

for the oxidation of the $Na_{0.65}WO_3$ electrode to more negative potentials

by 120-140 mV. This oxidation at more negative potential may result

from the EDTA complexing tungsten and driving the following reaction to

the right.

$$Na_xWO_3 + 2OH^- \ \text{--------} \ xNa^+ + WO_4^{2-} + H_2O + xe^- \qquad (8)$$
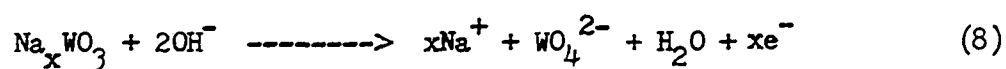
The EDTA also appears to affect the cathodic polarization wave for

the reduction of oxygen at the Na_xWO_3 electrode. The negative 20-30 mV·

potential shift in this wave may be the result of the EDTA hindering the

oxygen reduction reaction. If this shift in the cathodic wave is also

characteristic of other metallic electrodes the 20-30 mV shift observed

in chelometric titrations using the other tungsten bronze electrodes

(Figure 29) and the Pt, Cu and W electrodes (Figure 31) can be explained.

CONCLUSION

The sodium tungsten bronzes have been shown to be highly useful potentiometric-indicating electrodes for determining dissolved oxygen in aqueous solution and for indicating the equivalence point in metal-EDTA titrations.

The response to dissolved oxygen differs from that of conventional polarographic, voltammetric and galvanic electrochemical methods (81) in that a potential rather than a current is indicative of the oxygen concentration. Although the analytical applicability of the Na_xWO_3 electrode was only demonstrated at dissolved oxygen concentrations above 0.04 ppm ($P_{O_2} = 0.001$ atm), there is an additional 150-200 mV potential region available to perhaps extend the range of analysis another order of magnitude lower. The logarithmic potential response has in theory a distinct advantage over the linear current response of the conventional methods when working at extremely low concentrations. It becomes increasingly more difficult to instrumentally measure the smaller and smaller currents involved but no more difficult to measure a more negative potential.

The high degree of sensitivity and the magnitude of the potential change per unit change of oxygen concentration (120 mV/decade) demonstrate the utility of the Na_xWO_3 electrode for dissolved oxygen determinations. The simplicity and low cost of the electrode and the relative ease with which potential measurements can be made are additional advantages. The ability to incorporate the electrode into a flow-through system or perhaps a recirculating system suggests applicability for field measurements of

dissolved oxygen in river and lake waters. The major disadvantage however, is that the response is limited to basic solution and a deaerated reagent would have to be introduced into the sample. The membrane voltammetric and galvanic electrodes on the other hand, will operate over an extended pH range and in organic liquids (81).

An extremely useful application of the Na_xWO_3 electrode is the potentiometric detection of equivalence points in metal-EDTA titrations. As little as 0.01 millimole of metal can be easily measured in these titrations and the method is applicable for the determination of nonelectroactive as well as electro-active metals. Similar chelometric titrations have been demonstrated using a mercury electrode (78,94) and copper ion-selective electrodes (95,96) but these require the presence of an indicator ion for successful titrations. Equivalence-point detection with the Na_xWO_3 electrode appears to be a result of the electrode's direct response to the EDTA itself. The absence of any indicator is a distinct advantage when titrating for minute quantities of metal because corrections for the indicator blank are unnecessary. As in the case of the Na_xWO_3 oxygen electrode, the simple design and low cost of the electrode are additional advantages.

The potentiometric response of the Na_xWO_3 electrode in basic solution is attributed to a mixed potential established from the spontaneous oxidation of the electrode surface by dissolved oxygen. The simultaneous reduction of dissolved oxygen and oxidation of the Na_xWO_3 electrode over the same general potential range as the potentiometric response was demonstrated by voltammetry. A mixed potential mechanism explains the response to dissolved oxygen and the response in chelometric titrations.

Also explained by the mixed-potential mechanism are the many idiosyncra-
sies connected with the response of the Na_xWO_3 electrode. These include
the variability in electrode response, the effect of stirring, the loss
of O_2 response in LiOH and the enhancement of O_2 response in the presence
of trace Ag(I), and the uniqueness of the cubic Na_xWO_3 electrode in
responding to dissolved oxygen and the equivalence point in chelometric
titrations.

Future Studies

Although the Na_xWO_3 electrode has been demonstrated to be very useful
in dissolved oxygen determinations, there are two disadvantages to be
overcome in order to improve results. These are the slow response at low
oxygen concentrations and the variability in electrode response over a
period of time. The response characteristics may possibly be improved by
changing the composition of the Na_xWO_3 electrode. Incorporation of
Li_xWO_3 into Na_xWO_3 for example, will increase resistance toward oxidation
and minimize deterioration of the electrode surface. This may result in
a more stable response without too much sacrifice in response slope and
sensitivity. Incorporation of trace platinum in Na_xWO_3 electrodes is
known to catalyze the reduction of oxygen. This may result in a more
rapid response of the electrode to dissolved oxygen.

In this study, the application of the Na_xWO_3 electrode in chelometric
titrations was demonstrated only for EDTA. Additional studies are
warranted to determine if other complexing agents would cause a similar
mixed potential shift and be useful as titrants. Studies involving the
use of masking agents in conjunction with EDTA for selectively determining

metals in mixtures may also prove to be useful.

The voltammetric studies presented here have shown the cubic sodium tungsten bronzes to undergo oxidation in basic solution much more easily than the other alkali metal tungsten bronzes. Also demonstrated by voltammetry is the extremely interesting series of observations concerning oxidation at the hexagonal tungsten bronze electrode in basic solution. Oxidation occurs most readily at the K_xWO_3 electrode and least readily at the Cs_xWO_3 electrode with Rb_xWO_3 in between. Correlation of these observations with other properties of the tungsten bronzes would make a most interesting study.

LITERATURE CITED

1. P. G. Dickens and M. S. Whittingham, Quart. Rev. (London) $\underline{22}$(1), 30 (1968).

2. P. Hagenmueller, "Les Bronzes Oxygenes," Progress in Solid State Chemistry, Vol. 5, H. Reiss, Ed., Pergamon Press, Oxford, England, 1971, pp 71-144.

3. E. Banks and A. Wold, Prep. Inorg. React., $\underline{4}$, 237 (1968).

4. E. Schwarzmann and R. Birkenberg, Z. Naturforsch., B, $\underline{26}$(10), 1069 (1971).

5. P. G. Dickens, A. C. Halliwell, D. J. Murphy and M. S. Whittingham, Trans. Faraday Soc., $\underline{67}$(Part 3), 794 (1971).

6. F. Wöhler, Ann. Chim. Phys., $\underline{43}$(2), 29 (1823).

7. A. Laurent, Ann. Chim. Phys., $\underline{67}$, 215 (1838).

8. L. A. Hallopeau, Ann. Chim. Phys., $\underline{19}$, 117 (1900).

9. O. Brunner, Ph.D. Thesis, University of Zurich, Zurich, Switzerland, 1903.

10. E. Schaefer, Z. Anorg. Allg. Chem., $\underline{38}$, 158 (1904).

11. M. J. Sienko, J. Amer. Chem. Soc., $\underline{81}$, 5556 (1959).

12. M. E. Straumanis and S. S. Hsu, J. Amer. Chem. Soc., $\underline{72}$, 4027 (1950).

13. M. E. Straumanis, J. Amer. Chem. Soc., $\underline{71}$, 679 (1949).

14. E. O. Brimm, J. C. Brantley, J. H. Lorenz and M. H. Jellinek, J. Amer. Chem. Soc., $\underline{73}$, 5427 (1951).

15. W. McNeill, Ph.D. Thesis, Temple University, Philadelphia, Pa., 1961; Diss. Abstr. Int. B, $\underline{22}$, 60 (1961).

16. W. McNeill and L. E. Conroy, J. Chem. Phys., $\underline{36}$, 87 (1962).

17. W. Ostertag, Inorg. Chem., $\underline{5}$, 758 (1966).

18. B. Broyde, Inorg. Chem., $\underline{6}$, 1588 (1967).

19. A. Magneli and B. Blomberg, Acta Chem. Scand., $\underline{5}$, 372 (1951).

20. R. A. Bernoff and L. E. Conroy, J. Amer. Chem. Soc., $\underline{82}$, 6261 (1960).

21. L. E. Conroy and G. Podolsky, Inorg. Chem., $\underline{7}$, 614 (1968).

22. A. Magneli, Ark. Kemi, 1, 213 (1949).

23. D. Van Duyn, Rec. Trav. Chim. Pays-Bas, 61, 669 (1942).

24. B. L. Chamberland, Inorg. Chem., 8, 1183 (1969).

25. L. D. Ellerbeck, H. R. Shanks, P. H. Sidles and G. C. Danielson, J. Chem. Phys., 35, 298 (1961).

26. H. R. Shanks and G. C. Danielson, J. Appl. Phys., 38, 4923 (1967).

27. H. R. Shanks, J. Crystal Growth, 13-14, 433 (1972).

28. C. T. Hauck, A. Wold and E. Banks, Inorg. Syn., 12, 153 (1970).

29. A. Magneli and R. Nilsson, Acta Chem. Scand., 4, 398 (1950).

30. M. J. Sienko and T. B. N. Truong, J. Amer. Chem. Soc., 83, 3939 (1961).

31. R. A. Fredlein and A. Damjanovic, J. Solid State Chem., 4, 94 (1972).

32. L. Meites, E. Banks and C. E. Fleischmann, Anal. Chem., 44, 1133 (1972).

33. M. S. Whittingham and R. A. Huggins, National Bureau of Standards Special Publication N. 364, U. S. Government Printing Office, Washington, D. C., 1972, pp 51-62.

34. W. F. de Jong and H. J. Stek, A. Kristallogr., 83, 496 (1932).

35. W. F. de Jong, Z. Kristallogr., 81, 314 (1932).

36. G. Hagg, Nature, 135, 874 (1935).

37. G. Hagg, Z. Physik. Chem., B29, 192 (1935).

38. B. W. Brown and E. J. Banks, J. Amer. Chem. Soc., 76, 963 (1954).

39. R. J. Reuland and A. F. Voigt, Anal. Chem., 35, 1263 (1963).

40. A. Magneli, Acta Chem. Scand., 5, 670 (1951).

41. A. S. Ribnik, B. Post and E. Banks, "Phase Transitions in Sodium Tungsten Bronze," Advances in Chemistry Series, No. 39, American Chemical Society, Washington, D. C., 1963, pp 246-253.

42. A. Magneli, Nature, 169, 791 (1952).

43. A. Magneli, Acta Chem. Scand., 7, 315 (1953).

44. M. J. Sienko, "Electric and Magnetic Properties of the Tungsten and Vanadium Bronzes," Advances in Chemistry Series, No. 39, American Chemical Society, Washington, D. C., 1963, pp 224-236.

45. H. R. Shanks, P. H. Sidles and G. C. Danielson, "Electrical Properties of the Tungsten Bronzes," Advances in Chemistry Series, No. 39, American Chemical Society, Washington, D. C., 1963, pp 237-245.

46. L. D. Muhlestein and G. C. Danielson, Phys. Rev., 158, 825 (1967).

47. E. J. Huibregtse, Iowa State Coll. J. Sci., 26, 222 (1952).

48. J. D. Greiner, H. R. Shanks and D. C. Wallace, J. Chem. Phys., 36, 772 (1962).

49. A. R. Mackintosh, J. Chem. Phys., 38, 1991 (1963).

50. R. Fuchs, J. Chem. Phys., 42, 3781 (1965).

51. J. B. Goodenough, Bull. Soc. Chim. Fr., 1965, 1200 (1965).

52. A. Feretti, D. B. Rodgers and J. B. Goodenough, J. Phys. Chem. Solids, 26, 2007 (1965).

53. J. B. Goodenough, "Metallic Oxides," Progress in Solid State Chemistry, Vol. 5, H. Reiss, Ed., Pergamon Press, Oxford, England, 1971, pp 145-399.

54. M. E. Straumanis and G. F. Doctor, J. Amer. Chem. Soc., 73, 3492 (1951).

55. F. T. Jones, Ph.D. Thesis, Polytechnic Institute of Brooklyn, Brooklyn, N. Y., 1960; Diss. Abstr., Int. B, 21, 1390 (1960).

56. A. A. Balandin and N. P. Sokolova, Problemy Kinetiki i Kataliza, Akad. Nauk. S. S. S. R., No. 10, 363 (1960).

57. D. B. Sepa, D. S. Ovcin and M. V. Vojnovic, J. Electrochem. Soc., 119, 1285 (1972).

58. L. W. Niedrach and H. I. Zeliger, J. Electrochem. Soc., 116, 152 (1969).

59. D. B. Sepa, A. Damjanovic and J. O'M. Bockris, Electrochim. Acta, 12, 746 (1967).

60. A. Damjanovic, D. Sepa and J. O'M. Bockris, J. Res. Inst. Catal., Hokkaido Univ., 16, 1 (1968).

61. B. Barret, J. Catal., 10, 13 (1968).

62. J. H. Fishman, J. F. Henry and S. Tessore, Electrochim. Acta, 14, 1314 (1969).

63. J. O'M. Bockris, R. A. Fredlein and A. Damjanovic, U. S. Clearinghouse Fed. Sci. Tech. Inform., No. 706861, 1970, 37 pp.

64. R. A. Fredlein and J. McHardy, Power Sources Symp., Proc., 24, 175 (1970).

65. J. McHardy, K. L. Mittal, and J. O'M. Bockris, U. S. Nat. Tech. Inform. Serv., No. 747766, 1972, 92 pp.

66. J. McHardy, Ph.D. Thesis, University of Pennsylvania, Philadelphia, Pa., 1972; Diss. Abstr. Int. B, 33, 1484 (1972).

67. M. Voinor and H. Tannenberger in "From Electrocatalysis to Fuel Cells," G. Sandstede, Ed., Univ. Wash. Press, Seattle, Wash., 1972, pp 101-108.

68. J. McHardy and J. O'M. Bockris in "From Electrocatalysis to Fuel Cells," G. Sandstede, Ed., Univ. Wash. Press, Seattle, Wash., 1972, pp 109-112.

69. J. McHardy and J. O'M. Bockris, J. Electrochem. Soc., 120, 53 (1973).

70. J. O'M. Bockris and J. McHardy, J. Electrochem. Soc., 120, 61 (1973).

71. A. G. Koksharov and V. F. Ust-Kachkinsev, Uch. Zap. Perm. Gos. Univ., 111, 63 (1964); Chem. Abstr., 64, 1617g (1966).

72. A. G. Koksharov and V. F. Ust-Kachkinsev, Izv. Vyssh. Ucheb. Zaved. Khim. Khim. Tekhnol., 10, 243 (1967); Chem. Abstr., 67, 39512b (1967).

73. A. G. Koksharov and V. F. Ust-Kachkinsev, Uch. Zap. Perm. Gos. Univ., 178, 117 (1968); Chem. Abstr., 73, 61979e (1970).

74. M. A. Wechter, H. R. Shanks, G. Carter, G. M. Ebert, R. Guglielmino and A. F. Voigt, Anal. Chem., 44, 850 (1972).

75. A. Weser and E. Pungor, Acta Chim. Acad. Sci. Hung., 59, 319 (1969).

76. M. A. Wechter and A. F. Voigt, Anal. Chem., 38, 1681 (1966).

77. M. A. Wechter, H. R. Shanks and A. F. Voigt, Inorg. Chem., 7, 845 (1968).

78. A. I. Vogel, "Quantitative Inorganic Analysis," John Wiley and Sons, Inc., New York, N. Y., 1961.

79. R. C. Weast, S. M. Selby and C. D. Hodgman, Eds., "Handbook of Chemistry and Physics," 46th Ed., The Chemical Rubber Co., Cleveland, Ohio, 1964, 1965.

80. D. C. Johnson and S. Bruckenstein, Anal. Chem., 43, 1313 (1971).

81. J. P. Hoare, "The Electrochemistry of Oxygen," Interscience Publishers, New York, N. Y., 1968.

82. R. E. Davis, G. L. Horvath, and C. W. Tobias, Electrochim. Acta, 12, 287 (1967).

83. T. S. Light in "Ion Selective Electrodes, "R. A. Durst, Ed., National Bureau of Standards Special Publication 314, U. S. Government Printing Office, Washington, D. C., pp 354-355.

84. N. A. Lange and G. M. Forker, Eds., "Handbook of Chemistry," 10th ed, McGraw-Hill, New York, N. Y. 1967.

85. F. D. Snell and C. T. Snell, "Colorimetric Methods of Analysis," Vol. II A, D. Van Nostrand Co. Inc., Princeton, N. J., 1959, p 76.

86. G. Eisenman, Ed., "Glass Electrodes for Hydrogen and Other Cations," Marcel Dekker, Inc., New York, N. Y., 1967.

87. R. A. Durst, Ed., "Ion-Selective Electrodes," National Bureau of Standards Special Publication 314, U. S. Government Printing Office, Washington, D. C., 1969.

88. C. Wagner and W. Traud, Z. Electrochem., 44, 391 (1938).

89. P. Delahey, "Double Layer and Electrode Kinetics," Interscience Publishers, New York, N. Y., 1965, pp 172-173.

90. D. Gray and A. Cahill, J. Electrochem Soc., 116, 443 (1969).

91. I. M. Kolthoff, E. B. Sandell, E. J. Meehan and S. Bruckenstein, "Quantitative Chemical Analysis," 4th ed, Macmillan Co., London, England, 1969, pp 944-945.

92. J. Koryta, J. Dvorak and V. Bochackova, "Electrochemistry," Methuen and Co. Ltd., London, England, 1970, pp 318-321.

93. J. M. Herbelin, T. N. Andersen and H. Eyring, Electrochim. Acta, 15, 1455 (1970).

94. A. E. Martin and C. N. Reilley, Anal. Chem., 31, 992 (1959).

95. J. W. Ross, Jr. and M. S. Frant, Anal. Chem., 41, 1900 (1969).

96. E. W. Baumann and R. M. Wallace, Anal. Chem., 41, 2072 (1969).

ACKNOWLEDGMENTS

The author wishes to extend his gratitude to his major professor, Dr. Adolf F. Voigt, for his encouragement and assistance during the author's graduate study at Iowa State University.

Special thanks are also due to Dr. Margaret Wechter for her continued interest and support throughout this study.

The author would like to thank Dr. Dennis Johnson for his many helpful suggestions, and Mr. Howard Shanks for providing the tungsten bronze crystals used in this study.

The author wishes to express his appreciation to his wife, Pat, for an excellent job of editing and typing this dissertation.

;